ISTANBUL TECHNICAL UNIVERSITY ★ GRADUATE SCHOOL OF SCIENCE ENGINEERING AND TECHNOLOGY

ANALYSIS OF ELECTRIFICATION ON POWER CONSUMPTION OF A SHUTTLE BUS

M.Sc. THESIS

MEHMET ERCAN TEKİN

Department of Mechanical Engineering

Automotive Programme

June 2019

ISTANBUL TECHNICAL UNIVERSITY ★ GRADUATE SCHOOL OF SCIENCE ENGINEERING AND TECHNOLOGY

ANALYSIS OF ELECTRIFICATION ON POWER CONSUMPTION OF A SHUTTLE BUS

M.Sc. THESIS

MEHMET ERCAN TEKİN
(503161715)

Department of Mechanical Engineering

Automotive Programme

Thesis Advisor: Dr. Osman Taha Şen

June 2019

ISTANBUL TEKNİK ÜNİVERSİTESİ ★ FEN BİLİMLERİ ENSTİTÜSÜ

ÜNİVERSİTE RİNG SERVİSİ'NİN DİRENÇ ANALİZİ ARAŞTIRMASI VE REJENERATİF FRENLEMENİN ETKİLERİ

YÜKSEK LİSANS TEZİ

MEHMET ERCAN TEKİN
(503161715)

Makina Mühendisliği Anabilim Dalı

Otomotiv Programı

Tez Danışmanı: Dr. Osman Taha Şen

Haziran 2019

Mehmet Ercan Tekin, a M.Sc. student of ITU Graduate School of Science Engineering and Technology student ID 503161715, successfully defended the thesis entitled “ANALYSIS OF ELECTRIFICATION ON POWER CONSUMPTION OF A SHUTTLE BUS”, which he prepared after fulfilling the requirements specified in the associated legislations, before the jury whose signatures are below.

Thesis Advisor : **Dr. Osman Taha Şen** ....
İstanbul Technical University

Jury Members : **Doç. Dr. Özgen Akalın** ....
Istanbul Technical University

Dr. Tarkan Sandalcı ....
Yıldız Technical University

Date of Submission : 3 May 2019
Date of Defense : 10 June 2019

To my lovely family,

FOREWORD

In this thesis, analysis study made on the shuttle bus' power consumption in order to complete graduate program of Istanbul Technical University Automotive Engineering Programme. Aim of the study is to investigate power consumption of a shuttle bus in a specified route and analysis of electrification on power consumption. Regenerative braking rate was calculated with respect to the route information and speed data of the shuttle bus

During the study, data acquisition and data post-processing is done. Data was collected in different time zones on the same route and different results was a gain of this study. Deciding and finding the wrong measurements was another problem to be solved alternatvely in this study.

I would like to thank to my supervisor Dr. Osman Taha ŞEN for supporting me and guiding me all the time. I would also like to thank to my family for always encouraging me.

June 2019

Mehmet Ercan TEKİN
Mechanical Engineer

TABLE OF CONTENTS

Page

ABBREVIATIONS

API	**:** Application Program Interface
EV	**:** Electric Vehicle
GPS	**:** Global Positioning System
NYCC	**:** New York City Cycle
PHEV	**:** Plug-in Hybrid Electric Vehicle
TUIK	**:** Türkiye İstatistik Kurumu
VRLA	**:** Valve Regulated Lead Acid Battery

SYMBOLS

a	: Acceleration
Cd	: Drag Coefficient
D	: Distance
Kg	: Grade Coefficient
ρ	: Air Density
ρd	: Density of Diesel Fuel
Fa	: Aerodynamic Drag Resistance
Fbr	: Brake Force
Fg	: Grade Resistance
Fi	: Inertia
Fr	: Rolling Resistance
fr	: Rolling Resistance Coefficient
g	: Gravity
h	: Height
Hd	: Diesel Calorific Value
m	: Mass
P	: Power
t	: Time
v	: Speed

LIST OF TABLES

Page

LIST OF FIGURES

Page

ANALYSIS OF ELECTRIFICIATION ON POWER CONSUMPTION OF A SHUTTLE BUS

SUMMARY

Emission problems and depletion of fossil fuel reserves led the automotive sector to find alternative solutions. Electrification of the vehicles is one of the alternative solution to these problems and it is trying to be implemented by most of the automotive companies.

Despite of its performance and emission advantages, electric vehicles also have some some problems that prevent people from using it widely.This problem is the range of the electric vehicle. One of the system that can extend electric vehicle’s mileage is regenerative braking systems. This system simply aims to convert braking energy of the vehicle into the chemical energy that can be stored in battery system and can be used as a energy source to be ready when vehicle will be accelerated. Electric vehicle application can be also applied on buses and regenerative braking can be a good opportunity to save brake energy into the batteries.

In this study, the road information of the shuttle bus within the Istanbul Technical University was collected and a detailed power consumption analysis was performed and the amount of energy recovered by regenerative braking after a possible electrification application was calculated.

As a result of the measurements and calculations, the shuttle consumed 4.5kWh in total when the service went in first direction. In the calculations made according to the diesel fuel consumption, it was seen that the engine which produced 16kWh power along the whole route corresponded to the measured amount due to the efficiency. This situation shows that almost all of the resistances are calculated but the minor losses cannot be calculated.

It was observed that the shuttle bus spent most of the energy on inertia and slope along the route. This is because the vehicle has a very high mass. The high drag resistance in passenger cars has not reached very high values due to the fact that the shuttle does not go fast and the passenger cars have lower mass.

The amount of regenerative braking calculated on the assumptions made in this study has shown that the power consumed in the total route will be recovered by 26% in the worst case scenario and 33% in the best scenario. Therefore, rapid braking during the driving process is not suitable for the quick response and the regenerative braking method because the motor cannot provide this power completely. The differences in measurement also vary due to different crowd-density conditions and different driving characteristics.

As a result of this study, it has been shown that electrification of a service shuttle with a short distance route is appropriate. The high regenerative braking rate resulting from the calculations has shown that the vehicle can reach more distance with a single charge by extending the range further. All shuttles can be converted into electrical services with the charging stations that can be put at the last stops. The electrification of shuttle will help reduce the on-campus air pollution, help people breathe more comfortably and help to preserve nature

RİNG SERVİSİNİN ELEKTRİKLİLEŞTİRİLMESİYLE GÜÇ TÜKETİMİ ANALİZİ

ÖZET

Ulaşım ihtiyaçları dolayısıyla yükselen araç sayıları ve fosil yakıt kullanımları otomotiv sektörü için büyük problemler yaratmaktadır. Gerek fosil yakıt rezervlerinin tükenmesi, rezervlerin tükenmeye devam etmesinden kaynaklı olarak fiyatların yükselmesi, gerekse araçların kullanıldığı şehir içi ortamlarda hava kirliliğine sebebiyet vererek yaşam kalitesini düşürmesi otomotiv sektörünü alternatif güç kaynaklarına çalışmalar yapmaya yönlendirdi.

Şu anda alternatif çalışmalar arasında en yaygın çalışmalar ise elektrikli araçlar üzerine yapılıyor. Elektrikli araçlar basitçe batarya gibi bir enerji depolayabilen güç kaynağından aldığı enerjiyi elektrik motoru üzerinde hareket enerjisine çevirerek araçların hareket etmesini sağlamaktadır. Ancak batarya teknolojilerinin istenilen seviyede gelişememesi, hızlı şarj desteği olmaması menzilinin düşük olmasına ve kullanım kolaylığı sağlayamamasına sebep oluyor. Bu yüzden elektrikli araçların geliştirilmesi üzerine en çok pil ve enerji verimliliği çalışmaları yapılıyor.

Elektrikli araçların enerji verimliliğini arttırabilmek adına kullanılan yöntemlerden biri rejeneratif frenlemedir. Bu yöntemin esas amacı içten yanmalı motora sahip araçlarda sürtünme ile sağlanan frende kaybedilen enerjiyi pile geri depolayabilmektir. Bunun için elektrik motorunun bağlı olduğu tekerlerde frenleme esnasında elektrik motoru tarafından ters tork uygulanır ve elektrik motoru jeneratör olarak çalışmaya başlar. Böylelikle tekerleğin sahip olduğu kinetik enerji elektrik motorunun vasıtasıyla pile kimyasal enerji olarak geri depolanır. Bu olayların sonucunda ise araç yavaşlar.

Rejeneratif frenleme yönteminin kullanılması ile menzil sorunu yaşayan araçların menzili aracı fişe takmadan bir miktar daha uzatmayı sağlar ve verimliliği arttırır. Ancak bu bütün fren enerjisinin geri kazanılacağı anlamına gelmez. Arada bulunan komponentlerin verimleri ve düzensizlikler bu geri kazanımın kayıplara uğramasına sebep olur.

Bu çalışmada İstanbul Teknik Üniversitesi içerisinde bulunan ring servisinin yol bilgileri toplanarak detaylı güç tüketimi analizi yapılmıştır ve olası bir elektrikleştirme uygulaması sonrasında rejeneratif frenleme ile kazanılabilecek enerji miktarı hesaplanmıştır.

Çalışmanın en önemli süreçlerinden biri yol verisinin ve araç sürüş verilerinin toplanması esnasında oluşmuştur. Bu aşamada bir mobil telefon kullanılmıştır. Matlab Mobile uygulaması üzerinden cihazın üzerinden bulunan GPS alıcısından veriler kayıt edilmiştir. GPS üzerinden enlem, boylam, yükseklik ve hız bilgileri toplanabilmiştir. Mobil cihazın kullanılması daha fazla verinin toplanmasına ve daha gerçekçi sonuçlara ulaşılmasında fayda sağlamıştır. Bu cihazdan toplanan verilerl 1Hz frekansında toplanmıştır. Dolayısıyla her saniye için bir kayıt alınmıştır.

Veri toplaması esnasında enlem,boylam ve hız verilerinde bir tutarsızlık gözlenmemişken yükseklik verisinde tutarsızlıklar tespit edilmiştir. Bu durum GPS alıcılarının yükseklik ölçümlerinde problem oluşturduğunu göstermektedir. Bu durumu çözümlemek adına Google Elevation API kullanılmıştır. Google Elevation API enlem, boylam bilgilerinin verilmesi karşılığında o enlem ve boylamın bulunduğu noktanın yüksekliğinin edinilebildiği bir internet servisidir. Matlab üzerinden oluşturulan bir kod ile bu bilgiler toplanarak yol için edindiğimiz enlem, boylam noktaları için güvenilir yükseklik noktalarına sahip olunmuştur.

Bu çalışma kapsamında yolun coğrafi bilgileri, servisin hız bilgisi ölçüm cihazı ile toplanmış, bunun üzerine Matlab üzerinde yolun ivme haritası, sürtünme direnci haritası, yuvarlanma direnci haritası, yokuş direnci ve atalet kuvvetleri hesaplamaları yapılmıştır. Burada yapılan hesaplamalar sayesinde de aracın bir servis rotası esnasında anlık ve toplam olarak güç hesaplamaları yapılmıştır. Burada elde edilen atalet kuvvetlerinin analizi sayesinde aracın frenleme esnasındaki güç tüketimine ulaşılmıştır. Bu bilgi sayesinde de bazı varsayımlar kabul edilerek rejeneratif frenleme ile geri kazanılabilecek enerji miktarı hesaplanmıştır.

Yapılan hesaplamalar doğrultusunda, 12 durağa sahip bu rotada oluşan farklı sürüş karakteristikleri, servisin doluluğu ve trafik durumundaki farklılıklar çalışmanın farklı koşullarda da ölçüm yapmasını sağlamıştır. Böylelikle kampüsün daha yoğun veya daha tenha olduğu zamanlarda ring süreleri arasındaki farklar ve farklı sürüş karakteristiklerini gözlemlemek daha gerçekçi sonuçlar elde edilmesini sağlamıştır.

Yapılan ölçüm ve hesaplamaların sonucunda ise servisin yaklaşık olarak bir yöne gittiği zaman toplamda 4.5kWh güç tükettiği ölçülmüştür. Sahadan alınan dizel yakıt tüketimine göre yapılan hesaplamalarda bütün rota boyunca 16kWh güç üreten motorun verimlilikler dolayısıyla yaklaşık ölçülen miktara denk geldiği görülmüştür. Bu durum neredeyse dirençlerin tamamının hesaplandığını ancak kayıpların hesaplanamadığını göstermektedir.

Servis aracının rota boyunca en çok atalet ve yokuşa enerji harcadığı görülmüştür. Bu durum aracın çok yüksek bir kütleye sahip olmasından kaynaklanmaktadır. Binek araçlarda yüksek olarak görülen sürtünme direnci, gerek servisin hızlı gitmemesi gerekse binek araçların daha az kütleye sahip olmasından dolayı çok yüksek değerlere ulaşmamıştır.

Atalet kuvvetlerinin çok yüksek olmasından dolayı aracın frenlemeleri esnasında da çok yüksek miktarda güç harcanmaktadır. Bu durum sürtünme ile frenleme yapıldığında tamamen ısı enerjisine dönüşüp kullanılamaz hale geldiği için verimi düşürmektedir. Ancak elektrikli otobüs kullanımında rejeneratif frenleme ile geri kazanılarak menzil arttırılabilir ve bu durum verimliliği yükseltecektir.

Bu çalışmada yapılan varsayımlar üzerinde hesaplanan rejeneratif frenleme miktarı aracın toplamda harcadığı gücün en kötü senaryoda %26'sı en iyi senaryoda ise %33'ünün geri kazanılacağını göstermiştir. Burada sürüş esnasında yapılan ani frenlemeler çok yüksek fren kuvvetlerine sahip olduğundan dolayı, durmaya yakın esnadaki frenlemelerde motor üzerinde düzenli bir akım oluşturamadığından dolayı yok sayılarak hesaplanmıştır. Dolayısıyla, sürüş esnasında yapılan hızlıca frenlemeler hem hızlı tepki alabilmek adına hem de motorun bu gücü tamamen sağlayamamasından dolayı rejeneratif frenleme metodunu uygulamaya uygun değildir. Ölçüm farklılıkları da farklı yoğunluk koşullarında ve farklı sürüş karakteristiklerinden dolayı farklılıklar göstermektedir.

Bu çalışmanın sonucunda, kısa mesafeli rotaya sahip bir servis aracının elektriklileştirilmesinin uygun olabileceğini göstermiştir. Yapılan hesaplamalar sonucunda çıkan yüksek rejeneratif frenleme oranı da aracın menzilini daha fazla uzatarak tek şarj ile daha fazla yol alabileceğini göstermiştir. Son duraklara koyulabilecek şarj istasyonlarıyla da bütün servisler elektrikli servislere dönüştürülebilir. Servis içi kampüslerin elektriklileştirilmesi kampüs içi hava kirliliğini azaltarak kampüs içinde yaşayan insanların daha rahat nefes almasını ve doğayı korumaya yardımcı olmasını sağlayacaktır.

1. INTRODUCTION

Fossil fuel usage is creating major problems in the automotive industry. Both emission problems and depletion of fossil fuel reserves led the automotive sector to find alternative solutions. Electrification of the vehicles is one of the alternative solution to these problems and it is trying to be implemented by most of the automotive companies. Almost all of the automotive companies try to provide at least 1 electric or hybrid electric vehicle in all of their car segments. Also, governments and fuel companies started to add fast electric charging stations into their facilities.

Despite of its performance and emission advantages, there are some problems on electric vehicles that prevent people from using it widely. Range of the electric vehicles generally the point where people are reluctant to use it. Because of this reason, most of the studies on electric vehicle field are based on energy efficiency and battery systems that can provide better range.

One of the system that can extend electric vehicle's mileage is regenerative braking systems. This system simply aims to convert braking energy of the vehicle into the chemical energy that can be stored in battery system and can be used as a energy source when the traction system needs energy.

Electric vehicle applications are also used in public transportation vehicles like buses. In urban use, buses generally have low distance tours and it does not need to have long range. Further, electric buses can make higher rates of regenerative braking than passenger vehicles because of its high brake force requirements with respect to its mass and low acceleration movements. Regenerative braking application will be much more meaningful in the manner of energy efficiency when it is used in electric buses.

1.1 Purpose of Thesis

This study is based on calculations from the measurements taken from a university shuttle bus. Through these measurements, geographical information of the route, speed and acceleration profiles of the different driving characteristics, fuel consumption of the vehicle in the shuttle route, resistance calculations of the vehicle and detailed analysis of it, instant force and power demand of the vehicle in the shuttle route, energy consumed for braking, amount of brake energy to recover will be calculated. This study's main goal is to show effect of electrification and regenerative braking on a shuttle bus that used on a specific route. It is aimed to be measurements and calculations that can be a reference in possible electrification studies.

1.2 Regenerative Braking - Electric Vehicles

Electric vehicles are vehicles that provide the traction of the vehicle only from the electric motor. Generally, batteries are used to provide energy to the vehicle as a energy source and electric motor converts the stored energy to the rotational movement and this will be pass through to the for the movement of the vehicle(Husain,2003). Sample system diagram of the electric vehicle can be seen from the below figure 1.1 as:

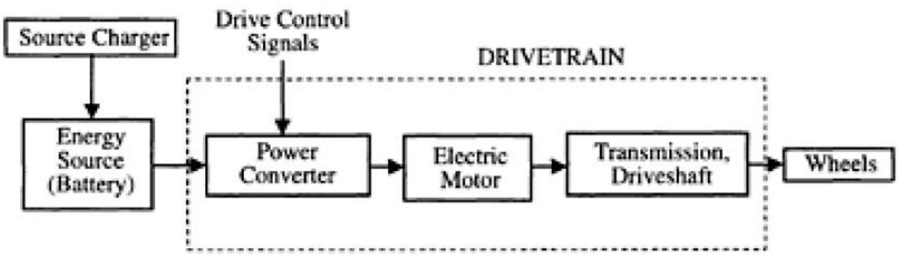

Figure 1.1: System Diagram of an Electric Vehicle

One of the main reasons for the low range of electric vehicles is the low energy capacity of the batteries and the weight burdens for both performance and safety reasons. Due to these reasons, every single efficiency gain on the power management of the electric vehicle will be crucial due to extend its range. The use of the electric motor as a generator is beneficial for energy gain through the movement of the vehicle.

While vehicle is braking, brake force applied to the brake pads on the wheels and vehicle will slow down due to the friction. During this process, kinetic energy of the vehicle converted into the heat because of the friction. In electric vehicles, there is an opportunity save this energy lost with using the electric motor as a generator and regenerate the energy as chemical energy on batteries. During the decelaration movement of the vehicle, electric motor act as generator and apply negative torque, vehicle starts to slow down and in this period battery will be charged through the power converter which is connected to the electric. Meantime, losses occur as an attempt to store an unstable current due to the variable speed and road conditions. But, As the electronic technologies developed, more energy is gained from this situation. Also, gain from the braking process of the vehicle is crucial for electric vehicles because of its low range.

Regenerative braking is also applied on electric bus applications. Buses apply too high brake force while slowing down due to its high amount of mass. This situation creates an advantage while regeneration occurs, because even if the speed of bus is slow, it has high rotational speeds. By this way, more energy can be regenerated to the batteries. This case provides much more brake regeneration on the batteries. In this study, investigation of forces applied on a shuttle bus spends on the resistances and the amount of gain achieved through regenerative braking will be examined.

1.3 Literature Review

Due to recent oil price crisis and an ever-increasing public awareness on environmental issues, an interest in electric vehicles (EV) has increased tremendously in Thailand and other Asian countries over the last few years(Premvaranon,2015). In this study, two different types of batteries tried on Electric bus which is used in Thailand Science Park as a campus fleet. These battery types are flooded lead acid battery and valve regulated lead acid battery(VRLA). Also, e-bus provides regenerative brake feature and there is comparative analysis between regenerative and non-regenerative. Paper mentions that performance of EV has generally been evaluated by implementing certain standard driving cycles on the vehicle via a chassis dynamometer test bench but these drive cycles do not represent the real driving scenarios. GPS was inserted on the e-bus for collecting the route data of the campus fleet.For each set of test, the total distance travelled was 21 km. (1.4 km/lap for 15 laps). They used 4 different drivers for considering the different driving scenarios of the drivers. From this study, the regenerative braking system could improve the usage of energy by 37% for both types of battery.

Another project based on coordinated control of the mechanical brake and electric motor brake on rear axis drive Hybrid electric bus for improving brake comfort without losing recovered energy from the regen. Project modeled in Trucksim and Matlab for simulations. If the bus is under a particular braking mode, there won't be a sudden change in the target value of motor braking force and mechanical braking force. There is no need to adopt coordinated control. Mechanical braking force and motor braking force are distributed according to the braking force required by driver. If the braking modes switch, there would be a sudden change in the target value of motor braking force and mechanical braking force. Coordinated control algorithm needs to be adopted(Zheng,2014).

Nowadays there are already electric buses operating in some parts of the world and one of the main concerns is their high weight (Perrotta,2012). This paper shows mathematical model of a driving cycle between two bus stops for the electric bus powertrain and its routes. The main objective is to verify how much of the energy recovered from regenerative braking can be absorbed by lithium-ion batteries and supercapacitors. Ultracapacitors can be a option to optimize efficiency of Electric vehicles that can be used together with batteries. Implementing the use of supercapacitors, which has a much higher power density - quick storage and release of energy - and thus are capable of absorbing a higher amount of the regenerative braking energy. This study also shows the regeneration percentage of the motor and it results with %65 regeneration of brake energy and %32 of total energy was regenerated to the batteries.

During the braking, another important point is braking feel inside the vehicle. Sangtarash and friends has studied on different regenerative brake strategies for optimal braking feel, optimal energy recovery and parallel braking for the best match of these 2 criterias. Optimal energy recovery model provies %36 regeneration but optimal braking feel model provides %12.2. Optimization of both criterias is provided %19.6 energy recovery from the brake in this study(Sangtarash,2008).

Another study of Perrotta is related with consumption analysis of energy according to the route specifications and other performance measures(Perrotta,2012). Caetano electric bus is used on the study. Some of the city cycls like New York City Cycle(NYCC) was applied on the bus and consumption analysis was made on deeply investigated. It is important to consider the efficiency of the motor when working as a generator, which is what happens during regenerative braking.. Thus, the amount of energy that can be recovered through regenerative braking for the NYCC is 0.69 kWh, which represents around 21% of the total energy of the cycle. It is important to state that, it was considered the battery pack could absorb all the energy in every braking episode, which is not entirely true.

Another study for the regenerative braking is about using hydraulic regenerative braking system as an alternative to the problems of electrical systems which is simulation study(Chen,2013). Results of simulations has shown that one-time charge driving distance of electric bus has been increased by 8.2%. After simulating influence of hydraulic components on regenerative braking system efficiency, optimization of hydraulic components parameters is done which laying foundation of dynamic modulating road test of hydraulic regenerative braking system.

Cikanek's study is about regenerative brake system on a hybrid electric vehicle(Cikanek, 2002). Alternative way for regenerative braking was dicussed in this study as parallel regenerative braking system for a PHEV that maximizes the regenerative braking force based on various vehicle attributes, without adding additional cost to the vehicle. The regenerative braking is performed through a high efficiency, single gear, direct drive transaxle for optimum braking efficiency. The engine is disengaged from the drive wheels during regenerative braking, eliminating engine frictional losses.

2. METHODOLOGY

2.1 Measurement of the Route

Measurements were made on the shuttle service that is traveling inside of Istanbul Technical University – Ayazaga Campus. Shuttle service has two endpoints and the routes are almost in the form of a turn of the way. One way has a distance of 4.5 km and that can be seen from the Figure 2.1.Measurements was executed with the mobile device that has GPS module. Mobile device approximately placed in the middle of the vehicle. Measurements was started from the beginning of the route and data was recorded until the end of the shuttle. Turn way recorded as a different measurement due to avoid effect of the waiting time at the last stop.

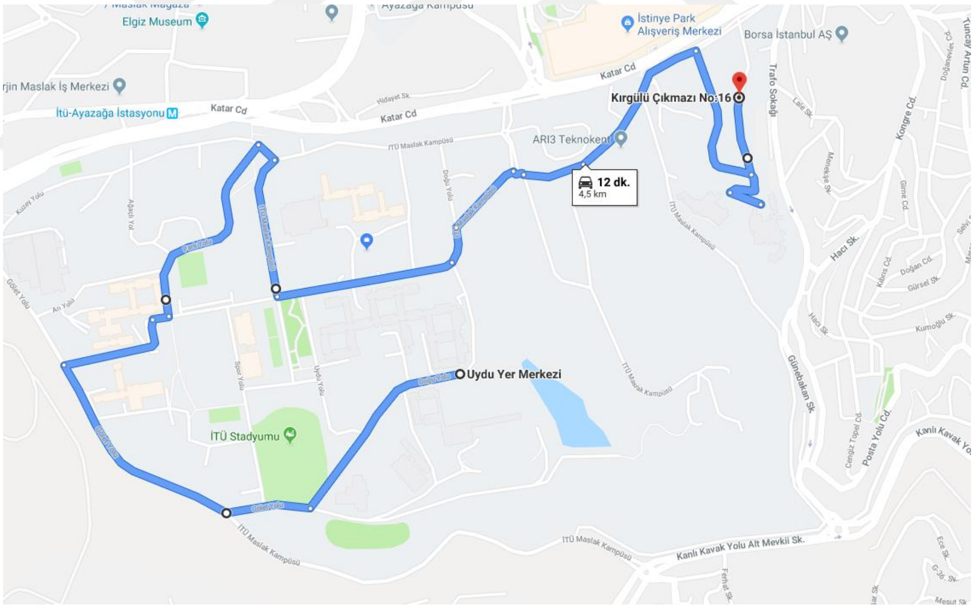

Figure 2.1: Route of the Shuttle Drive

2.1.1 Measurement Device

Apple iPhone 6s mobile phone device used as measurement device. GPS feature of the device provided the necessary information about the measurement. It collects the data in 1Hz frequency. So, it recorded the data in every second of the route. During real-time measurement conditions, this device has been selected due to its portability and data that can be recorded over it. Measurement device can be seen in the Figure 2.2.

Figure 2.2: Measurement Device

2.1.2 MATLAB Mobile Application

MATLAB supports the acquisition of data from the built-in sensors on Apple iPhone. With MATLAB mobile app Support Package for Apple iOS Sensors, data can be logged or query the most recent data available from the supported sensors on from the Apple iPhone. Logged data can be processed and analyzed on the MATLAB software on the computer.

In this study, location data acquisiton was used to collect the data of the shuttle route with the 1 Hertz frequency. Matlab Mobile App's data collection screen can be seen from the Figure 2.3. Also, collected sensor data is listed in following as:

- Latitude [degrees]
- Longitude [degrees]
- Altitude [m]
- Horizontal Accuracy [m]
- Speed [m/s]
- Course [degrees]

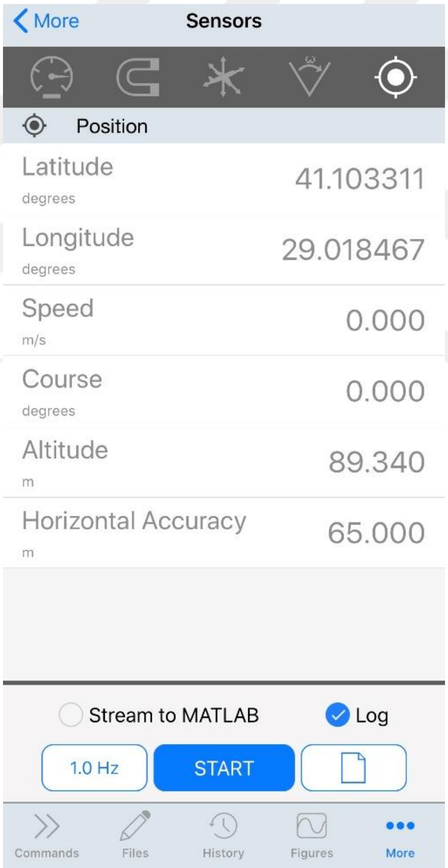

Figure 2.3: MATLAB Mobile App

2.1.3 Google Elevation API

While observing the collected data altitude data has discrepancies between the different measurement datasets. But, it should be all the same in all the measurements because route is same in all measurements. Google Elevation API was used to solve this situation. The Elevation API provides a simple interface to query locations on the earth for elevation data. Additionally, it allows to get sampled elevation data along paths which helps on calculating elevation changes along routes.

Collected latitude, longitude data from the Matlab mobile was used in Google Elevation API to get altitude information of the necessary geographic points. By this way, necessary geographical informations collected for calculations.

2.1.4 Shuttle Bus

Isuzu Novo Citi bus is used inside the campus for shuttle service. This service take a campus tour in every 20 minutes. Technical details of the shuttle can be seen from the Table 2.1. Also, shuttle bus can be seen from the Figure 2.4. Since there was no official data on fuel consumption, information was taken from drivers who were driving on this route all day. This condition may provide more realistic calculations and comparison on the further stages of the study. Also, there is no official data for the drag coefficient of the shuttle. This is specified as 0.7 after literature review.

Table 2.1: Technical details of Isuzu Novo Citi

	Isuzu Novo Citi
Length	7505 mm
Height	3332 mm
Width	2275 mm
Mass (Empty)	5600 kg
Fuel Consumption	35 lt / 100 km
Drag Coefficient (Cd)	0.7
Seat Number	21
Power	148 kW

2.1.5 System Coefficients & Assumptions

Some values that would be required during the calculations could not be measured during the measurements, assumptions were accepted as a result of the investigations. First one is the average human body weight selected as 71.5kg with respect to TUIK records. Due to the passenger circulation, it is hard to mention constant passenger number for this service. But, it is assumed as average 18 passenger with respect to the investigation while executing measurements. Selected system coefficients can be seen on the Table 2.2. Road surface coefficient selected as 1.2 for heavy truck contact with the asphalt(Gillespie).

Table 2.2: System Coefficients

Road Surface Coefficient (Ch)	1.2
Air Density(ρ)	1.2 kg/m^3
Gravity(g)	9.81 m/s^2
Diesel calorific value (Hd)	44000 kj/kg
Density of diesel fuel (ρ_d)	0.832 kg/lt

2.2 Formulations

In this section, calculations and formulations will be explained with the use of data and coefficients obtained from the measurements.

2.2.1 Acceleration Formulation

Acceleration is the rate of change of speed per unit of time. Speed data was collected from the measurement device will be used to calculate the average acceleration between two data points. Acceleration can be obtained from the following equation [2.1]:

$$a_n = \frac{v_{n+1} - v_n}{t_{n+1} - t_n} \quad [2.1]$$

Acceleration calculation will provide acceleration map of the route and will be used in Inertia force calculation. It is one of the important data that shows the different driving characteristics.

2.2.2 Aerodynamic Drag Resistance Formulation

All resistance acting on the vehicle will be examined one by one. The first resistance here is aerodynamic resistance. It represents the resistance of the air acting on the vehicle which is moving with a definite speed. Aerodynamic drag resistance can be obtained from the following equation [2.2]:

$$F_a = \frac{1}{2}\rho C_d A v^2 \qquad [2.2]$$

A is the projection area of the vehicle normal to moving direction which is generally directed to the air, v is the speed of the vehicle.

2.2.3 Rolling Resistance Formulation

Rolling resistance represents the resistance that caused by the contact of the ground and tire while the bus is moving. Rolling resistance can be obtained from the following equation [2.3] for the bus:

$$F_r = f_r mg \qquad [2.3]$$

f_r is the rolling resistance coefficient which can be calculated with the following equation [2.4]:

$$f_r = \left(\left(0.0041 + (0.000041.(v).2.237)\right).C_h\right) \qquad [2.4]$$

Rolling resistance is not calculated on the stationary positions of the bus like bus stops. Because there is no friction actuated between tire and road if the bus does not have any movement.

2.2.4 Grade Resistance Formulation

Grade resistance is caused by the projection of the weight of the vehicle in the direction of movement due to the angle formed during the climbing an uphill. When climbing the hill, it acts as a resistance and creates a support force when climbing downhill. Due to the obtained data, grade resistance will be calculated in a different way. Firstly, distance between two data points are calculated as [2.5]

$$D_n = \frac{1}{2}(v_{n+1} + v_n)(t_{n+1} - t_n) \quad [2.5]$$

D represents the distance between two points. After that, the coefficient of height difference is calculated by the following equation [2.6]

$$k_g = \frac{(h_{n+1} - h_n)}{D_n} \quad [2.6]$$

h represents the altitude value of the data point. k_g represents the grade coefficient of the data point. Grade resistance can be calculated by the following equation [2.7]:

$$F_g = k_g mg \quad [2.7]$$

2.2.5 Inertia Formulation

Inertia represents the net force applied on the vehicle. Inertia directly related with the acceleration of the vehicle. If acceleration is in positive direction it effects as tractive force but if it is negative it effects as brake force and brake force is one of the most important data for this study. It can be calculated by the following equation [2.8]:

$$F_i = ma \quad [2.8]$$

2.2.6 Brake Force Formulation

Braking force is applied during the deceleration movement of the vehicle. Negative acceleration values represents the braking stages of the vehicle. So, when the acceleration value is negative, brake force can be calculated by the following equation [2.9]:

$$F_{br} = ma \quad [2.9]$$

2.2.7 Power Formulation

Power in mechanical systems is the combination of forces and movement. In particular, power is the product of a force on an object and the object's velocity. Any of the particular resistance or total resistance values can be used to calculate power demand of the vehicle by the following equation [2.10]:

$$P = (0.001)Fv \quad [2.10]$$

Due to the unit of the velocity(m/s) formulation converted into kW.

2.2.8 Regenerative Brake Formulations

Due to the data obtained, the ratio of the braking on the front and rear axle is not achievable. Therefore, it is assumed that regenerative braking is applied on all wheels which is the condition of highest level energy recovery on the shuttle bus. All of the brake energy can not be used on regenerative braking due to the losses on heat, noise, inefficiencies etc.

Due to these situations, some of the assumptions will be made for the further calculations with respect to literature survey. During low speed movements, regenerative braking will not be used because low rotational speed could not provide necessary current on the system. The lower limit assumed that 15km/h in passenger vehicles. But, shuttle bus should assumed differently because rotational speed is rising faster than the passenger vehicles. It is assumed that 9km/h.

During regeneration, electric motor could not provide more than the maximum motor power. In real conditions, electric motors that are used in electric vehicles can act like generator up to %40 of maximum traction power of the electric motor. So, more than 60kW will be neglected in this study.

2.2.9 Fuel Consumption Formulations

Currently, shuttle bus has a internal combustion engine which is powered by diesel fuel. In this route, fuel energy that is provided by the internal combustion engine of the shuttle bus can be calculated in kWh by Equation 2.11:

$$FuelEnergy = \frac{\rho_d * H_d * FuelConsumption * 0{,}045}{3600} \quad [2.11]$$

0,045 coefficient was added due to the 4.5km route distance which converts the fuel consumption into route's consumption. If this calculation was executed, it can be reached that 16 kWh is used by internal combustion engine in this route. But , efficiency of the internal combustion engine is assumed as %30-35 due to the route conditions like bus stops and traffic.

3. CALCULATIONS & GRAPHS

In the different crowd density of the campus condition and different time zones, there was 9 dataset collection was executed. These situations led to differentiations between measurements and also show different driving characteristic because of different drivers and variable traffic condition inside the campus. These differentiations can be observed from these calculations and it will provide to see best case and worst case for the purpose of the study. Since the time of the journeys changed in each measurement, the number of data collected in each measurement was different. Data post-processing is executed on MATLAB software on computer. The number of data collected in the measurements can be observed in the table below [Table 3.1]:

Table 3.1: Dataset Information Table

Dataset	Start Point→End Point	End Point → Start Point
1	709 Data Points	658 Data Points
2	658 Data Points	936 Data Points
3	1025 Data Points	883 Data Points
4	911 Data Points	847 Data Points
5	861 Data Points	724 Data Points
6	806 Data Points	776 Data Points
7	822 Data Points	605 Data Points
8	784 Data Points	617 Data Points
9	847 Data Points	772 Data Points

Critical points of the collected datasets are specified in the following tables Table 3.2 and Table 3.3 which shows the duration of the route, distance calculation which is derivated from speed data, average speed of the route, maximum speed of the route, minimum and maximum altitude of the route.

Table 3.2: Overview of First Route (Gölet Dorm. → Vadi Dorm.)

#	Duration (s)	Distance (km)	Avg. Speed (km/h)	Max Speed (km/h)	Min Altitude (m)	Max Altitude (m)
1	709	4,11	20,87	41,76	66.98	131.86
2	1185	4,09	12,43	38,2	66,56	132.48
3	1025	4,11	14,44	39,31	66,93	131,87
4	911	4,12	16,28	41,78	66,93	131,96
5	861	4,10	17,14	41,76	66,98	131,88
6	806	4,10	18,31	42,55	67,00	131,97
7	822	4,04	17,69	40,03	66,93	131,88
8	784	4,08	18,73	43,24	66,98	132,03
9	847	4,13	17,55	37,98	66,98	131,87

Table 3.3: Overview of Turn Route (Vadi Dorm. → Gölet Dorm.)

#	Duration (s)	Distance (km)	Avg. Speed (km/h)	Max Speed (km/h)	Min Altitude (m)	Max Altitude (m)
1	658	3,76	20,57	46,40	66,93	131,87
2	936	3,84	14,77	39,46	66,93	131,87
3	883	3,85	15,70	42,95	66,91	131,88
4	847	3,81	16,19	40,43	66,91	131,88
5	724	3,75	18,65	44,32	66,96	131,87
6	776	3,79	17,58	42,59	66,95	131,88
7	605	4,04	24,04	43,99	66,97	131,87
8	617	3,81	22,23	44,21	66,98	131,86
9	772	3,79	17,67	40,28	66,96	131,87

From these tables, it can be seen that duration, average speed and maximum speed values were different between different datasets due to the different driving characteristics and different crowd intensity inside of the campus. Average speed values vary between 12,43 km/h to 24,04 km/h. This shows some of the drivers prefer fast driving scenarios than the others. But, distance and altitude values are consistent in all datasets. This shows reliability of the collected data.

3.1 Speed Profile

Speed data directly taken from the measurement device as a raw data. The speed profile will be one of the main values to see the stops on the driving route, see the driver's driving characteristics between these points and influence the power calculations to be made on it in the future. Maximum speed values and its timepoints shown in Table 3.4 and Table 3.5. These data shows that maximum speed do not happen in the same points of the route and it is not dependent with the other values.

Table 3.4: Max Speed of First Route (Gölet Dorm. → Vadi Dorm.)

#	Max Speed Time(s)	Max Speed (m/s)
1	35	11,6
2	111	10,6
3	205	10,9
4	59	11,6
5	136	11,6
6	740	11,8
7	456	11,1
8	81	12,0
9	626	10,6

Table 3.5: Max Speed of Turn Route (Vadi Dorm. → Gölet Dorm.)

#	Max Speed Time(s)	Max Speed (m/s)
1	516	12,9
2	836	11,0
3	774	11,9
4	440	11,2
5	279	12,3
6	752	11,8
7	208	12,2
8	539	12,3
9	748	11,2

Generally, vehicles completing the route in a similar time, had similar speed profiles. This situation can be seen from the Figure 3.1.1 which compares the speed profile of the 6th and 7th dataset that collected on the first route.

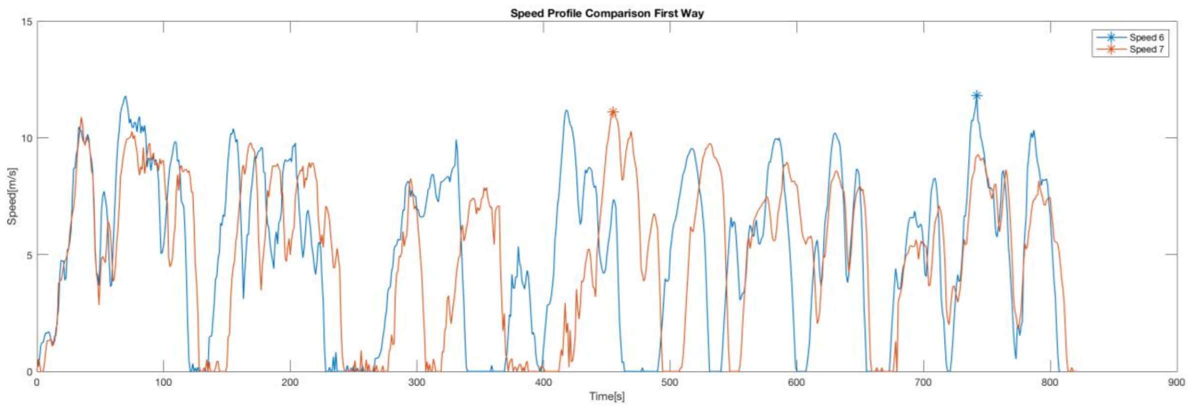

Figure 3.1.1: Speed Profile Comparison of First Route

(Gölet Dorm → Vadi Dorm)

Speed profiles generally show similar profiles. only minor deviations were observed due to the time elapsed at the stops. The data collected here will have a major impact on the power calculations. All of the speed profiles can be seen from Appendix A.

3.2 Acceleration Profile

Acceleration is important value which shows the vehicle's capacity to gain speed. Of course, the acceleration has a great effect on the energy the vehicle consumes. The easiest way to examine the driver's sudden acceleration and sudden deceleration movements is to examine the acceleration maps. Maximum acceleration values and its timepoints shown in Table 3.6 and Table 3.7. These points usually occur when approaching or leaving the stops. Acceleration values derived from Equation 2.1.

Table 3.6: Maximum Acceleration of First Route (Gölet Dorm. → Vadi Dorm.)

#	Max Acc Time(s)	Max Acc (m/s2)
1	94	2,75
2	89	1,80
3	90	2,68
4	456	3,76
5	276	2,25
6	776	2,83
7	680	2,97
8	212	2,10
9	215	1,92

Table 3.7: Maximum Acceleration of Turn Route (Vadi Dorm. → Gölet Dorm.)

#	Time(s)	Max Acc (m/s2)
1	508	3,85
2	874	3,91
3	364	1,77
4	814	3,69
5	430	3,34
6	638	2,72
7	438	3,24
8	461	2,59
9	18	2,87

As for the speed profile, the comparison of the sixth and seventh data can be accessed from Figure 3.2.1:

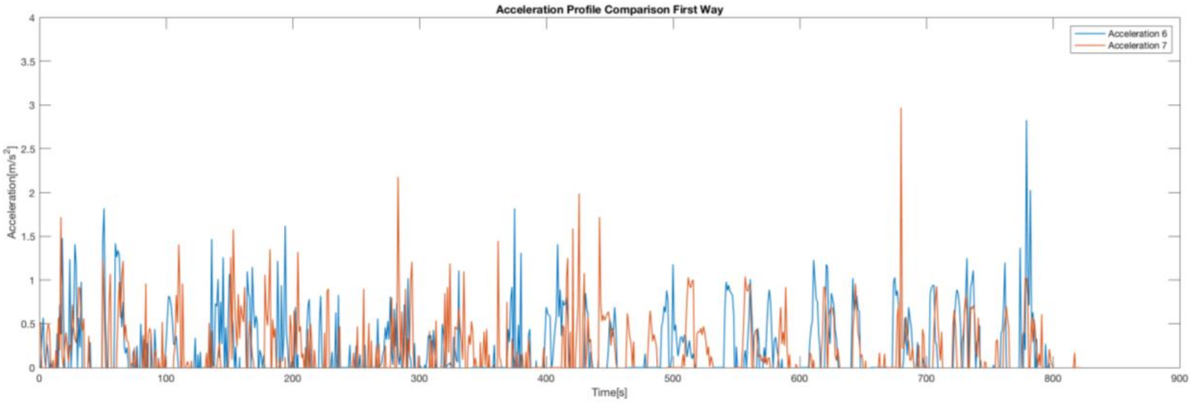

Figure 3.2.1: Acceleration Profile Comparison of First Route

(Gölet Dorm → Vadi Dorm)

Like the speed profile, the vehicles that complete the route in a similar time in the acceleration profile appear to have similar acceleration profiles. The time spent at the stops caused the graph to shift slightly, but the significant part was similar to each other. However, the highest accelerations can be observed when approaching and leaving the stopping points. Therefore, the maximum and minimum acceleration points do not correspond to the same regions in each measurement. The fact that drivers make their acceleration or deceleration movements as slow as possible can provide great advantages in terms of both driving comfort and power consumption. All of the acceleration profiles generated for all datasets, it can be seen from the

3.3 Altitude Profile

Altitude profile of the route requested from the Google Cloud service with using Elevation API with respect to the latitude,longitude information of all datapoints. Compared altitude vs time graph can be seen from the Figure 3.3.1 in first direction and Figure 3.3.2 in second direction.

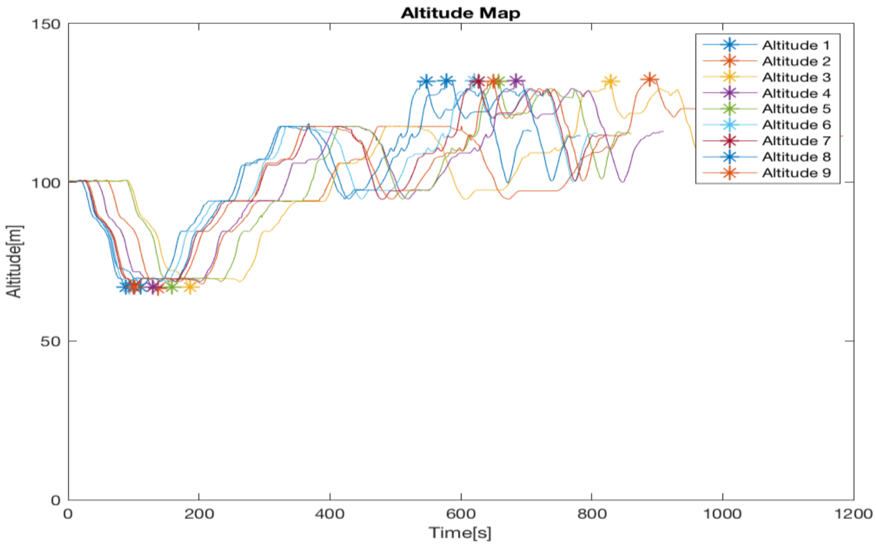

Figure 3.3.1: Altitude Map Comparison of First Direction Measurement

(Start Point → End Point)

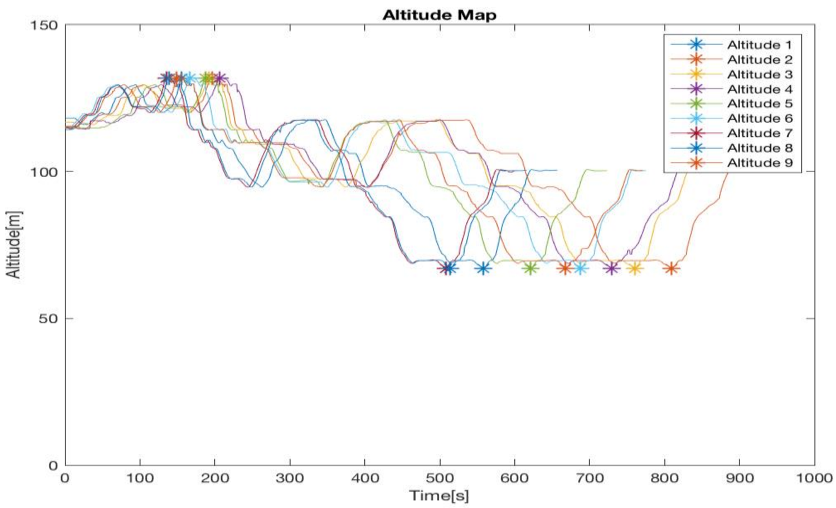

Figure 3.3.2: Altitude Map Comparison of Second Direction Measurements

(End Point → Start Point)

3.4 Route Mapping with Speed Profile

Latitude, longitude, altitude and speed values led to create 2D and 3D mapping with the colorization of speed values. These graphs will allow to see the bus stops at which the service stops and comparison and validation of the geographic data we collected with the measurement device and map. Blue areas show the bus stops. Almost all of the measurements plotted the same graph. Due to that, only selected ones of the first direction and second added to the following Figure 3.4.1, Figure 3.4.2, Figure 3.4.3, Figure 3.4.4:

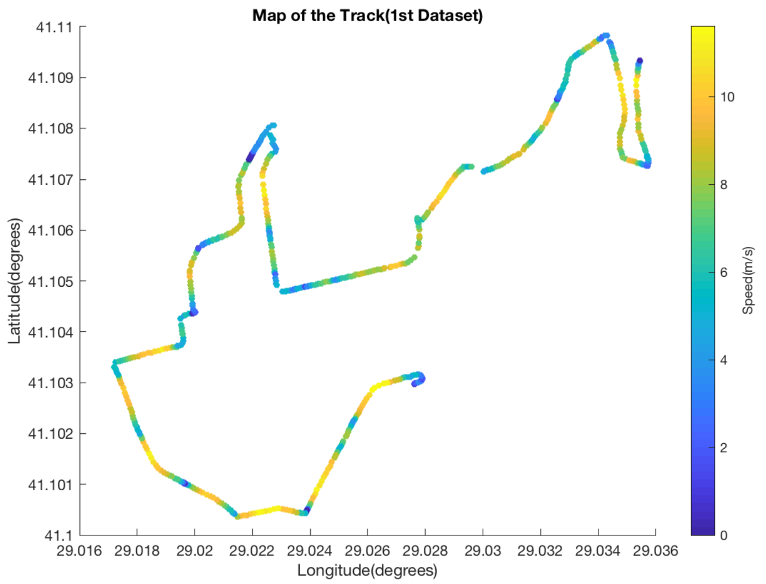

Figure 3.4.1: 2D Map of the Route

(Start Point → End Point)

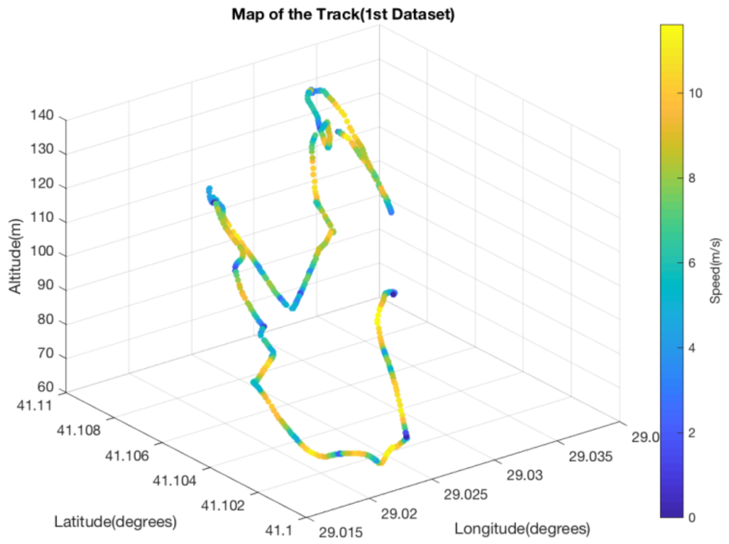

Figure 3.4.2: 3D Map of the Route

(Start Point → End Point)

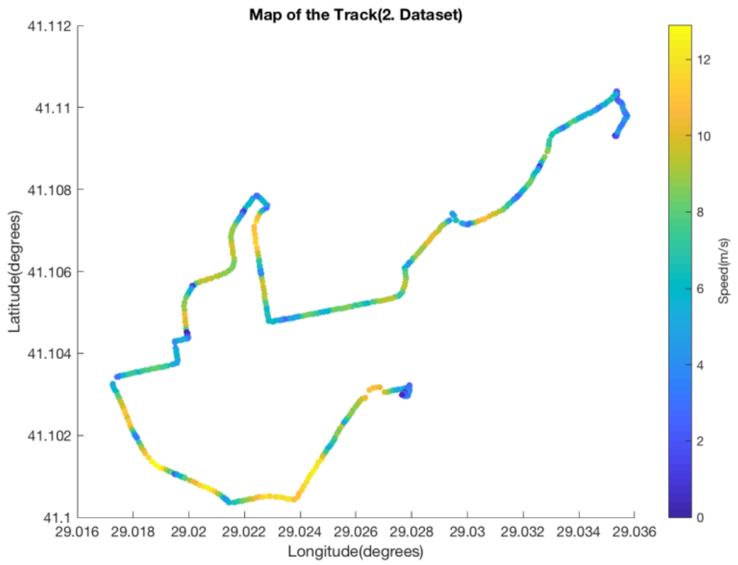

Figure 3.4.3: 2D Map of the Route

(End Point → Start Point)

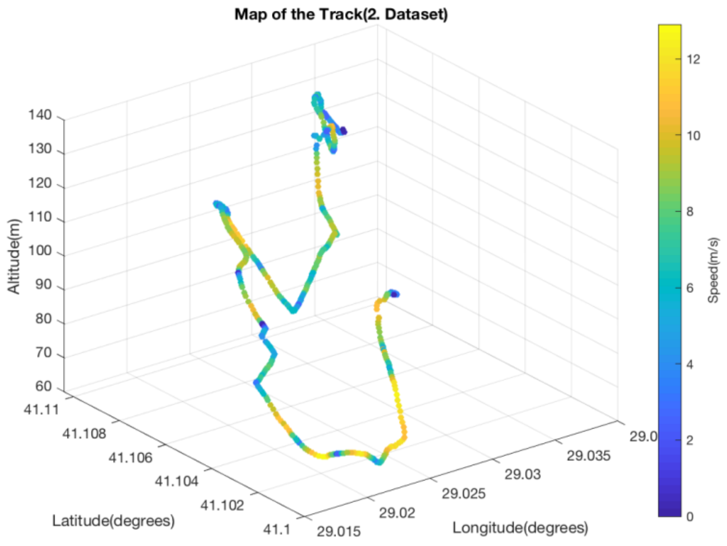

Figure 3.4.4: 3D Map of the Route

(Start Point → End Point)

3.5 Instant Specific Resistance Profile

Vehicles are subjected to some resistance forces as they move. The aerodynamic drag resistance, rolling resistance, grade resistance and inertial force to which the shuttle vehicle is subjected are calculated in accordance with the formulations specified, and other resistances are ignored as minor resistances. Since there is not enough information about the rotating mechanisms, inertia of rotating parts are not taken into account in the resistance calculations.

As in the other sections of the sixth and seventh data you can access instantaneous comparison charts from the Figure 3.5.1:

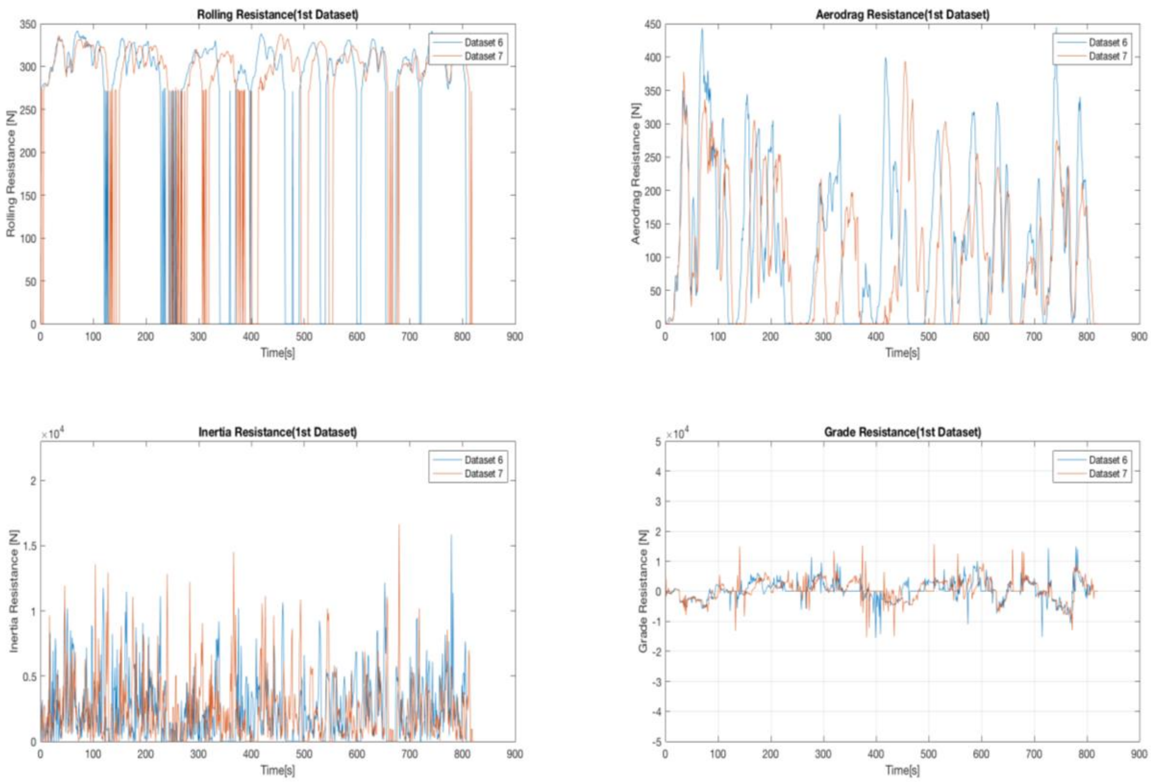

Figure 3.5.1: Instant Resistance Profile Comparison of First Route

(Gölet Dorm → Vadi Dorm)

Resistance values other than inertia forces are similar in different datasets. Sudden changes in acceleration have led to dissimilar situations in the inertia forces, but this has also revealed that different driving characteristics are applied. At this point, it can be seen that the mass-dependent resistances reach very high values. Resistance graphs of each dataset can be seen from Appendix C.

Maximum instant resistance values are shown in Table 3.8 and Table 3.9.

Table 3.8: Maximum Instant Resistances of First Route (Gölet Dorm. → Vadi Dorm.)

#	Max Rolling Resistance (N)	Max Aerodrag Resistance (N)	Max Grade Resistance (N)	Max Inertia Resistance (N)
1	340,42	428,4	14579	21000
2	334,43	358,4	15902	11480
3	336,31	379,65	16328	15008
4	340,48	429,14	15863	21056
5	340,42	428,4	16247	16576
6	341,75	444,81	14890	15848
7	337,52	393,68	15738	16632
8	404,13	459,22	15189	17094
9	334,07	354,35	15739	11144

Table 3.9: Maximum Instant Resistance of Turn Route (Vadi Dorm. → Gölet Dorm.)

#	Max Rolling Resistance (N)	Max Aerodrag Resistance (N)	Max Grade Resistance (N)	Max Inertia Resistance (N)
1	348,22	528,98	13605	25704
2	336,55	382,43	15991	21896
3	342,41	453,12	15291	12488
4	338,19	401,51	15234	20664
5	344,72	482,45	15601	18704
6	341,81	445,56	13794	15232
7	344.17	475,42	15510	18144
8	344,53	480,1	15130	21000
9	337,94	398,65	12409	16072

The highest values of the resistance forces other than inertia are generally at similar levels. The momentary large accelerations in inertia led to differences in maximum values.

Compared drag resistance vs time graph can be seen from the Figure 3.5.2 in first direction and Figure 3.5.3 in second direction.

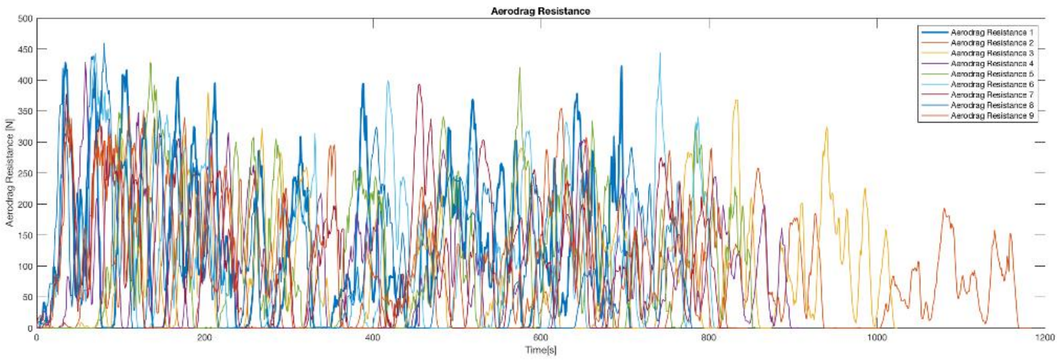

Figure 3.5.2: Drag Resistance Comparison of First Direction Measurement

(Start Point → End Point)

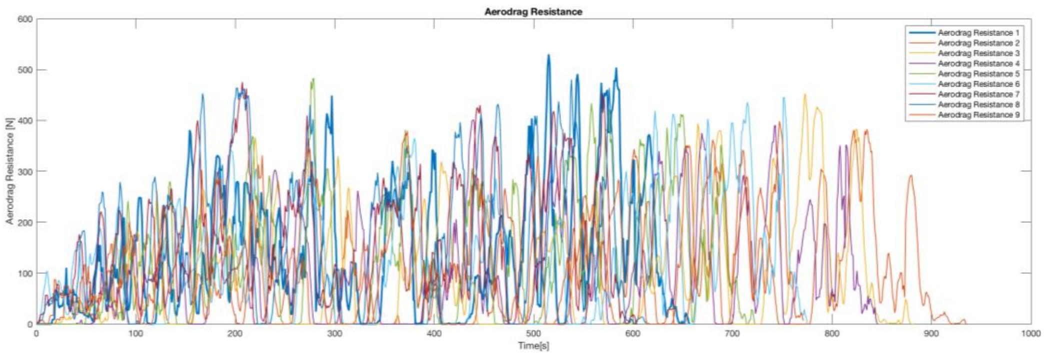

Figure 3.5.3: Drag Resistance Comparison of Second Direction Measurements

(End Point → Start Point)

Compared rolling resistance vs time graph can be seen from the Figure 3.5.4 in first direction and Figure 3.5.5 in second direction.

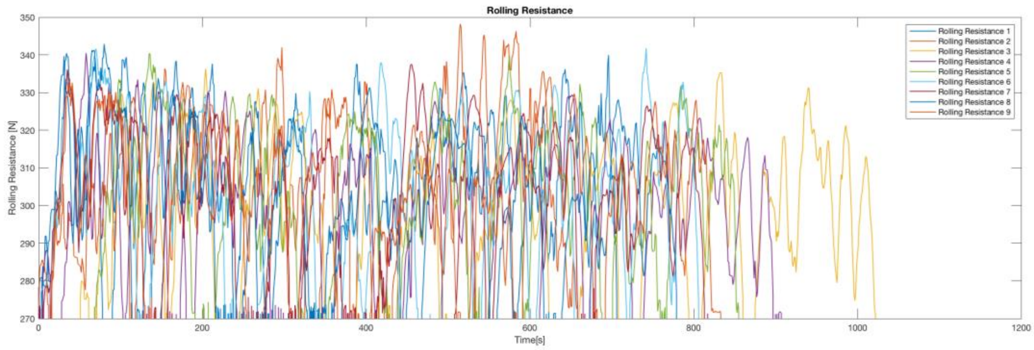

Figure 3.5.4: Rolling Resistance Comparison of First Direction Measurement

(Start Point → End Point)

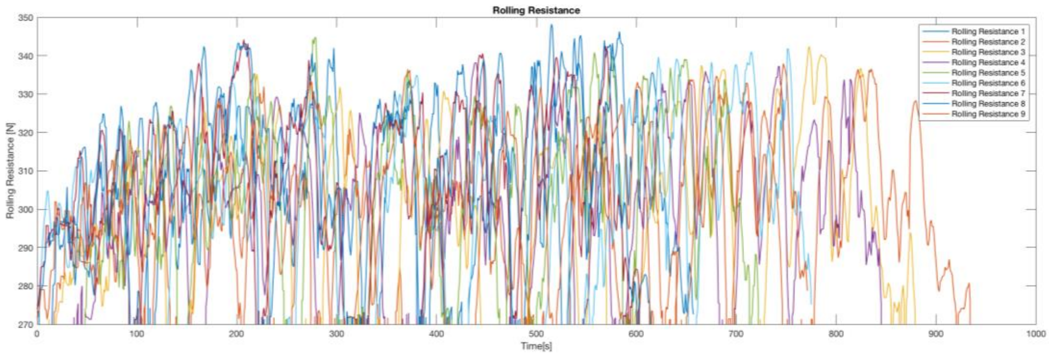

Figure 3.5.5: Rolling Resistance Comparison of Second Direction Measurements

(End Point → Start Point)

Compared grade resistance vs time graph can be seen from the Figure 3.5.6 in first direction and Figure 3.5.7 in second direction.

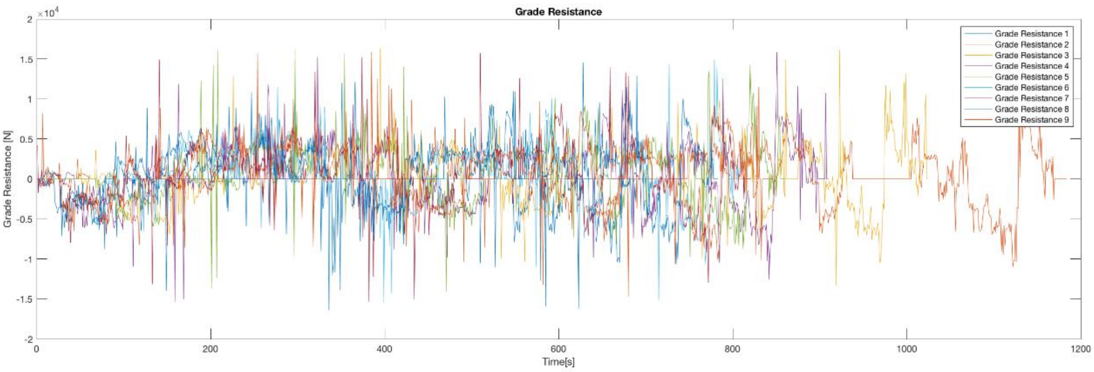

Figure 3.5.6: Grade Resistance Comparison of First Direction Measurement

(Start Point → End Point)

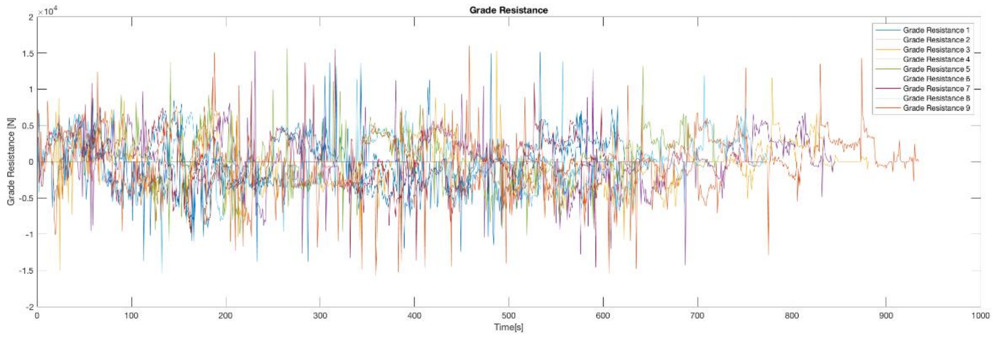

Figure 3.5.7: Grade Resistance Comparison of Second Direction Measurements

(End Point → Start Point)

Compared inertia vs time graph can be seen from the Figure 3.5.8 in first direction and Figure 3.5.9 in second direction.

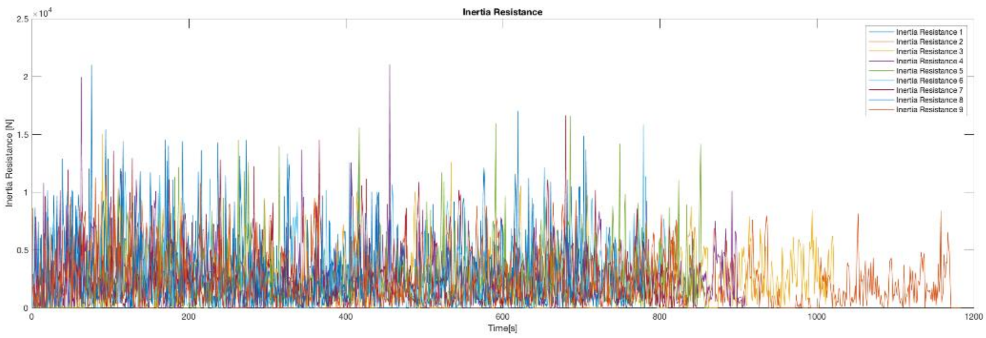

Figure 3.5.8: Inertia Comparison of First Direction Measurement

(Start Point → End Point)

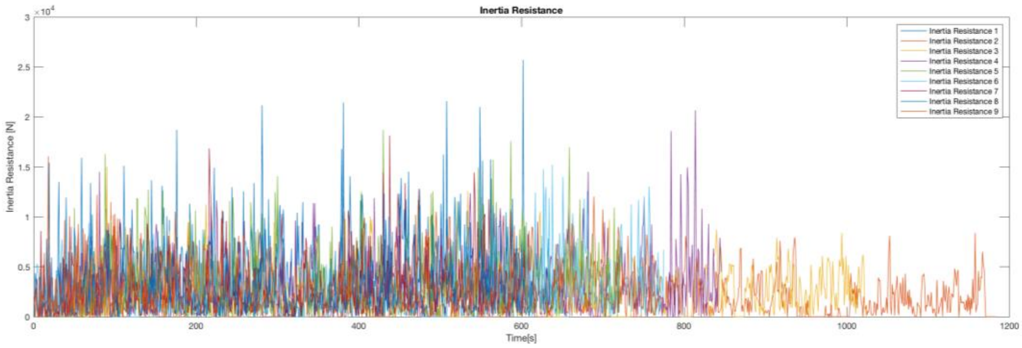

Figure 3.5.9: Inertia Comparison of Second Direction Measurements

(End Point → Start Point)

3.6 Instant Total Resistance Profile

If all the resistances are summed up momentarily, all forces applied to the vehicle at that moment will be seen. In fact, this force means the traction force of the vehicle. Total Resistance graphs of all datasets can be seen at the Appendix D.

If summation made for all dataset resistance forces, the total resistance force applied for each dataset can be calculated. Thus, the forces consumed for each dataset can be examined both in total and in terms of resistance forces.

Total resistance values are shown in Table 3.10 and Table 3.11.

Table 3.10: Total Resistance of First Route (Gölet Dorm. → Vadi Dorm.)

#	Total Rolling Resistance (N)	Total Aerodrag Resistance (N)	Total Grade Resistance (N)	Total Inertia Resistance (N)	Total Resistance (N)
1	200279	100145	101986	2236274	2638685
2	252096	79560	339244	2013847	2684477
3	226179	87788	370571	2165640	2850181
4	225718	87798	262082	2243365	2818680
5	211527	96539	305210	2097151	2710427
6	203817	98025	179917	2017797	2499285
7	212028	92358	347989	1951682	2604058
8	247275	95237	348819	2193337	2884347
9	217686	91726	178302	1936919	2424362

Table 3.11: Total Resistance of Turn Route (Vadi Dorm. → Gölet Dorm.)

#	Total Rolling Resistance (N)	Total Aerodrag Resistance (N)	Total Grade Resistance (N)	Total Inertia Resistance (N)	Total Resistance (N)
1	185190	92540	-141197	2300232	2436769
2	231045	78593	-249592	2240540	2300586
3	203530	88646	-98649	2078493	2272021
4	208185	83725	-113823	2360337	2538425
5	118801	92369	-25172	2226410	2480067
6	186723	90224	-167717	1939859	2048816
7	180048	96258	-48760	1845045	2072316
8	176530	100077	-105074	1990543	2162076
9	201579	86324	-134514	2047929	2201046

When the total resistance measurements are taken, the resistances that the vehicle uses the most force are seen as inertia and hill resistance due to the mass of the vehicle. This gives an advantage to the vehicle, as a more downhill route is followed. In addition, aerodynamic and friction resistances exert a very low amount of force compared to the total resistance.

3.7 Instant Power Demand Profile and Power Consumption

Total resistance and speed data can provide total power demand of the vehicle by using the Equation 2.10. Total Power graphics of every measurement can be seen from the Appendix E which will show instant power profile of every dataset. One of the most critical data that is obtained for this study is total power consumption. It can be reached from the following tables Table 3.12 and Table 3.13:

Table 3.12: Total Power Consumption of First Route (Gölet Dorm. → Vadi Dorm.)

#	Total Power Consumption(kWh)
1	4.53
2	3.35
3	3.70
4	3.74
5	3.90
6	3.80
7	3.40
8	4.09
9	3.63

Table 3.13: Total Power Consumption of Turn Route (Vadi Dorm. → Gölet Dorm.)

#	Total Power Consumption(kWh)
1	4.07
2	3.33
3	3.37
4	3.66
5	3.83
6	3.39
7	3.49
8	3.77
9	3.21

All the power the vehicle consumes on a route has been calculated and ranges from 3.21 kWh to 4.53 kWh. This is very dependent on the traffic conditions and driving characteristics of the vehicle. A vehicle that slows down and accelerates very quickly and frequently consumes more power. This can be confirmed by the previously calculated resistance and speed graphs.

3.8 Brake Force Profile

As it can be seen from the inertia forces, very high values of inertia force are applied in acceleration and deceleration stages of shuttle vehicles. At this point it is also very important to examine the braking forces. The braking forces applied in each measurement are evaluated in the case of inertia negative and the total braking force and maximum braking force with the timepoint in each measurement can be seen from the Table 3.14 and Table 3.15:

Table 3.14: Maximum and Total Brake Force of First Route (Gölet Dorm. → Vadi Dorm.)

#	Time(s)	Max Brake Force (N)	Total Brake Force (N)
1	76	21000	1117399
2	95	11479	1007853
3	212	11256	1082839
4	63	19938	1125971
5	686	16576	1051625
6	650	12152	1009980
7	366	14504	975865
8	170	17094	1097619
9	128	11144	969506

Table 3.15: Maximum and Total Brake Force of Turn Route (Vadi Dorm. → Gölet Dorm.)

#	Time(s)	Max Brake Force (N)	Total Brake Force (N)
1	602	25704	1149041
2	641	17304	1120286
3	794	12488	1039220
4	784	18592	1180168
5	587	17584	1113187
6	627	14784	968666
7	216	16851	924725
8	549	21000	995491
9	78	12208	1020476

In the measurements, it is seen that the braking force reaches very high values such as 21kN. Also, brake power can be calculated with the brake force and speed data. This is also calculated for each measurement and can be achieved from the Appendix F.

3.9 Power Consumption Charts

Through the resistance and power data obtained, power consumption percentages of every type of resistances along the route are calculated. Power consumption charts of every measurement can be seen from the Appendix G. Comparison of the power consumed for braking with respect to the other resistances and total power for this vehicle can be seen from the Figure 3.9.1 and Figure 3.9.2.

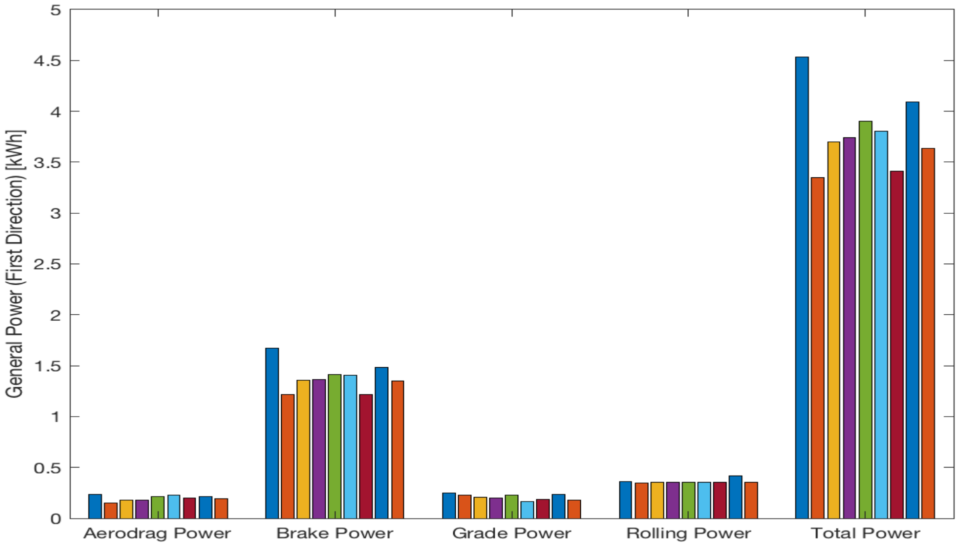

Figure 3.9.1: Power Consumption Chart (Gölet Dorm. → Vadi Dorm.)

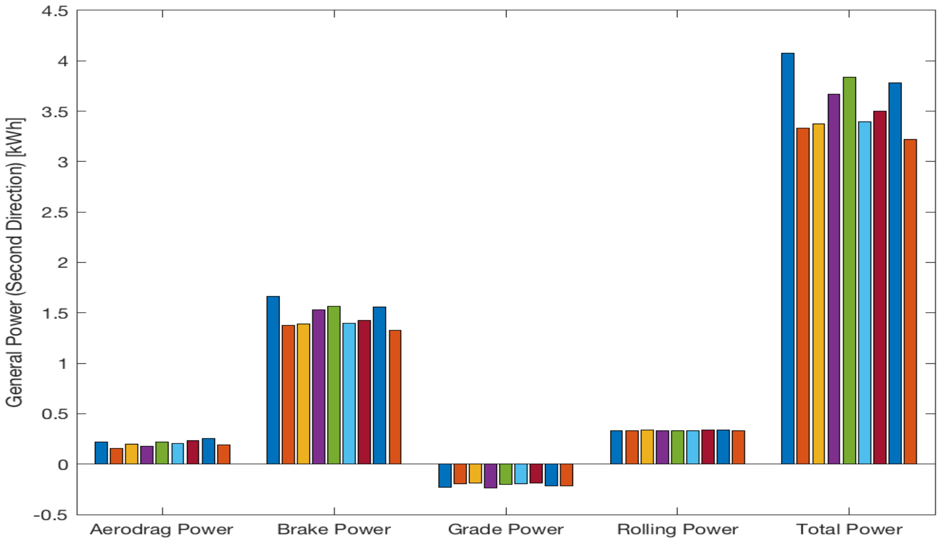

Figure 3.9.2: Power Consumption Chart (Vadi Dorm. → Gölet Dorm.)

When these graphs are analyzed, it is observed that a large part of the total spent power is spent on braking. Very high forces are stopped by friction when braking systems are used. This leads to very high energy loss. Recovering some of the energy lost here with a possible use of an electric vehicle would be efficient.

3.10 Regenerative Brake Graphs

Specific conditions of the regenerative braking is specified at the Section 2.2.8. During regeneration, electric motor could not provide more than the maximum motor power. In real conditions, electric motors that are used in electric vehicles can act like generator up to %40 of maximum traction power of the electric motor (Perotta, 2012). According to these assumptions, brake power calculations can be arranged and total amount of energy that can be recovered can be seen from the following Table 3.16.:

Table 3.16: Regenerative Brake Power Table

Dataset	Gölet Dorm→Vadi Dorm	Vadi Dorm → Gölet Dorm
1	1.31 kWh	1.09 kWh
2	1.11 kWh	1.28 kWh
3	1.28 kWh	1.27 kWh
4	1.24 kWh	1.29 kWh
5	1.31 kWh	1.20 kWh
6	1.17 kWh	1.17 kWh
7	1.09 kWh	1.15 kWh
8	1.08 kWh	1.26 kWh
9	1.26 kWh	1.24 kWh

Regenerative brake power map of every measurement can be seen from the Appendix H. It can be seen that despite the limitations of regenerative braking, a large part of the energy lost during braking can be recovered. This is also an amount that can provide great benefit to the range problem experienced in electric vehicles. Even on the worst drive route, it is seen that 65% of the power spent on the brake can be recovered as long as there is room in the battery.

4. CONCLUSION AND DISCUSSION

In this study, the power consumption of the shuttle service serving within the university campus and the electrification application is deeply analysed. Route, altitude and speed information were required before starting to study and these data was collected with the selected measurement device. Route information was collected and checked succesfully that there is no incosistent situation.

First significant data is the speed profile. Every measurement have different route times but in general speed profile of the measurement seems similar. Time difference is related with the crowd intensity of the school. Because it took different time in bus stop locations to hop on/off. There is also little difference on speed profile that can be realistic for different driver profiles.

After speed profile, acceleration profile was calculated. It is directly calculated from the average speed difference between data points, therefore it is consistent. Acceleration profile is too important to have braking period information of the route. Generally it has 0.3g in its peak points and it is suitable for fast stopping points.

Altitude profile is taken from Google service and it is too crucial for calculating the grade resistance of the shuttle bus. Taken data seems consistent in every measurement, time consumed on bus stops shows the difference in these graphics. It shows that 70m difference between lowest point and highest point of the route.

After picking up all the route information, Route was plotted and bus stop number was checked with the real scenario. Blue points shows us that there is 12 bus stops can be seen from the 2D and 3D maps of the route.

After the determination of the required coefficients, the forces applied on the vehicle were analyzed. Rolling Resistance, Grade Resistance, Aerodynamic Drag Resistance and Inertia Resistance were plotted. The differences between being a bus vehicle instead of a passenger vehicle were observed. Drag resistance and rolling resistance values have less effect than the other resistance. Because shuttle bus does not move on with high speeds. But grade and inertia forces are calculated too much because of their relation with the mass of the vehicle. Compared to each measurement, similar results were found. Only some of the grade resistance calculations have some differences between measurements because of the log frequency of the measurement device. If the vehicle drives too fast, device may miss some of the necessary informations between two data points.

When all effected forces are summed up, it shows the instant force applied on the vehicle. Same direction measurements have consistent graphics with a little differences. Negative results occurs on the braking process and downhill riding.

When the force values converted into the power, effect of the slope observed. Because, peak points are located in big altitude difference areas. This graphs also shows some of the measurements have measurement errors on few points that have meaningless peaks. But it can be ignored among so many data. It can be a checkpoint that instant power demand met by the internal combustion engine that used in the shuttle.

One of the most important measurements of the study is the power spent on the brake. Brake power profiles shows 2 important points on the analysis. These are driving characteristics and consumption of shuttle bus. Between these variable brake power graphs brake power demand varies between 30-60 kW instantly and it can be related with the sudden stop characteristics and mass of the vehicle. Sudden stops will be hard to regenerate because of its high power demand instantly, also it effects the passenger comfort inside of the shuttle. Slow decelerations on braking observed to be more convenient.

Bar charts show that the comparison of power consumption of each resistance type of the route. These charts shows that every route takes almost 4.5kWh in first direction and 3.5kWh in second direction which is consistent when we calculated the fuel consumption of the current shuttle bus. On second direction there is negative grade power consumption due to reaching low point from high point. These charts also shows the importance of the brake power consumptions. It is the second highest power consuming part of the route.

The last calculations are the regenerative braking calculations which revealed very important results for this study. It shows that sudden stops drops the efficiency of the regenerative braking. It also shows that low speed regenerative braking problems are not cause too much effect on the result. In the worst scenario, there can be %26 of the total power consumption can be regenerated under selected assumptions and in the best scenario, %33 of the total power consumption can be regenerated to the batteries. This can be examined from the Table 4.1 and Table 4.2:

Table 4.1: Power Analysis Table (Gölet Dorm. → Vadi Dorm.)

#	ICE Power Consumption (kWh)	Total Power Consumption (kWh)	Total Brake Power (kWh)	Available Regenerative Brake Power (kWh)	Brake Efficiency (%)	Total Efficiency (%)
1	16	4,53	1,67	1,31	78,44	28,92
2	16	3,35	1,21	1,11	91,74	33,13
3	16	3,7	1,35	1,28	94,81	34,59
4	16	3,74	1,36	1,24	91,18	33,16
5	16	3,9	1,41	1,31	92,91	33,59
6	16	3,8	1,4	1,17	83,57	30,79
7	16	3,4	1,21	1,09	90,08	32,06
8	16	4,09	1,47	1,08	73,47	26,41
9	16	3,63	1,34	1,26	94,03	34,71

Table 4.2: Power Analysis Table (Vadi Dorm. → Gölet Dorm.)

#	ICE Power Consumption (kWh)	Total Power Consumption (kWh)	Total Brake Power (kWh)	Available Regenerative Brake Power (kWh)	Brake Efficiency (%)	Total Efficiency (%)
1	16	4,07	1,67	1,09	65,27	26,78
2	16	3,33	1,38	1,28	92,75	38,44
3	16	3,37	1,39	1,27	91,37	37,69
4	16	3,66	1,53	1,29	84,31	35,25
5	16	3,83	1,56	1,2	76,92	31,33
6	16	3,39	1,4	1,17	83,57	34,51
7	16	3,49	1,43	1,15	80,42	32,95
8	16	3,77	1,56	1,26	80,77	33,42
9	16	3,21	1,32	1,24	93,94	38,63

These measurements and study shows that a bus that can be used for short distances can be very suitable for the electrification. On the route of this study is very appropriate for electric bus because of its high rate of regeneration. Shuttle route can be completed too many times in 1 day and if there is a possibility of charging at the last stops, there will be no problems. Large amounts of regenerative braking that is calculated on this study will increase the efficiency of this route. The electrification of on-campus services will also benefit the reduction of air pollution on-campus and will lead to more comfortable breathing.

REFERENCES

Arat, M., Duringhof, H., Hagnander, J., and L. Simoes, E., (2017) "Use of Electric Driveline for a Cooperative Braking Strategy," SAE Int. J. Passeng. Cars – Electron. Electr. Syst. 10(2):2017

Cikanek, S.R. & Bailey, K.E.. (2002). Regenerative braking system for a Hybrid Electric Vehicle. Proceedings of the American Control Conference. 4. 3129 - 3134 vol.4. 10.1109/ACC.2002.1025270.

Deborah Perrotta[a],(2012). On the potential of regenerative braking of electric buses as a function of their itinerary, 15th meeting of the EURO Working Group on Transportation

He, R., Zheng, H., and Zong, C., (2014) "Braking Force Distribution and Coordinated Control Algorithm for Hybrid Electric Bus based on EBS," SAE Technical Paper

Perrotta, D., Teixeira, A., Silva, H., Ribeiro, B. (2012), "Electrical Bus Performance Modeling for Urban Environments," SAE Int. J. Alt. Power. 1(1)

Premvaranon, P., Soparat, J., Teralapsuwan, A., Sritham, W. (2015), "A Feasibility Study on Effect of Battery and Driving Conditions on Performance of an Electric Bus," SAE Technical Paper

Ruan, J. and Walker, P., (2014) "An Optimal Regenerative Braking Energy Recovery System for Two-Speed Dual Clutch Transmission-Based Electric Vehicles," SAE Technical Paper

Sangtarash, Farhad & Esfahanian, Vahid & Nehzati, Hassan & Haddadi, Samaneh & Amiri Bavanpour, Meisam & Haghpanah, Babak. (2008). Effect of Different Regenerative Braking Strategies on Braking Performance and Fuel Economy in a Hybrid Electric Bus Employing CRUISE Vehicle Simulation. SAE International Journal of Fuels and Lubricants.

J. J. Chen, et al., "Design of Hybrid Electric Bus on Regenerative Braking System", Applied Mechanics and Materials, Vols. 300-301, pp. 333-337, 2013

Ehsani M., Gao Y., Emadi A. (2010). *Modern Electric, Hybrid Electric, and Fuel Cell Vehicles Fundamentals, Theory and Design*. Boca Raton, FL.: CRC Press – Taylor & Francis Group.

Ehsani M., Miller J.M., Emadi A. (2004). *Vehicular Electric Power Systems Land, Sea, Air, and Space Vehicles*. Marcel Dekker, Inc

Husain I., (2005). *Electric and Hybrid Vehicles Design Fundamentals.* CRC Press – Taylor & Francis Group.

Larminie J., Lowry J., (2012). *Electric Vehicle Technology Explained Second Edition,* John Wiley & Sons Ltd.

Gillespie, T., (1992) *"Fundamentals of Vehicle Dynamics"*, SAE Publishers. Warmedale, PA.

Wong, J. Y. (Jo Yung), (2001), *Theory of ground vehicles - 3rd ed,* John Wiley & Sons Ltd.

Url-1<https://www.mathworks.com/hardware-support/iphone-sensor.html>, Date retrieved 23.03.2019

Url-2<https://developers.google.com/maps/documentation/elevation/intro>, Date retrieved 18.02.2019

Url-3 <https://www.isuzu.com.tr/tr/otobus/novo-citi/>, Date retrieved 13.01.2019

Url-4<https://electrek.co/2018/04/24/regenerative-braking-how-it-works/>, Date retrieved 22.10.2018

Url-5<https://learn.adafruit.com/all-about-batteries/power-capacity-and-power-capability>, Date retrieved 04.04.2019

APPENDICES

APPENDIX A: Speed Profiles of the Collected Dataset
APPENDIX B: Acceleration Profiles of the Collected Dataset
APPENDIX C: Resistance Maps of the Collected Dataset
APPENDIX D: Total Resistance Profile of the Collected Dataset
APPENDIX E: Total Power Map of the Collected Dataset
APPENDIX F: Brake Power Map of the Collected Dataset
APPENDIX G: Power Consumption Chart of Collected Dataset
APPENDIX H: Regenerative Brake Power Map of Collected Dataset

APPENDIX A

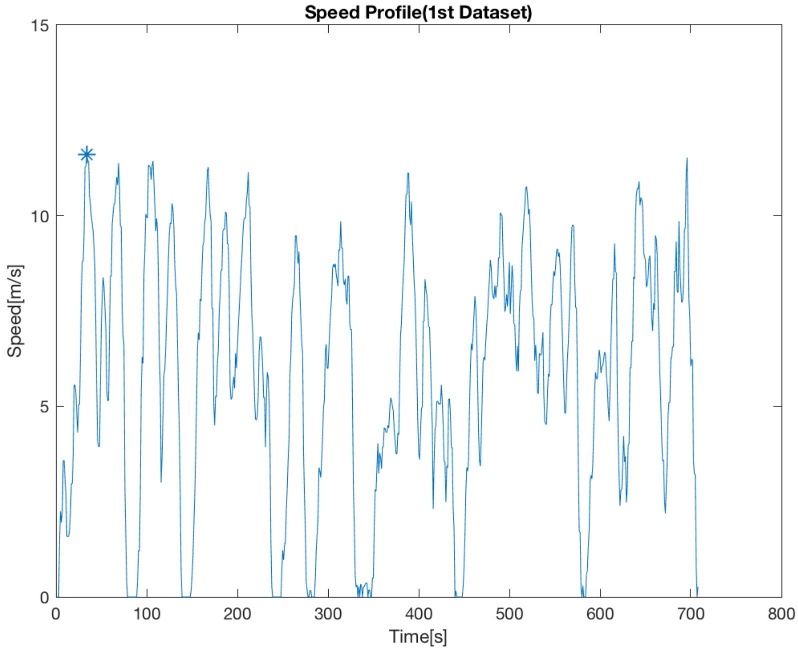

Figure A.1 : Speed Profile of 1.Measurement (1.(Start point → End point))

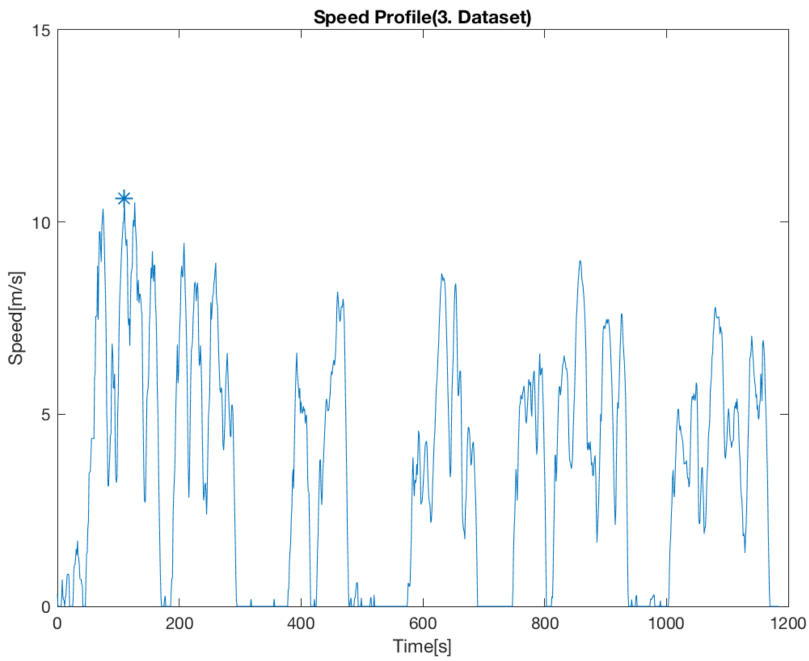

Figure A.2 : Speed Profile of 3.Measurement (2. (Start point → End point))

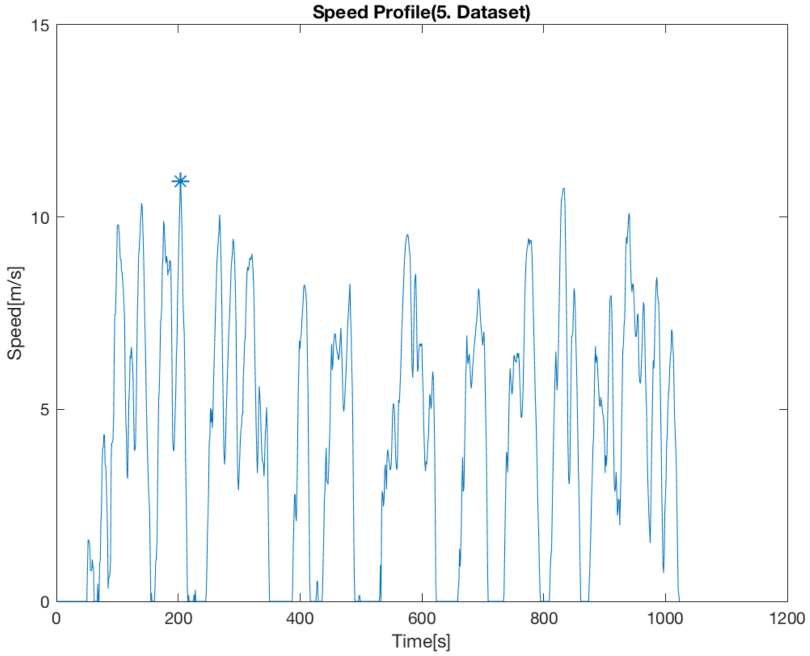

Figure A.3 : Speed Profile of 5.Measurement (3.(Start point → End point))

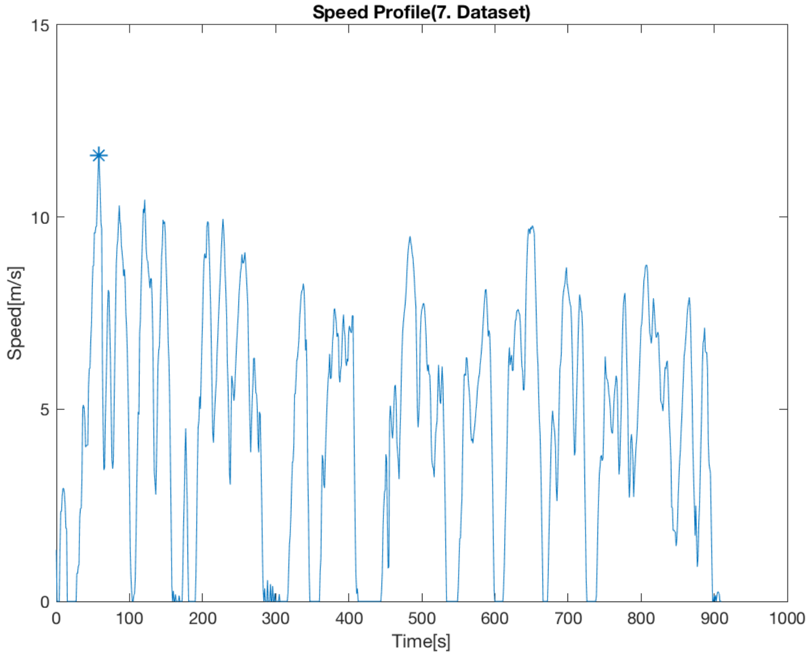

Figure A.4 : Speed Profile of 7.Measurement (4. (Start point → End point))

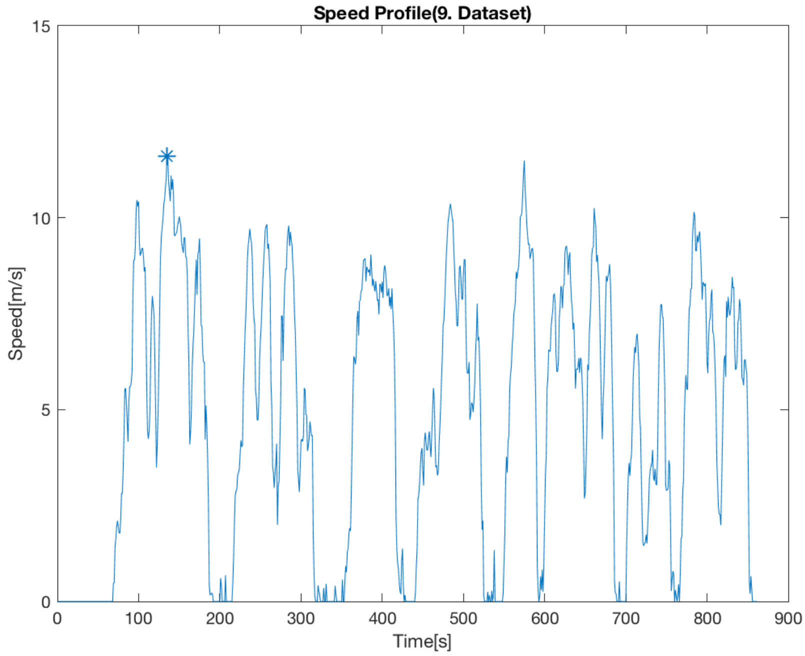

Figure A.5 : Speed Profile of 9.Measurement (5.(Start point → End point))

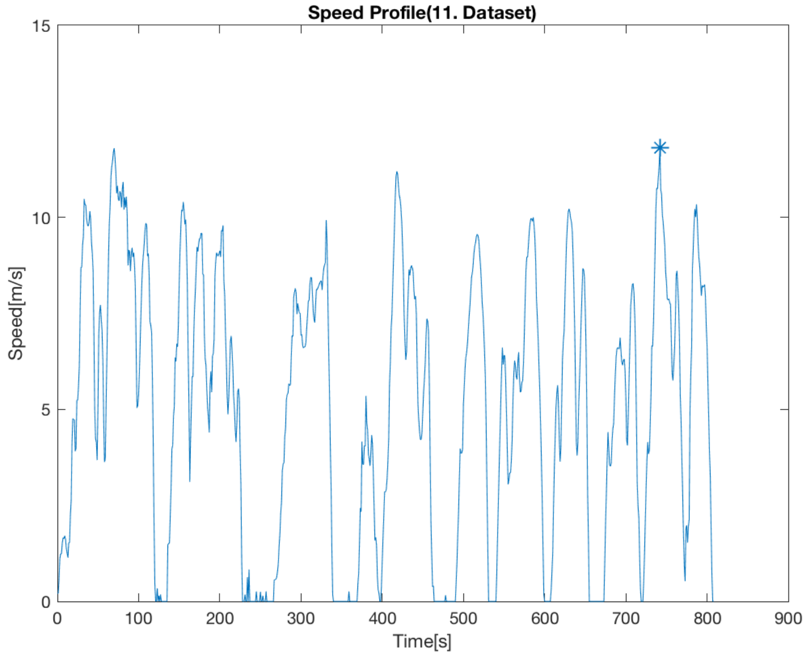

Figure A.6 : Speed Profile of 11.Measurement (6. (Start point → End point))

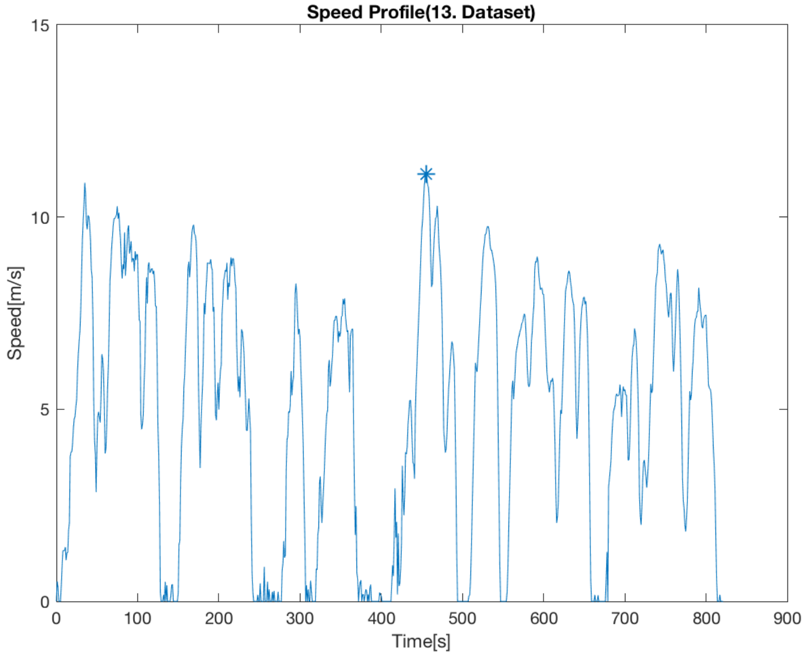

Figure A.7 : Speed Profile of 13.Measurement (7.(Start point → End point))

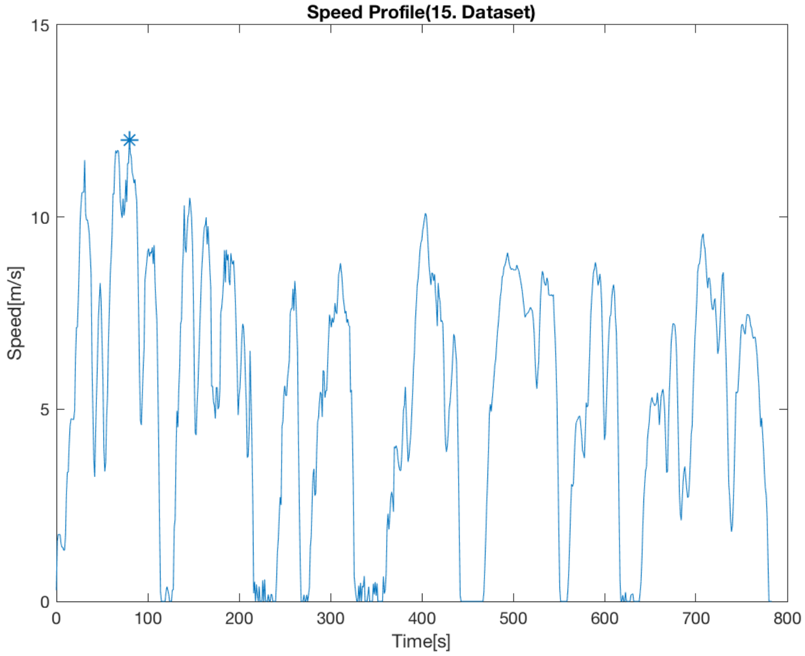

Figure A.8 : Speed Profile of 15.Measurement (8. (Start point → End point))

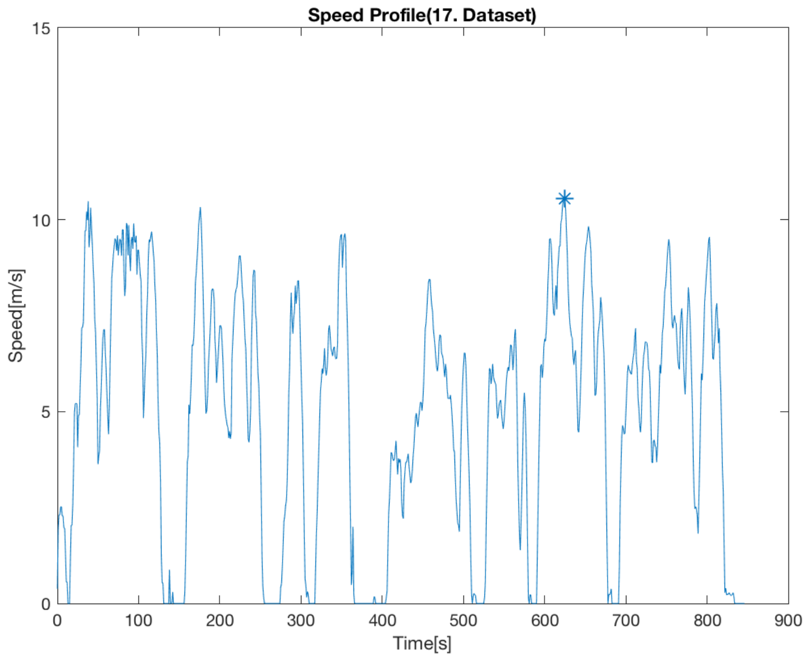

Figure A.9 : Speed Profile of 17.Measurement (9.(Start point End point))

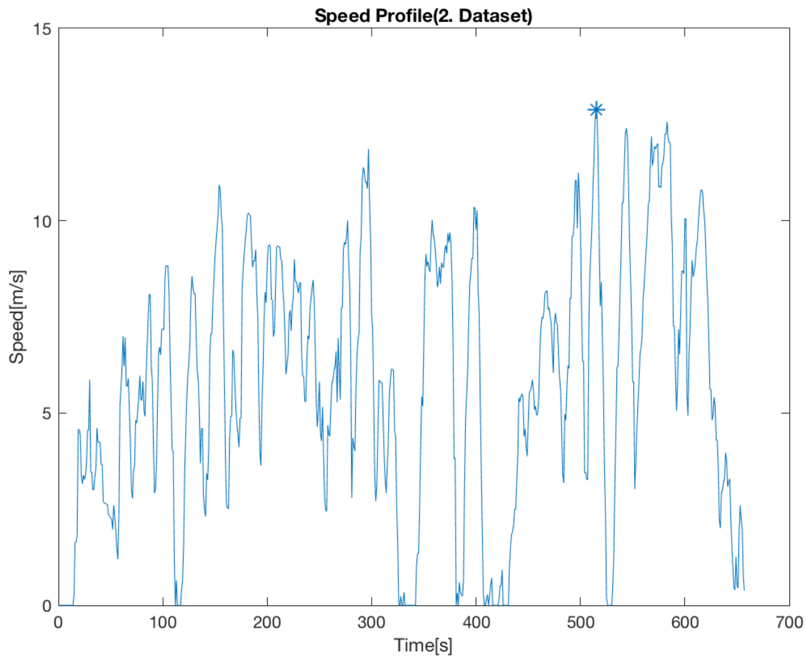

Figure A.10 : Speed Profile of 2.Measurement (1.(End point→ Start point))

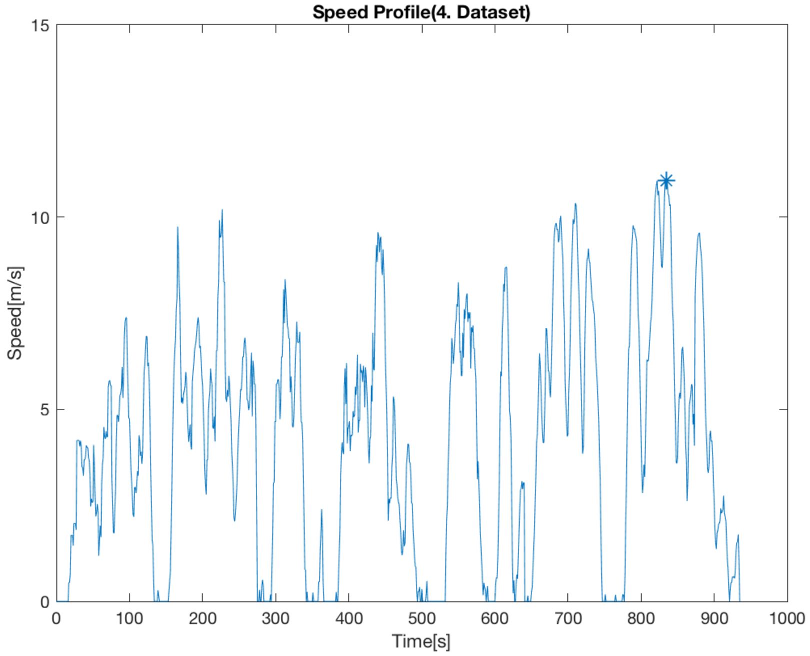

Figure A.11 : Speed Profile of 4.Measurement (2.(End point□ Start point))

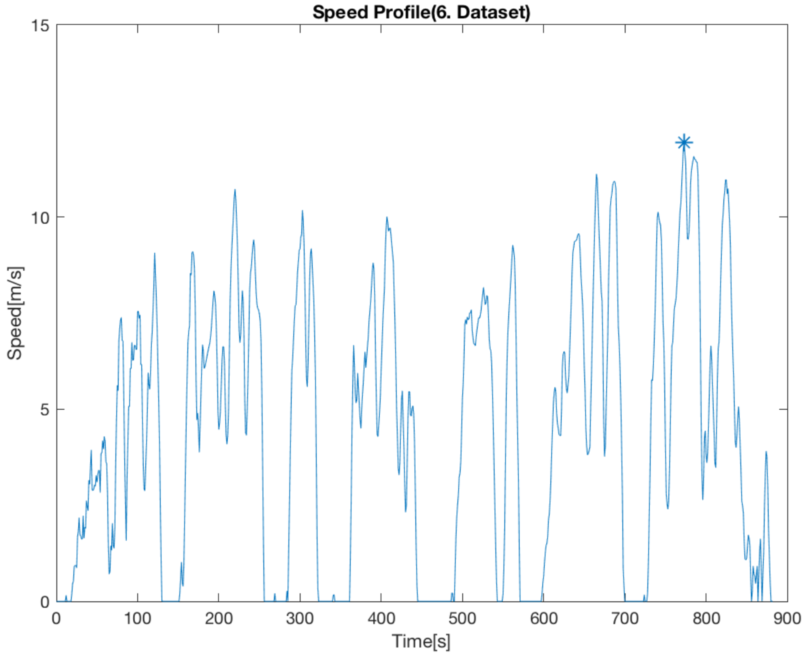

Figure A.12 : Speed Profile of 6.Measurement (3.(End point→ Start point))

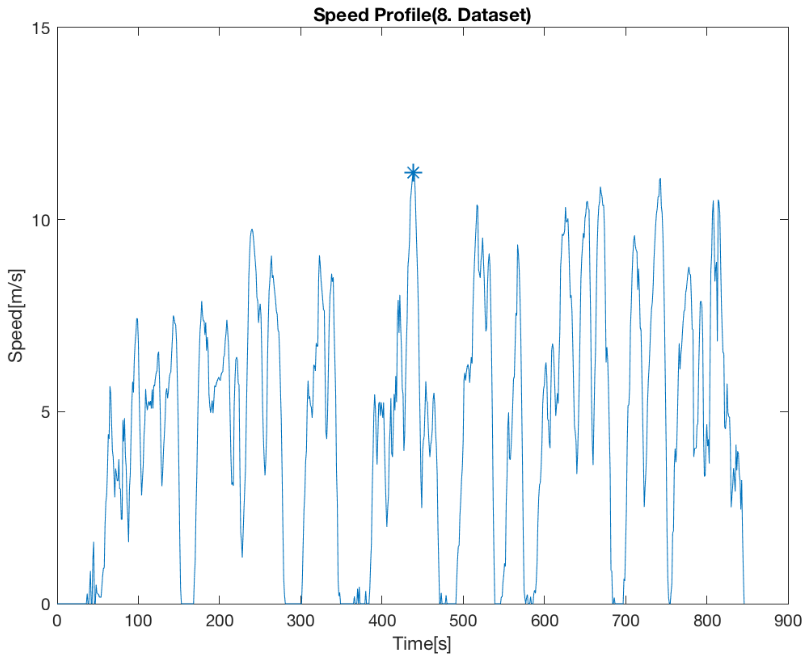

Figure A.13 : Speed Profile of 8.Measurement (4.(End point→ Start point))

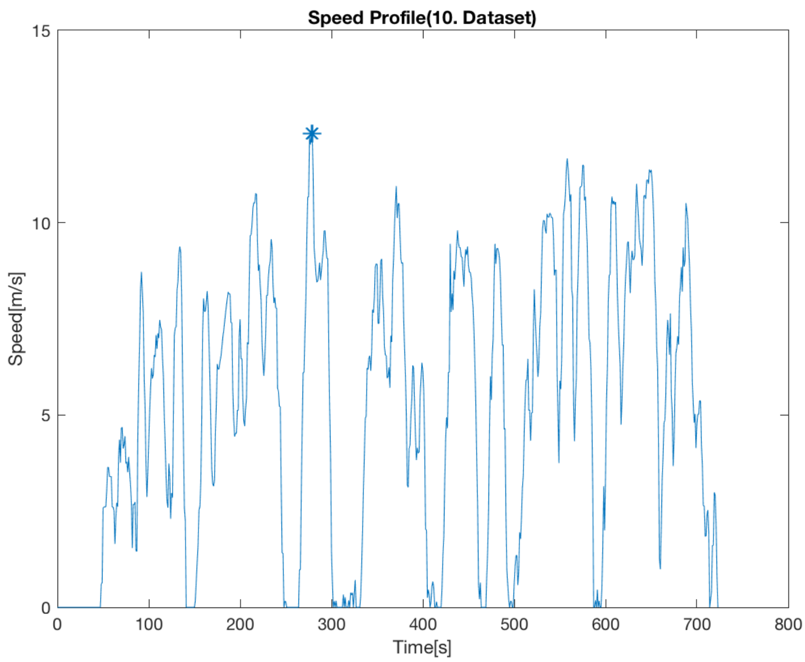

Figure A.14 : Speed Profile of 10.Measurement (5.(End point→ Start point))

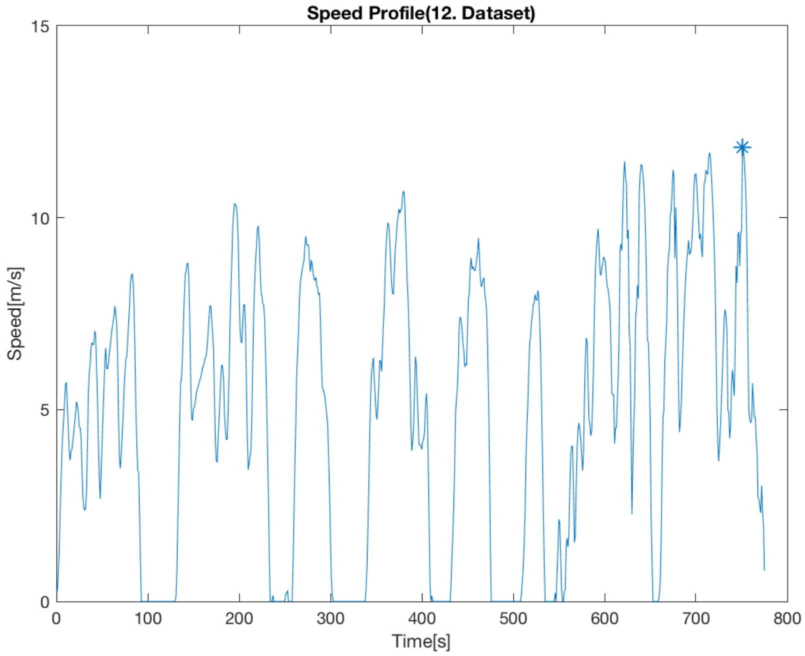

Figure A.15 : Speed Profile of 12.Measurement (6.(End point→ Start point))

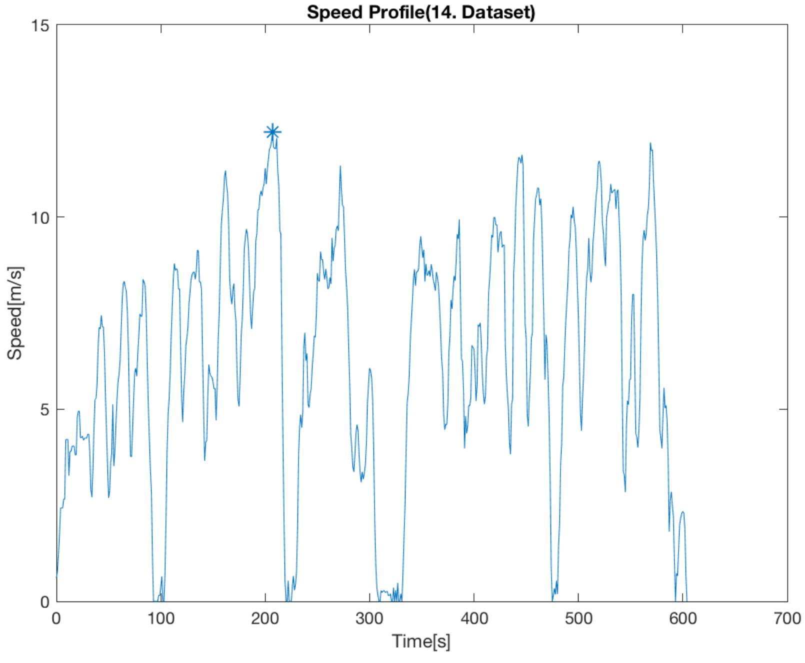

Figure A.16 : Speed Profile of 14.Measurement (7.(End point→ Start point))

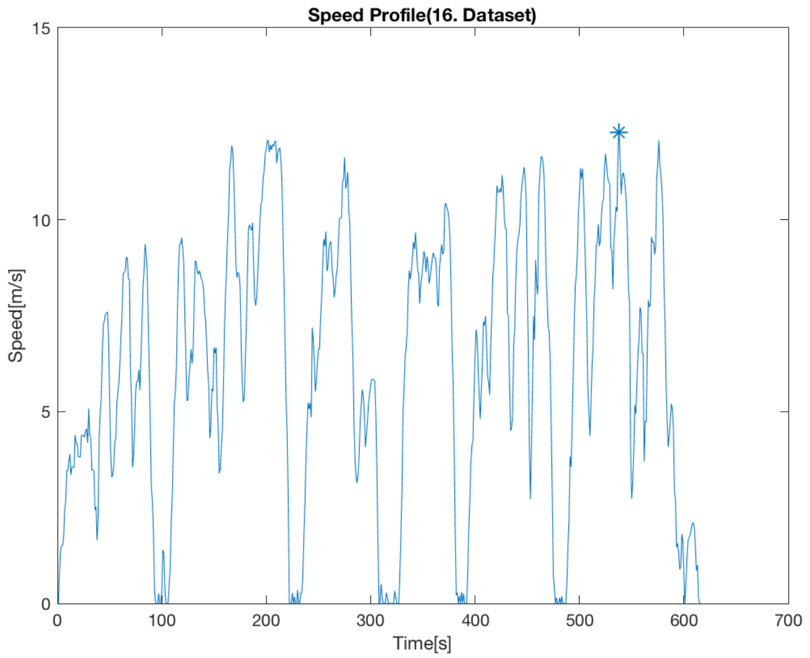

Figure A.17 : Speed Profile of 16.Measurement (8.(End point→ Start point))

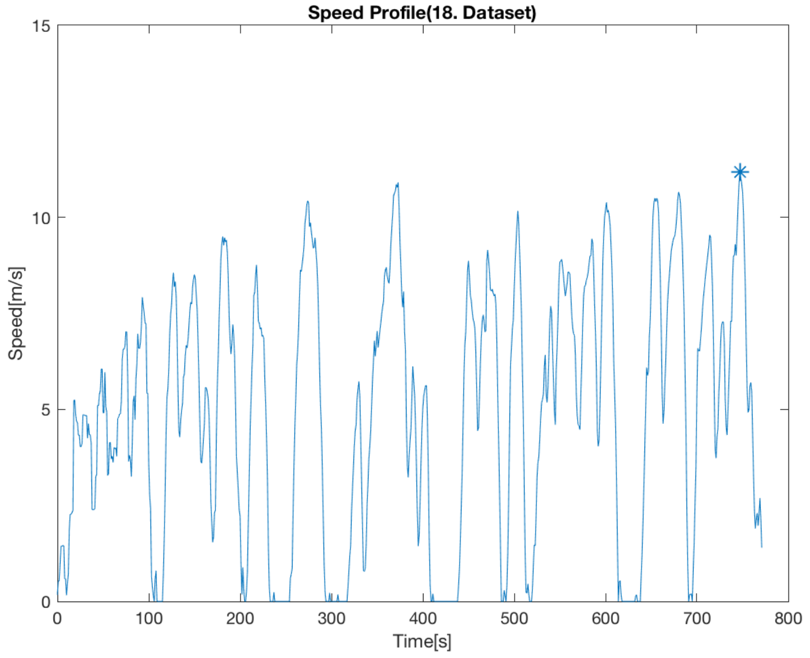

Figure A.18 : Speed Profile of 18.Measurement (9.(End point→ Start point))

APPENDIX B

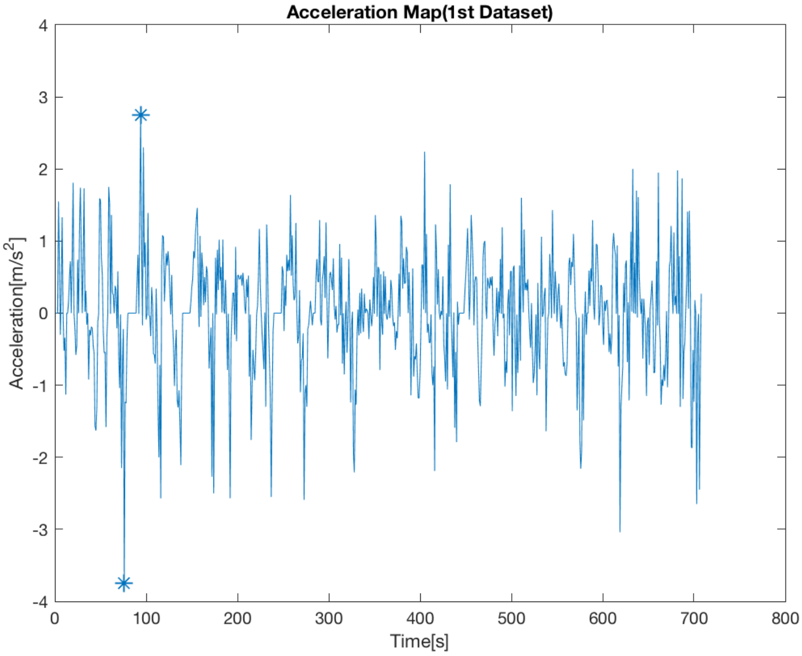

Figure B.1 : Acceleration Profile of 1.Measurement (1.(Start point → End point))

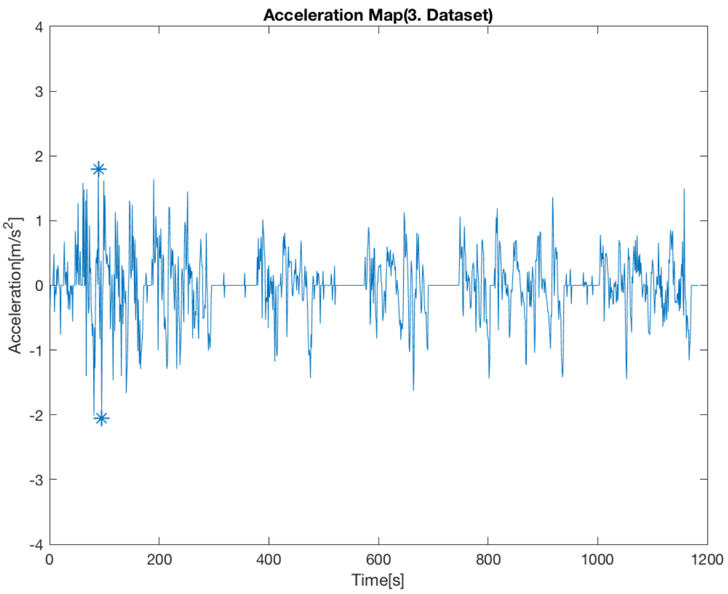

Figure B.2 : Acceleration Profile of 3.Measurement (2. (Start point → End point))

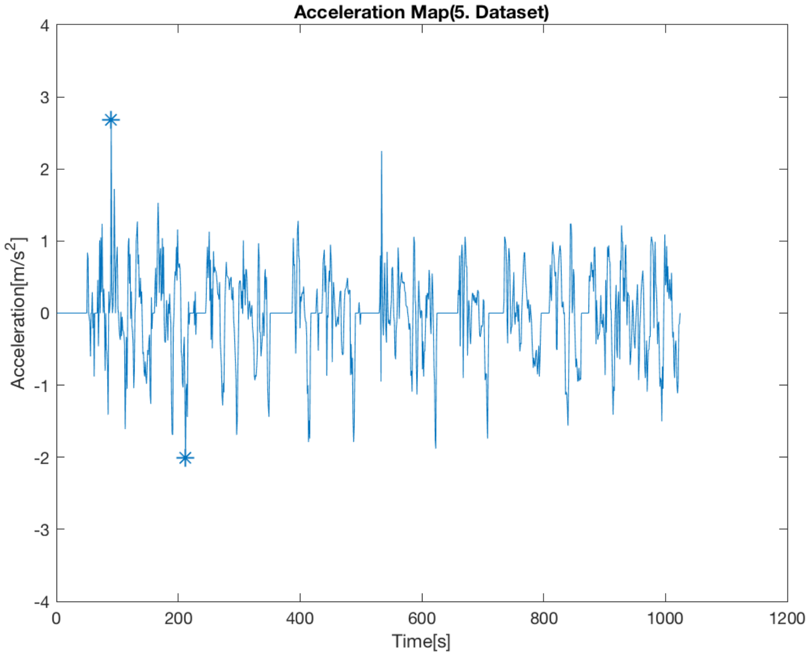

Figure B.3 : Acceleration Profile of 5.Measurement (3.(Start point → End point))

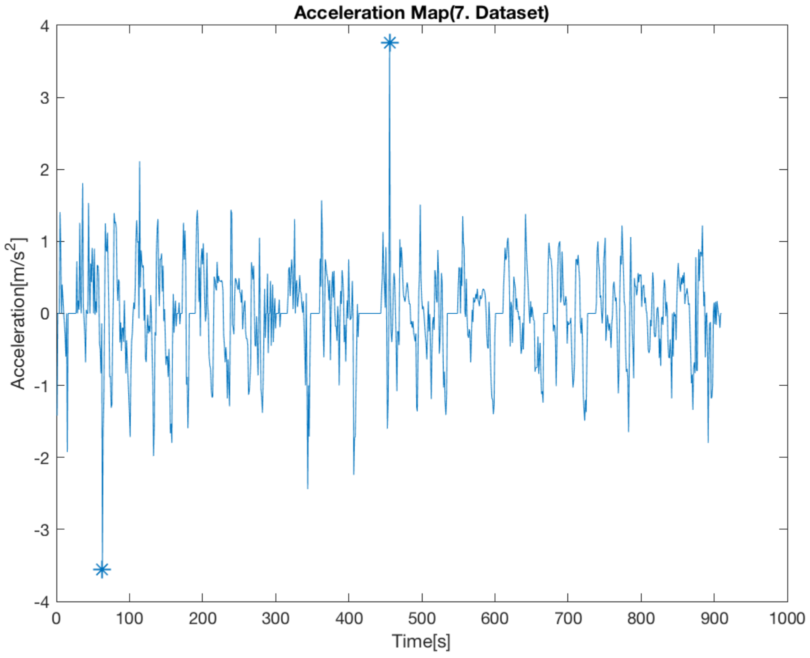

Figure B.4 : Acceleration Profile of 7.Measurement (4. (Start point → End point))

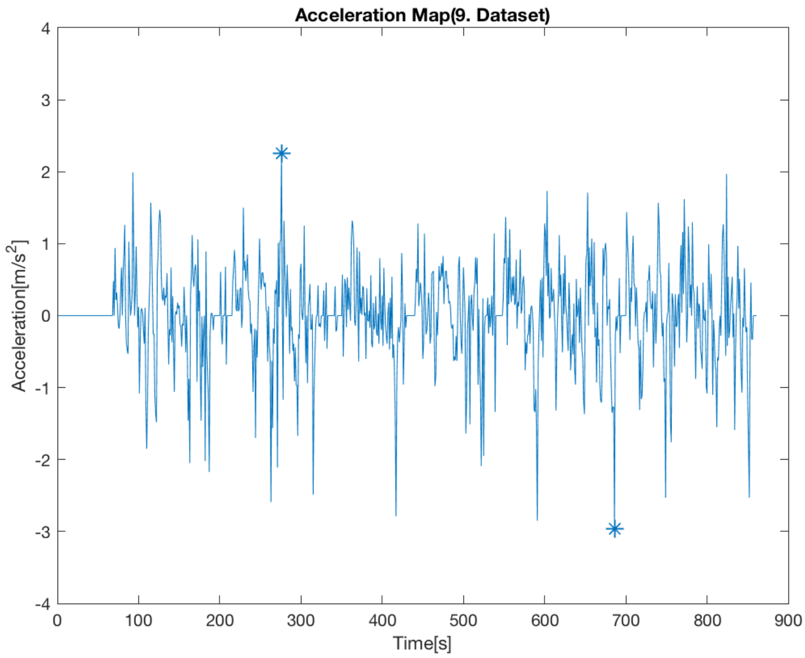

Figure B.5 : Acceleration Profile of 9.Measurement (5.(Start point → End point))

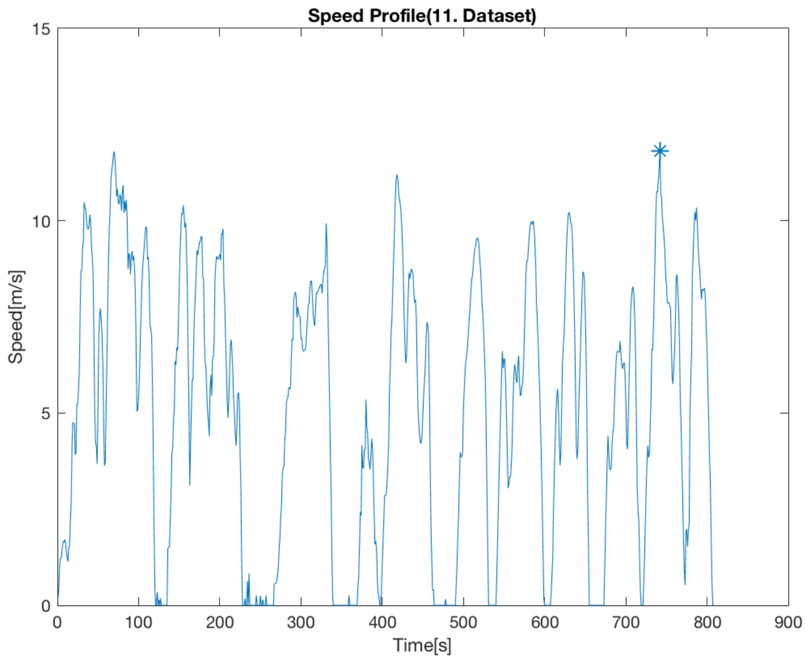

Figure B.6 : Acceleration Profile of 11.Measurement (6. (Start point → End point))

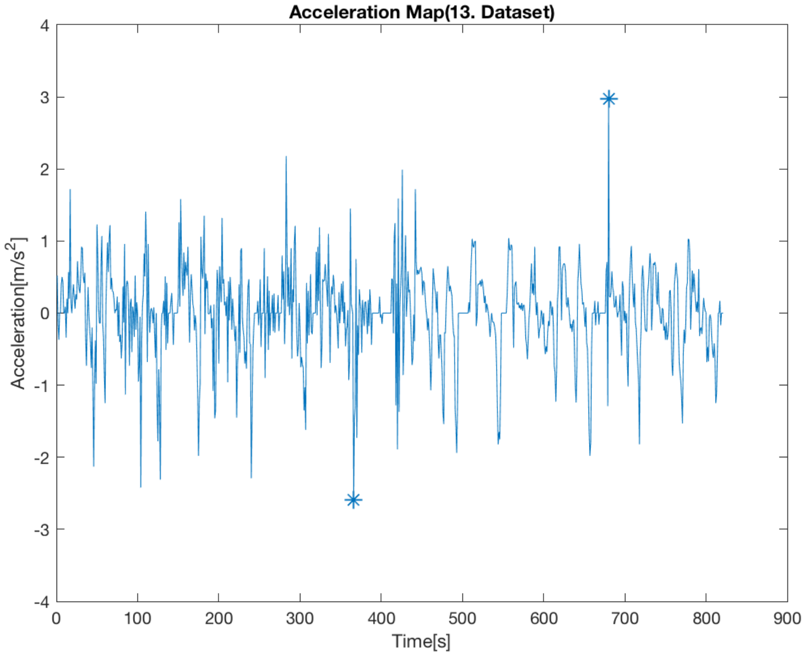

Figure B.7 : Acceleration Profile of 13.Measurement (7.(Start point → End point))

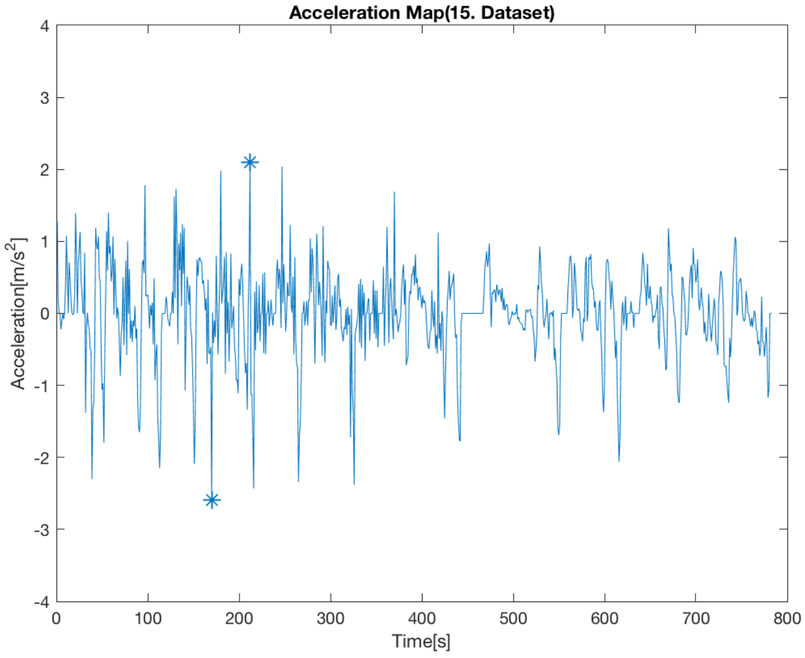

Figure B.8 : Acceleration Profile of 15.Measurement (8. (Start point → End point))

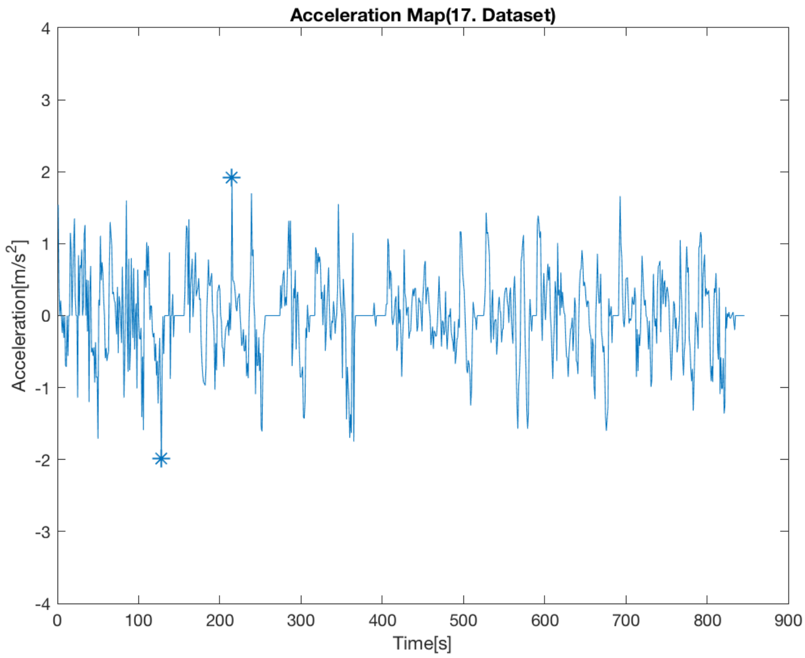

Figure B.9 : Acceleration Profile of 17.Measurement (9.(Start point → End point))

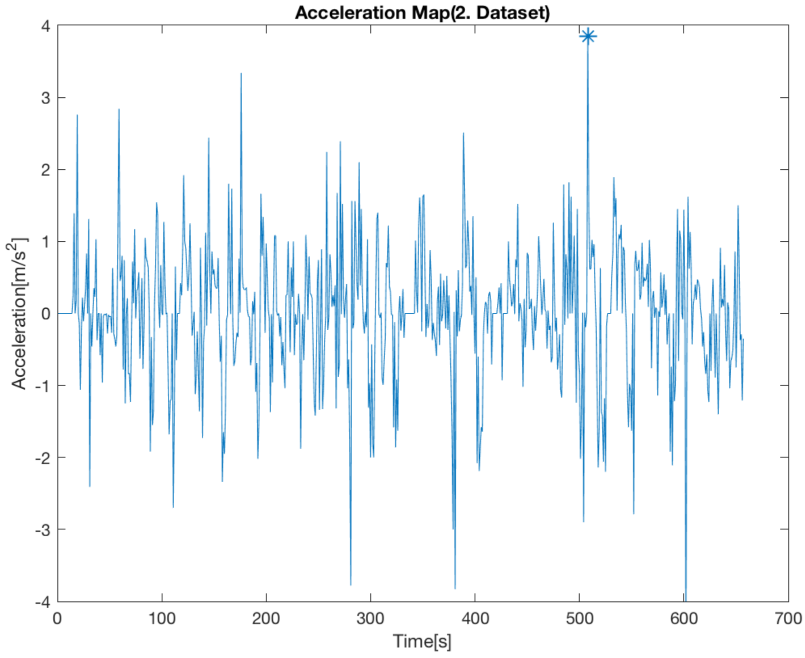

Figure B.10 : Acceleration Profile of 2.Measurement (1.(End point→ Start point))

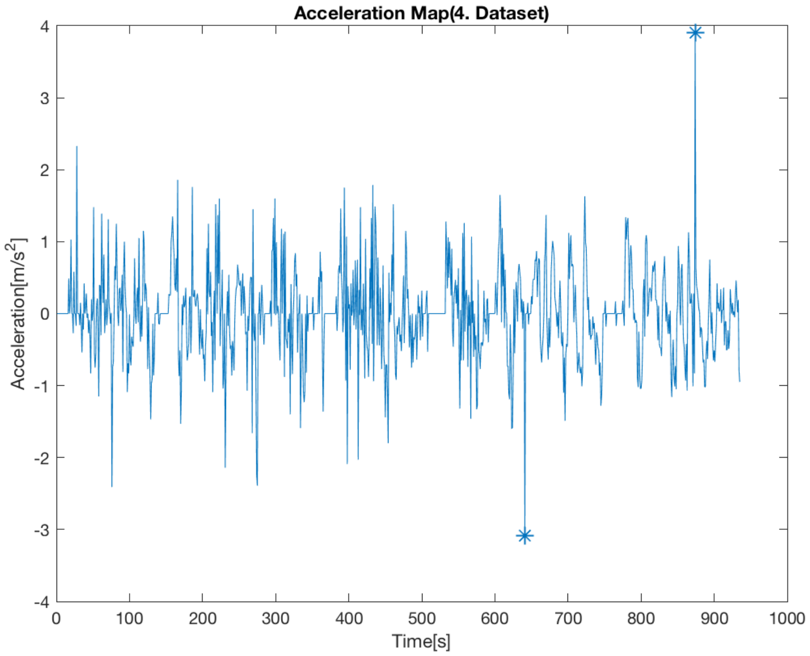

Figure B.11 : Acceleration Profile of 4.Measurement (2.(End point→ Start point))

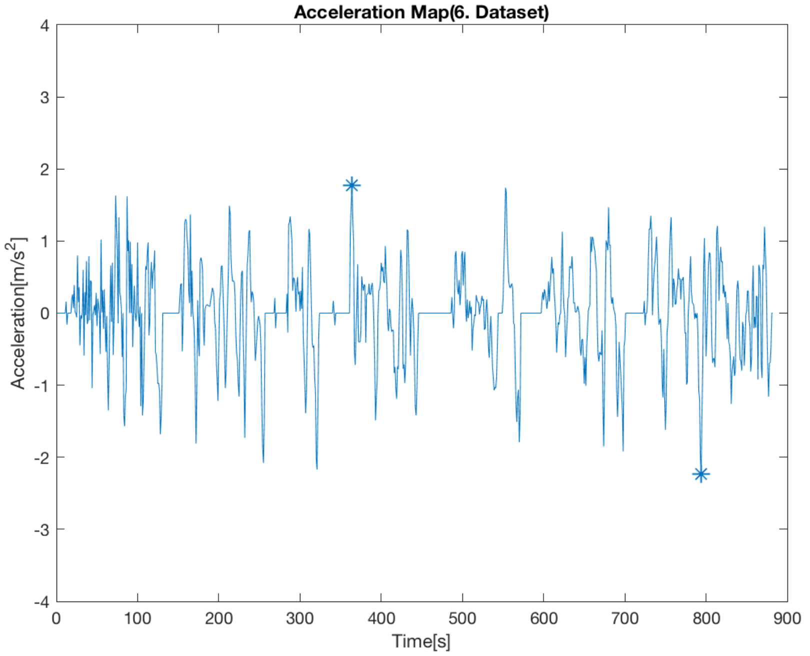

Figure B.12 : Acceleration Profile of 6.Measurement (3.(End point→ Start point))

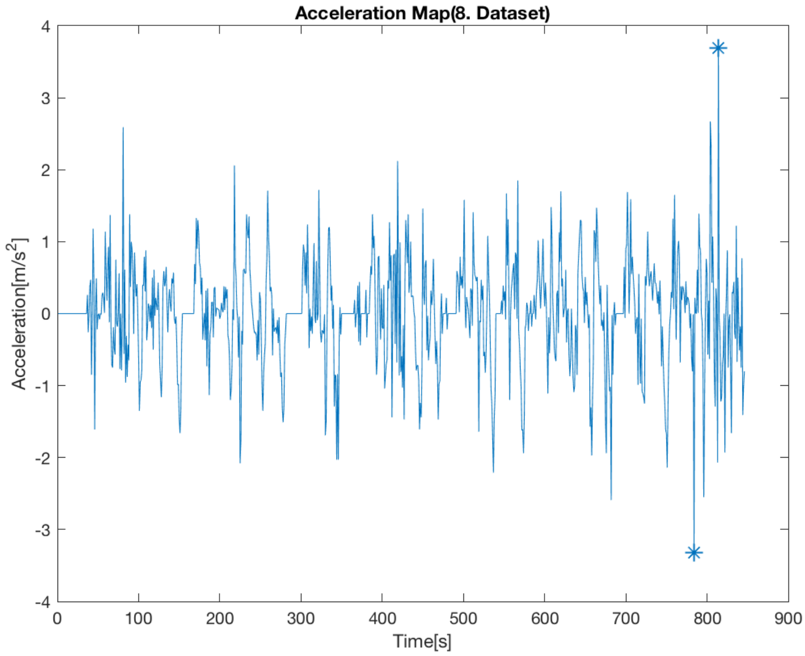

Figure B.13 : Acceleration Profile of 8.Measurement (4.(End point→ Start point))

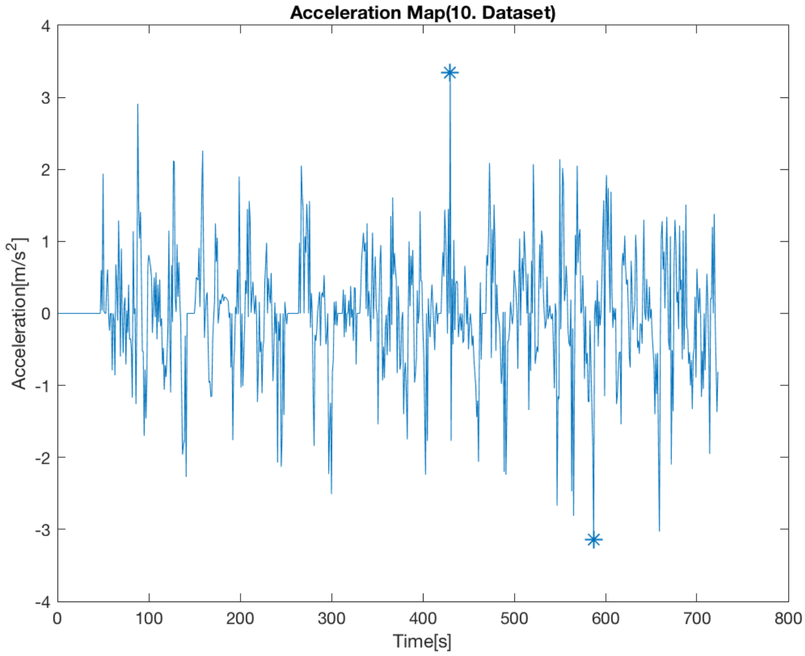

Figure B.14 : Acceleration Profile of 10.Measurement (5.(End point→ Start point))

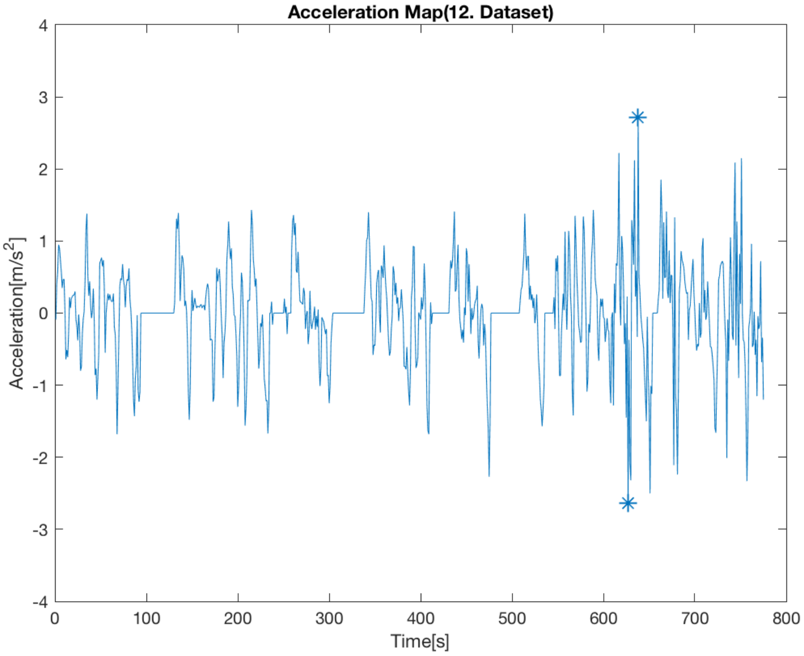

Figure B.15 : Acceleration Profile of 12.Measurement (6.(End point→ Start point))

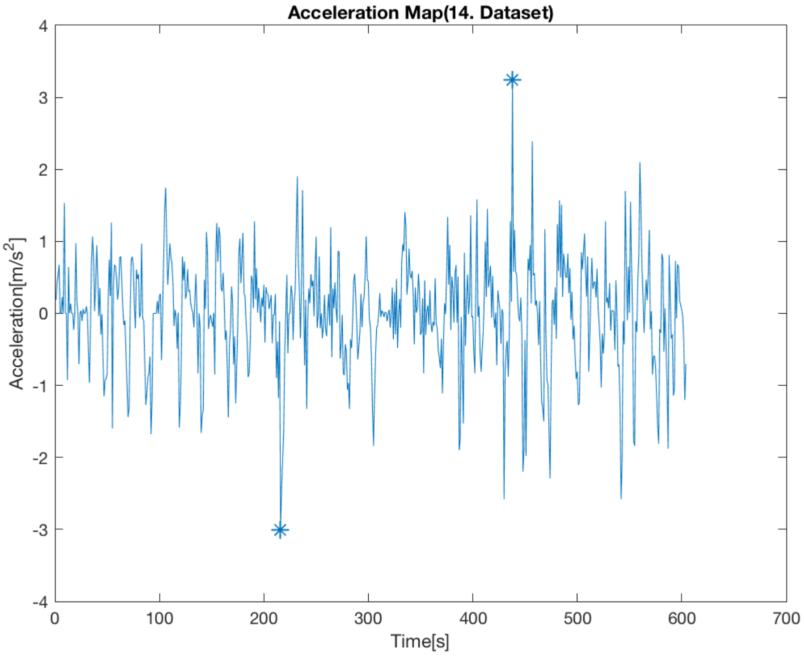

Figure B.16 : Acceleration Profile of 14.Measurement (7.(End point→ Start point))

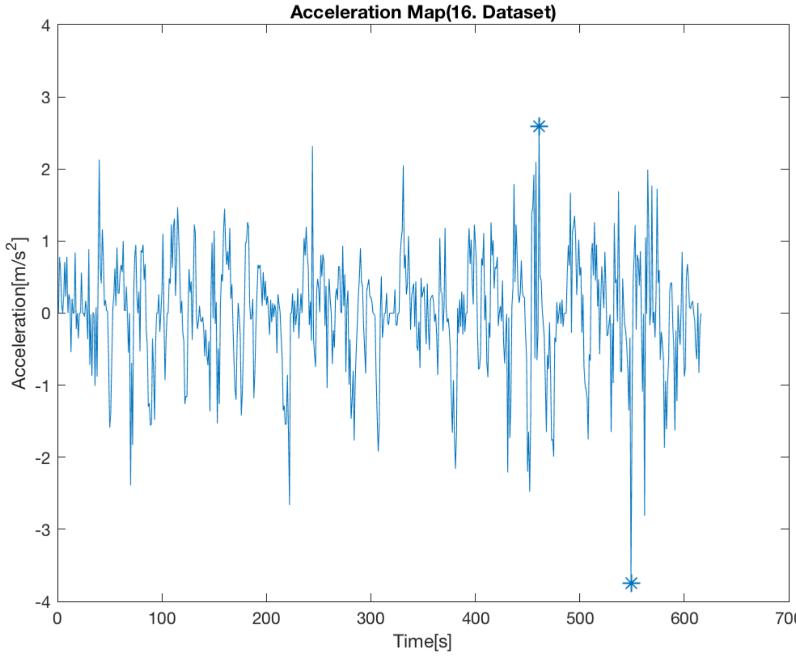

Figure B.17 : Acceleration Profile of 16.Measurement (8.(End point→ Start point))

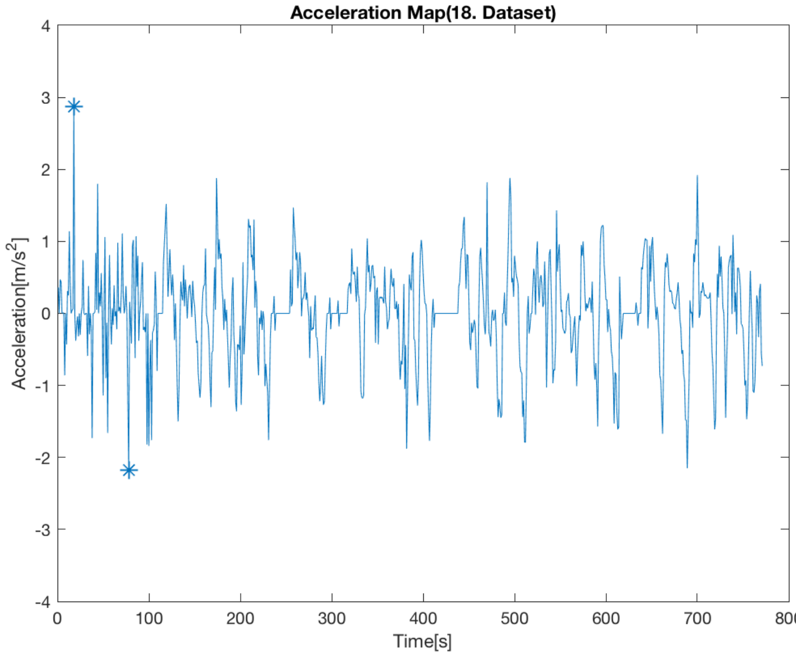

Figure B.18 : Acceleration Profile of 18.Measurement (9.(End point→ Start point))

APPENDIX C

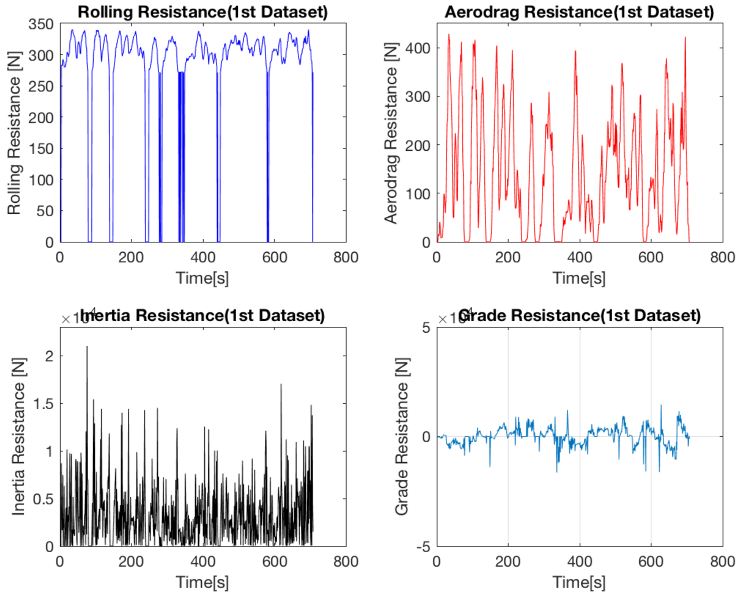

Figure C.1 : Resistance Map of 1.Measurement (1.(Start point → End point))

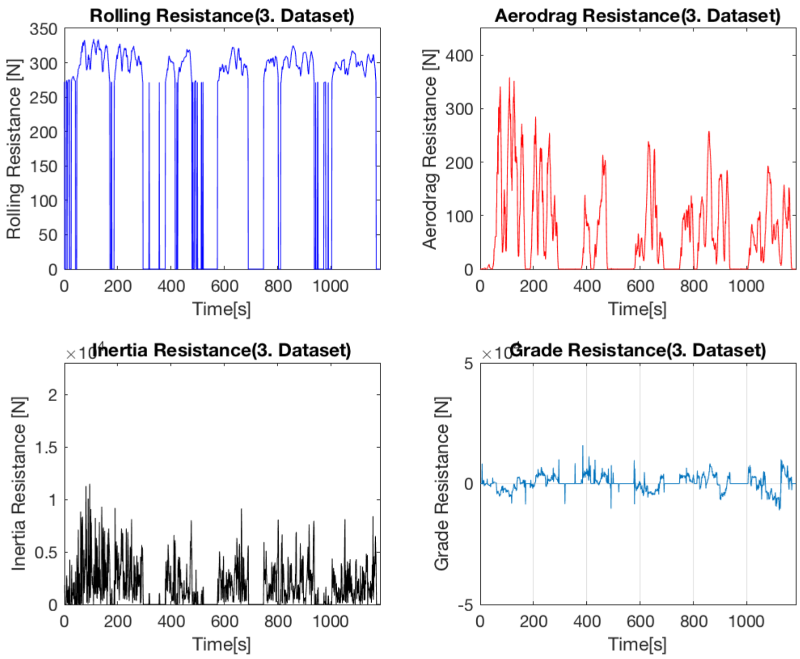

Figure C.2 : Resistance Map of 3.Measurement (2. (Start point → End point))

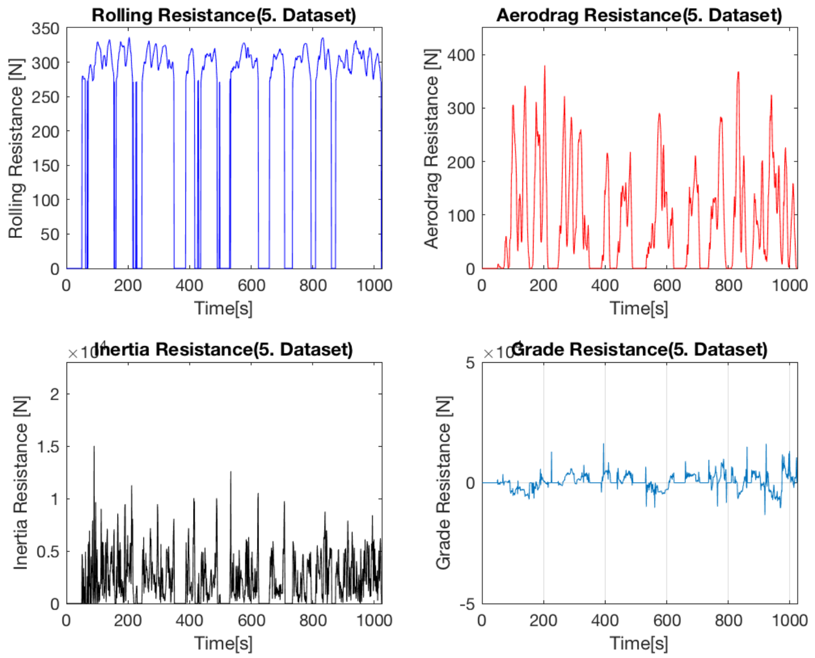

Figure C.3 : Resistance Map of 5.Measurement (3.(Start point → End point))

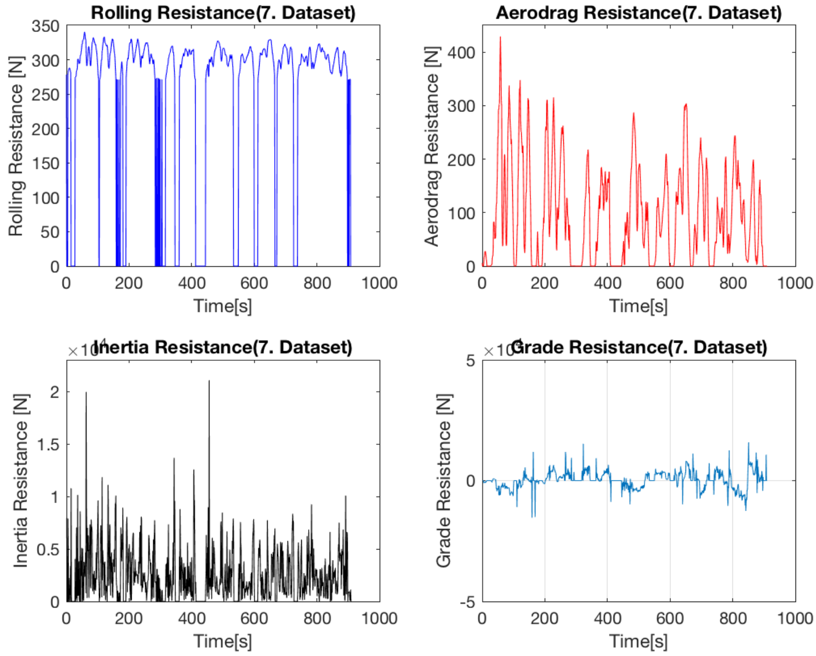

Figure C.4 : Resistance Map of 7.Measurement (4. (Start point → End point))

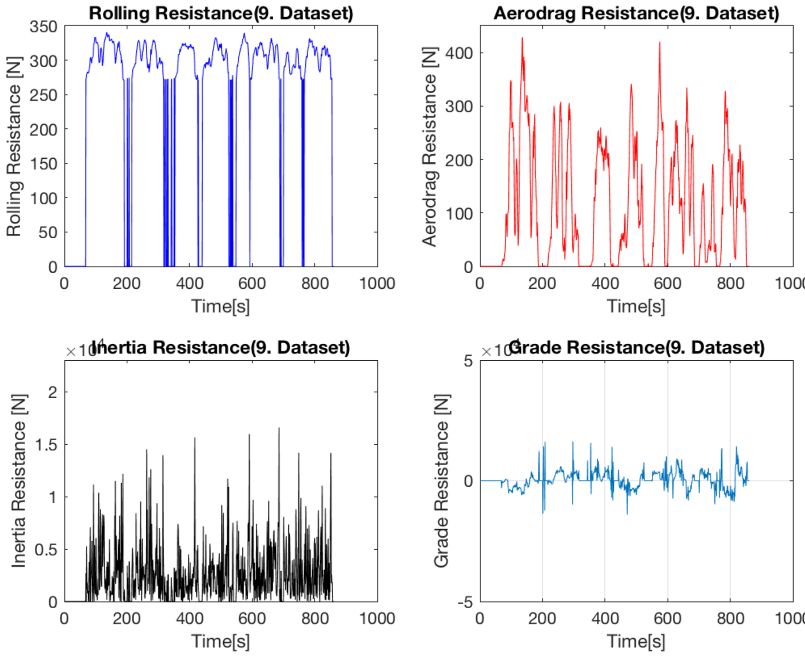

Figure C.5 : Resistance Map of 9.Measurement (5.(Start point → End point))

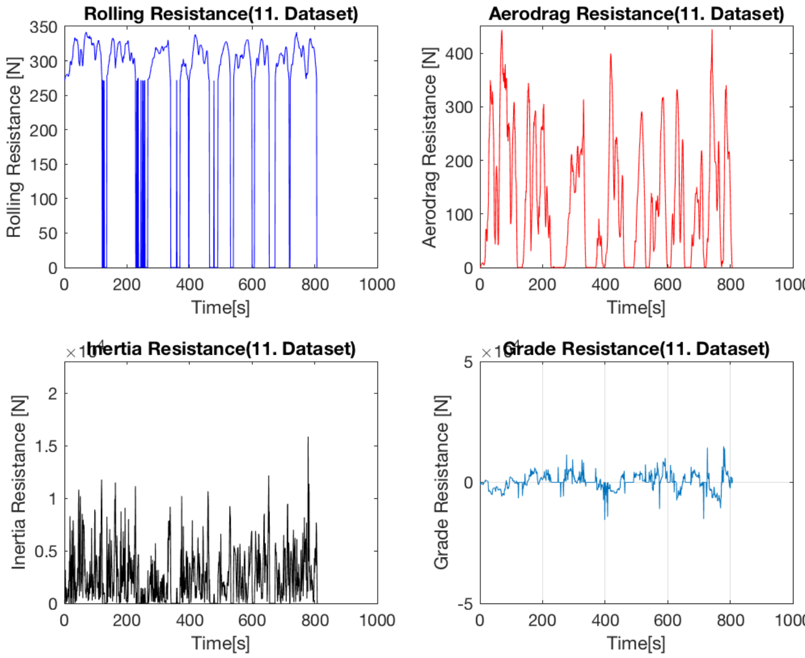

Figure C.6 : Resistance Map of 11.Measurement (6. (Start point → End point))

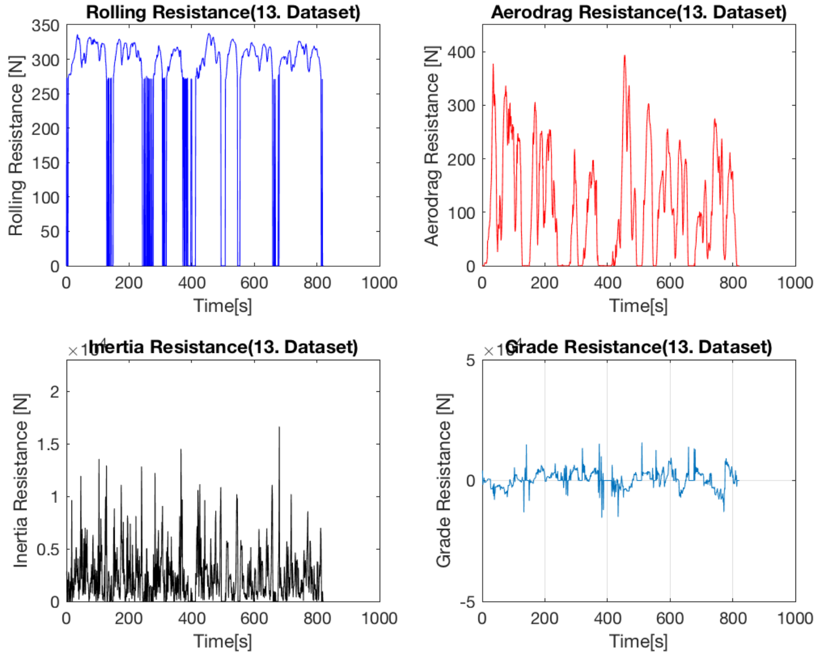

Figure C.7 : Resistance Map of 13.Measurement (7.(Start point → End point))

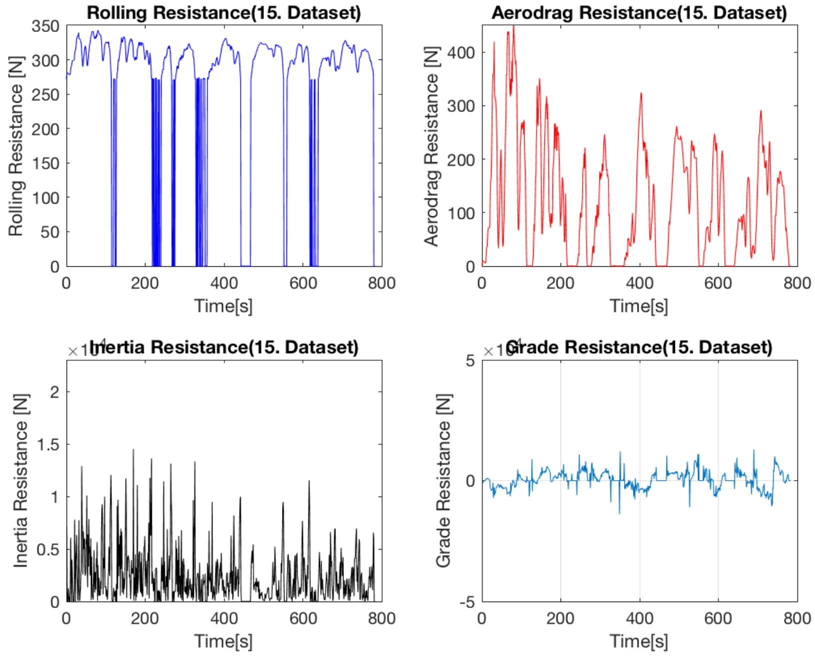

Figure C.8 : Resistance Map of 15.Measurement (8. (Start point → End point))

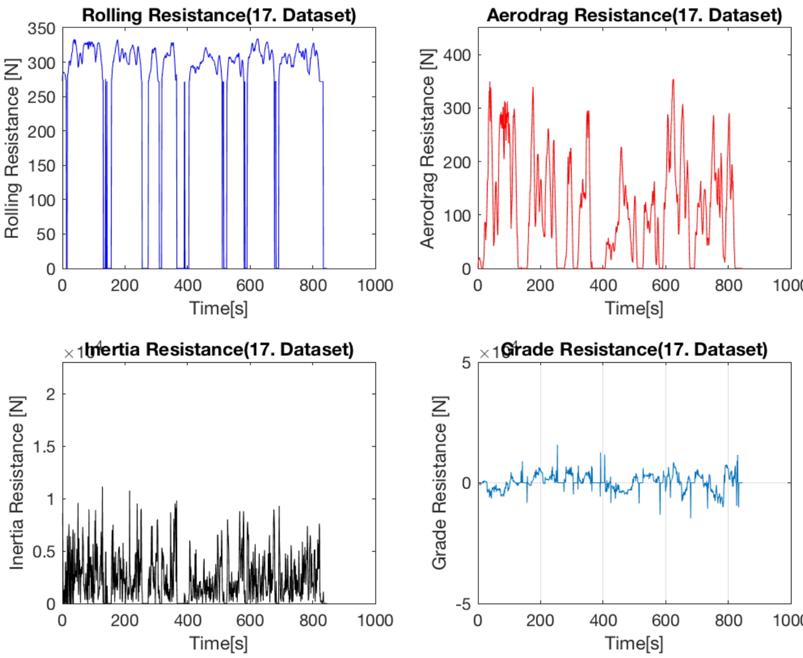

Figure C.9 : Resistance Map of 17.Measurement (9.(Start point → End point))

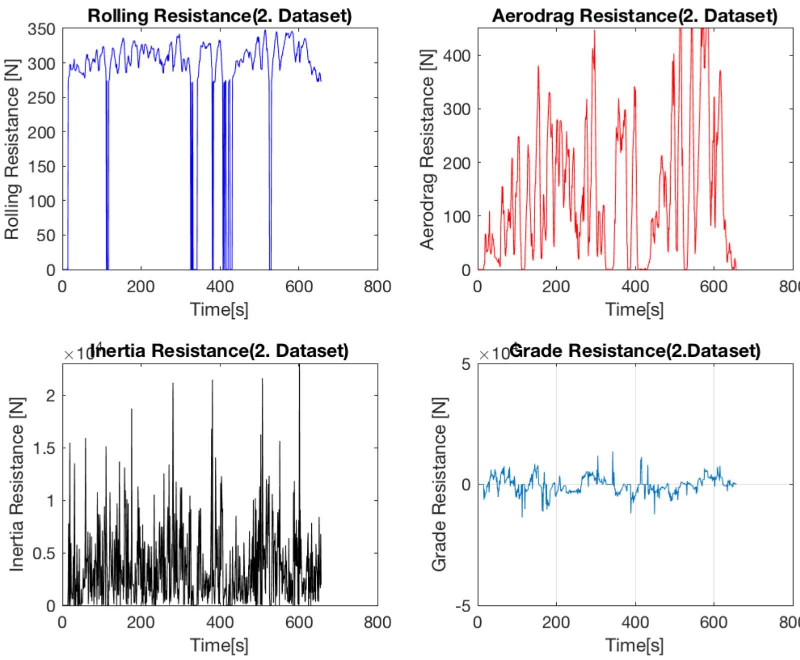

Figure C.10 : Resistance Map of 2.Measurement (1.(End point→ Start point))

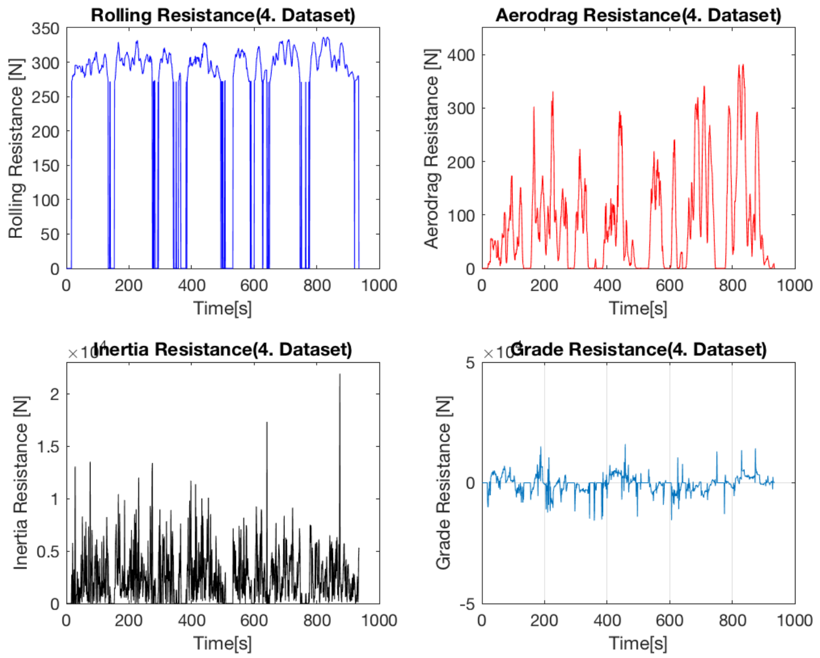

Figure C.11 : Resistance Map of 4.Measurement (2.(End point→ Start point))

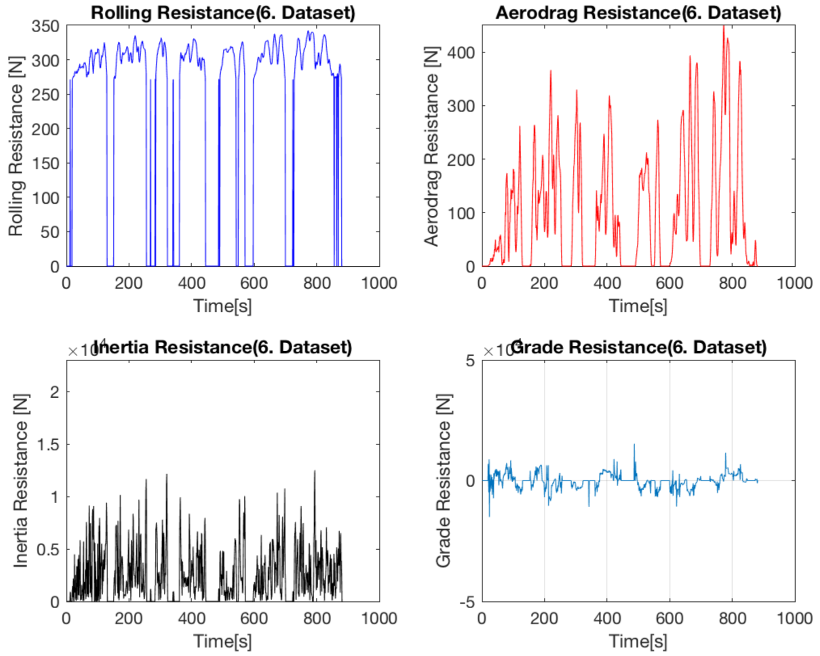

Figure C.12 : Resistance Map of 6.Measurement (3.(End point→ Start point))

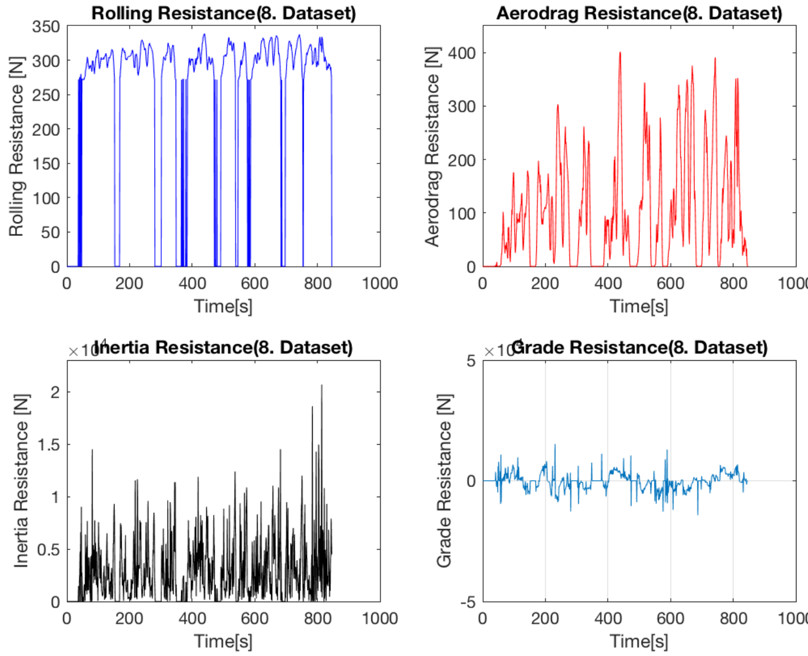

Figure C.13 : Resistance Map of 8.Measurement (4.(End point→ Start point))

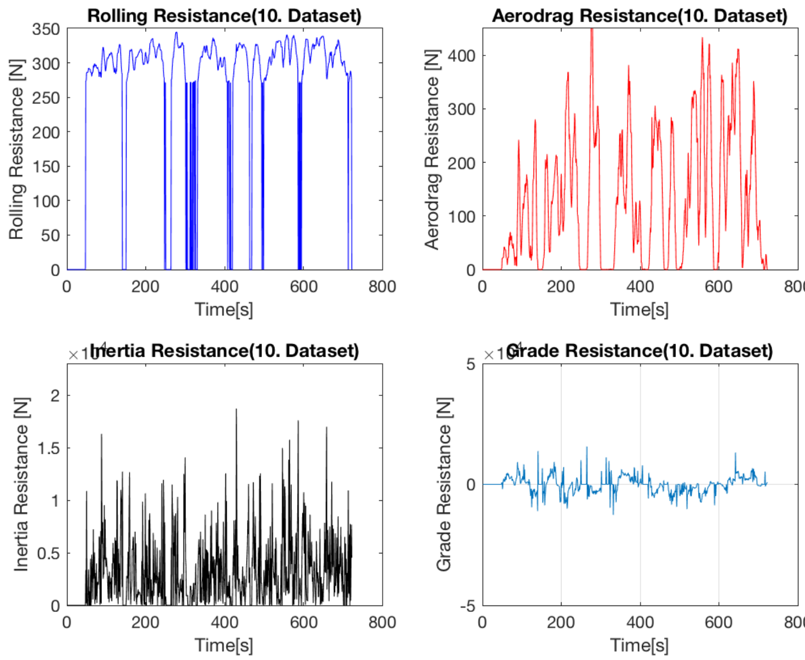

Figure C.14 : Resistance Map of 10.Measurement (5.(End point→ Start point))

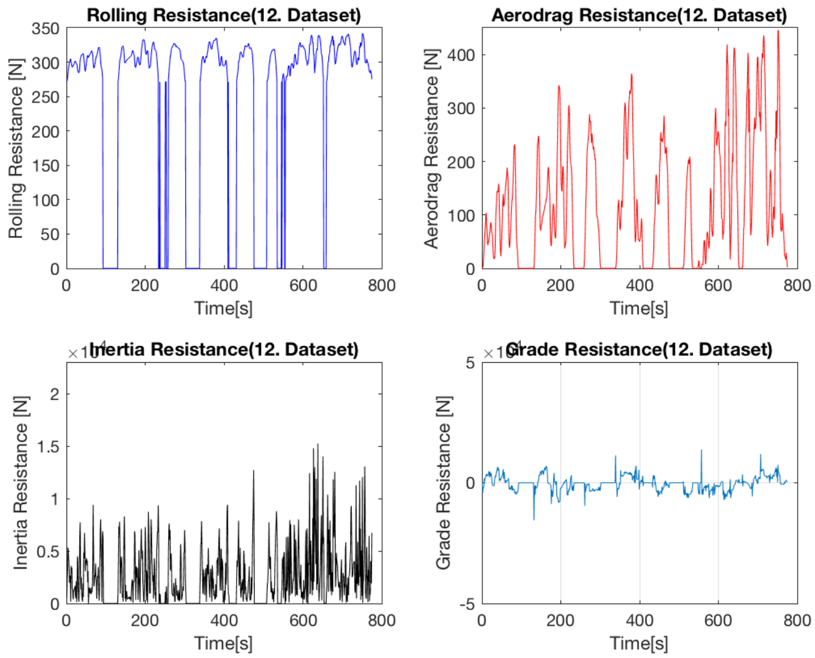

Figure C.15 : Resistance Map of 12.Measurement (6.(End point→ Start point))

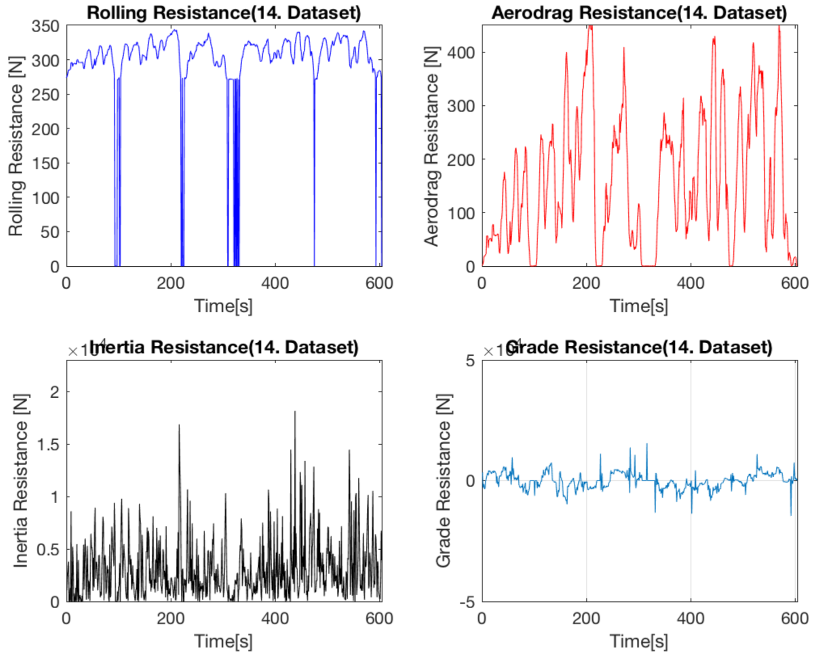

Figure C.16 : Resistance Map of 14.Measurement (7.(End point→ Start point))

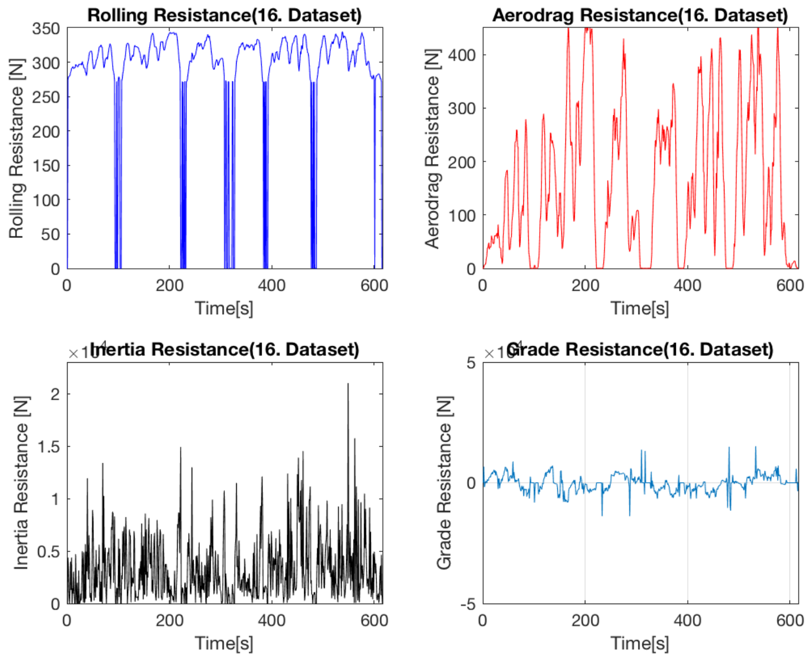

Figure C.17 : Resistance Map of 16.Measurement (8.(End point→ Start point))

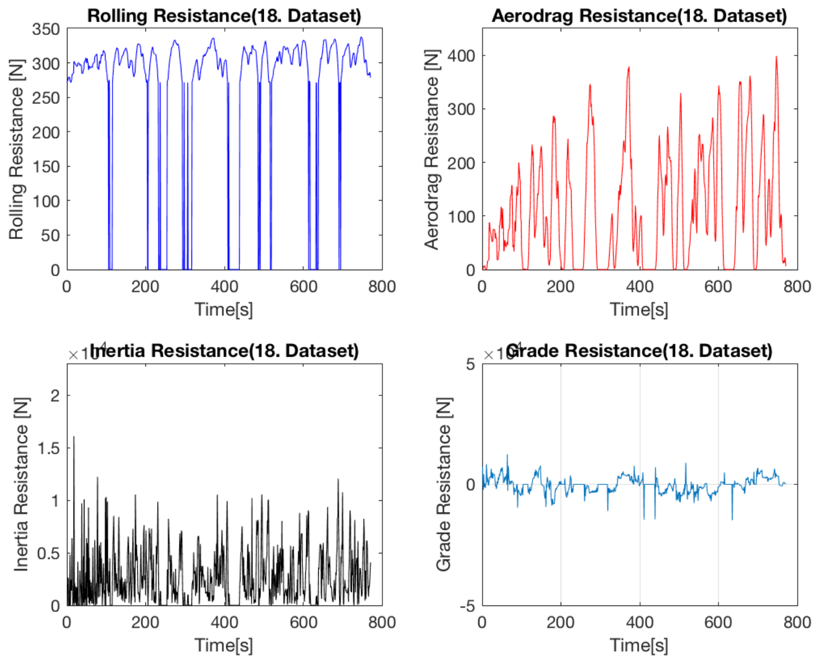

Figure C.18 : Resistance Map of 18.Measurement (9.(End point→ Start point))

APPENDIX D

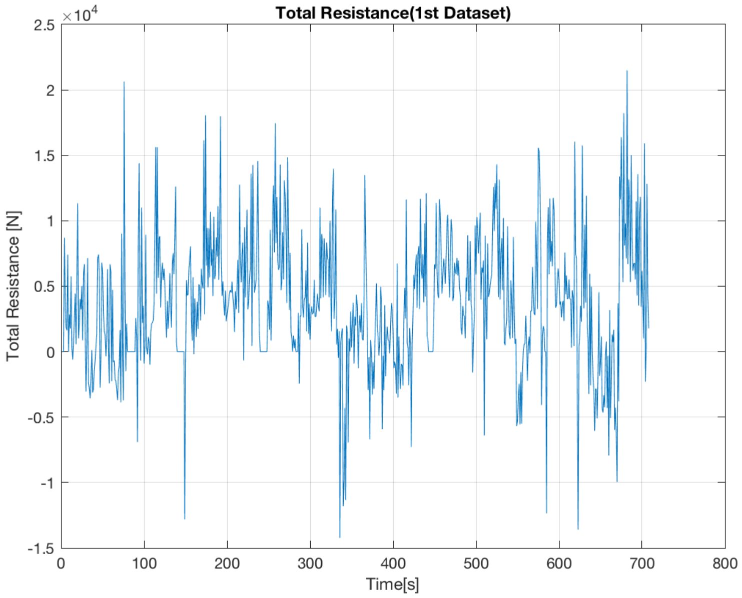

Figure D.1 : Total Resistance Map of 1.Measurement (1.(Start point → End point))

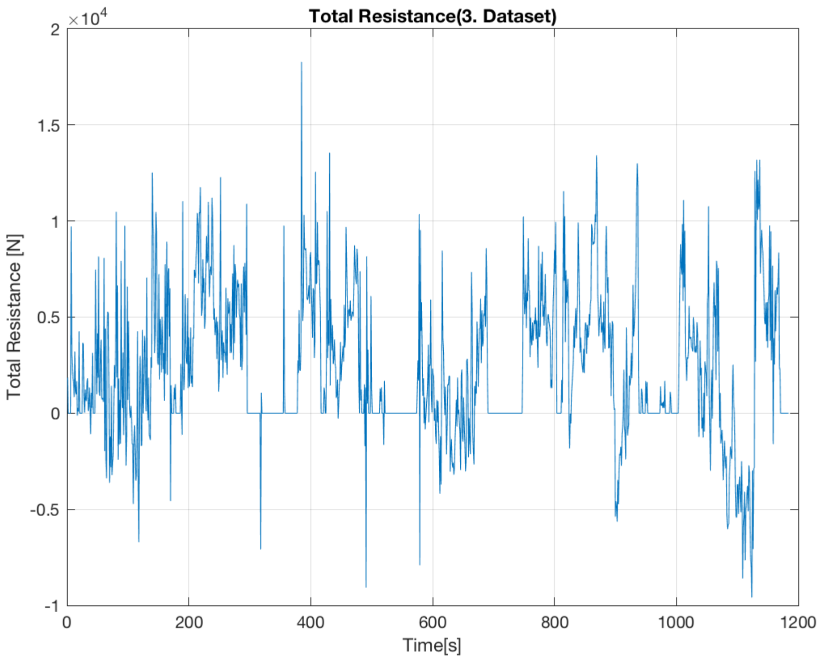

Figure D.2 : Total Resistance Map of 3.Measurement (2. (Start point → End point))

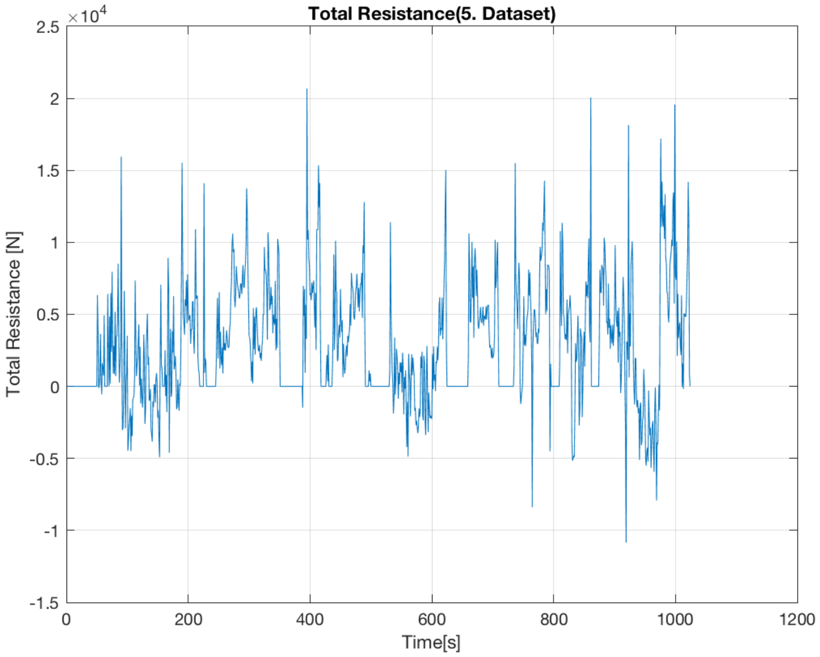

Figure D.3 : Total Resistance Map of 5.Measurement (3.(Start point → End point))

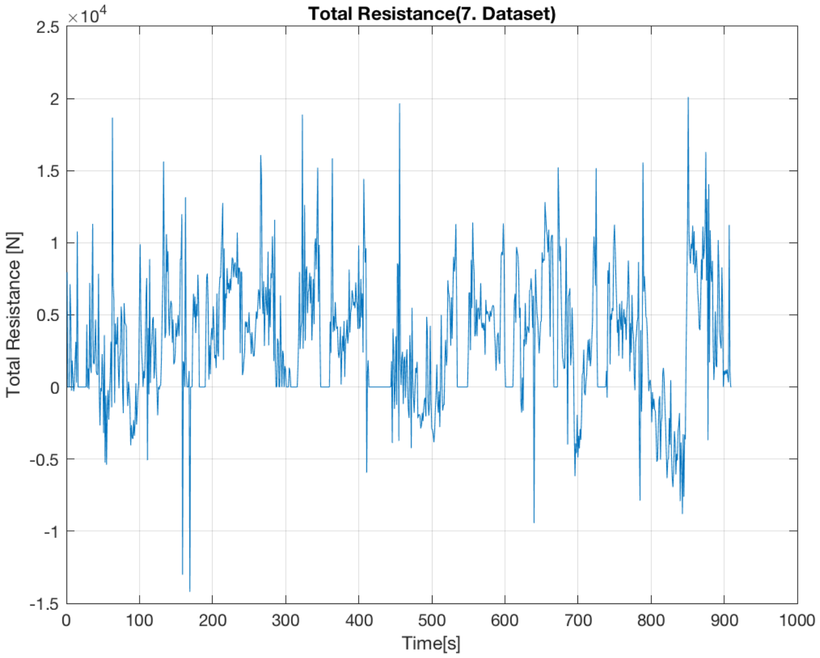

Figure D.4 : Total Resistance Map of 7.Measurement (4. (Start point → End point))

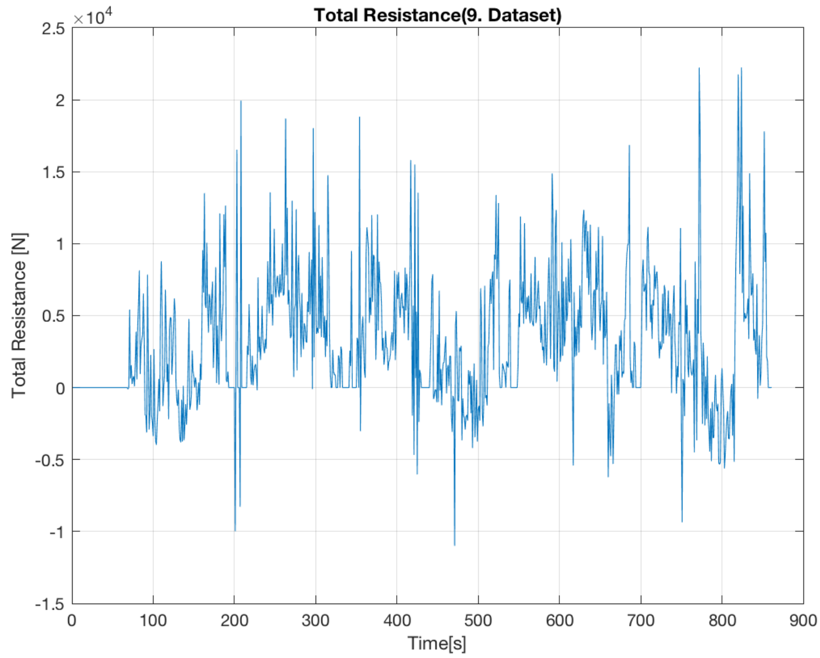

Figure D.5 : Total Resistance Map of 9.Measurement (5.(Start point → End point))

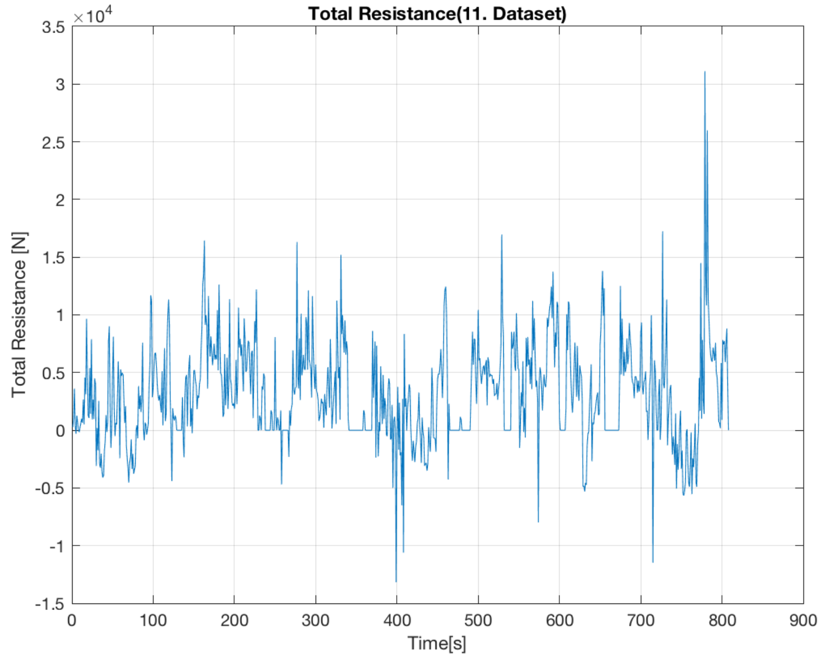

Figure D.6 : Total Resistance Map of 11.Measurement (6. (Start point → End point))

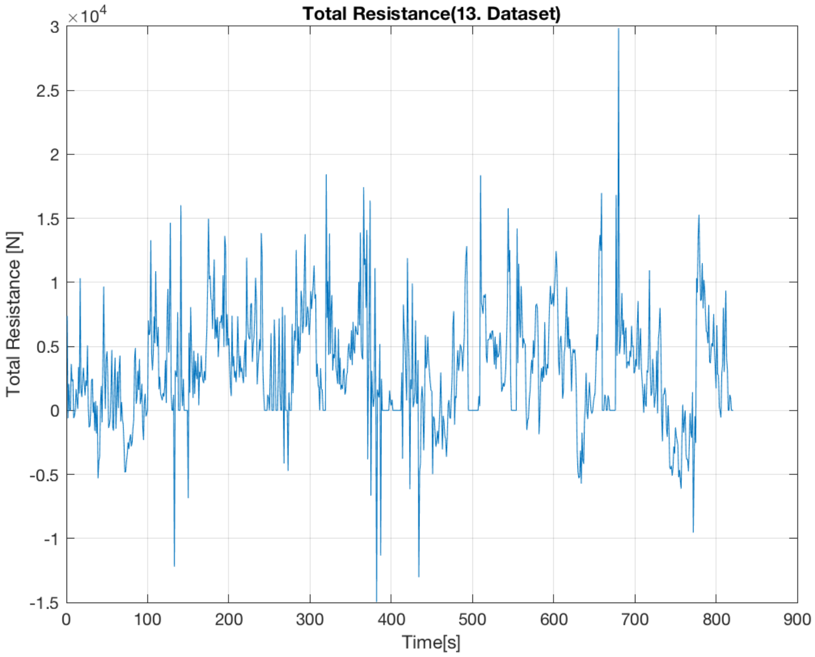

Figure D.7 : Total Resistance Map of 13.Measurement (7.(Start point → End point))

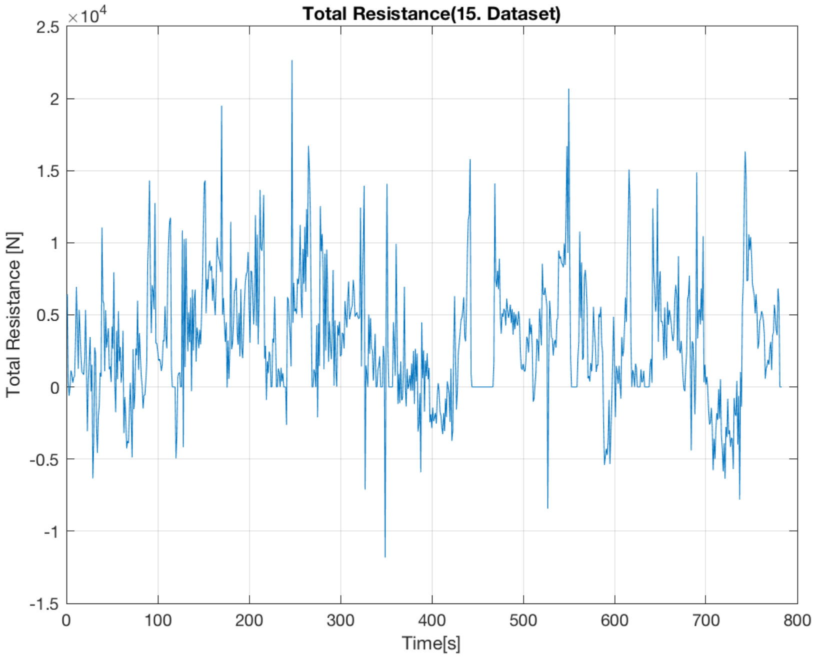

Figure D.8 : Total Resistance Map of 15.Measurement (8. (Start point → End point))

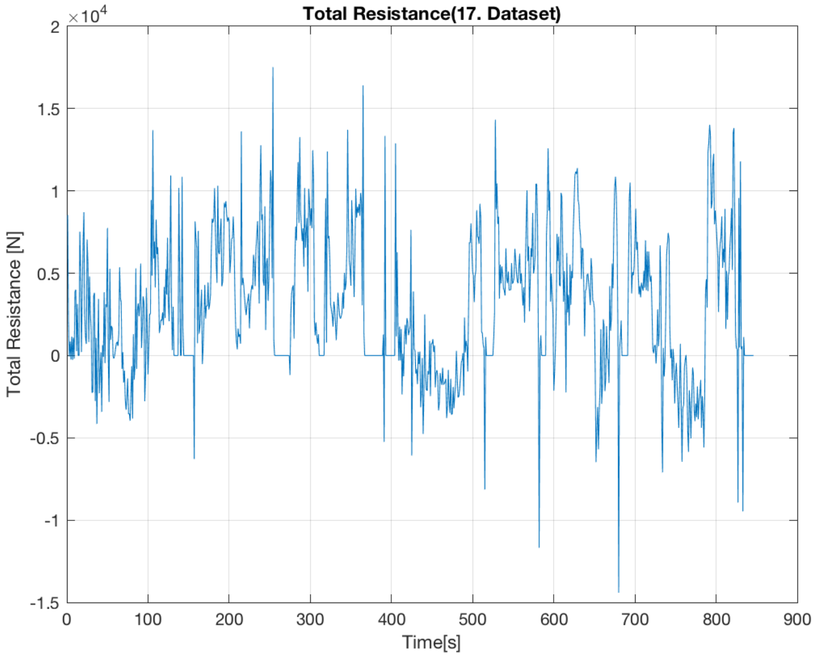

Figure D.9 : Total Resistance Map of 17.Measurement (9.(Start point → End point))

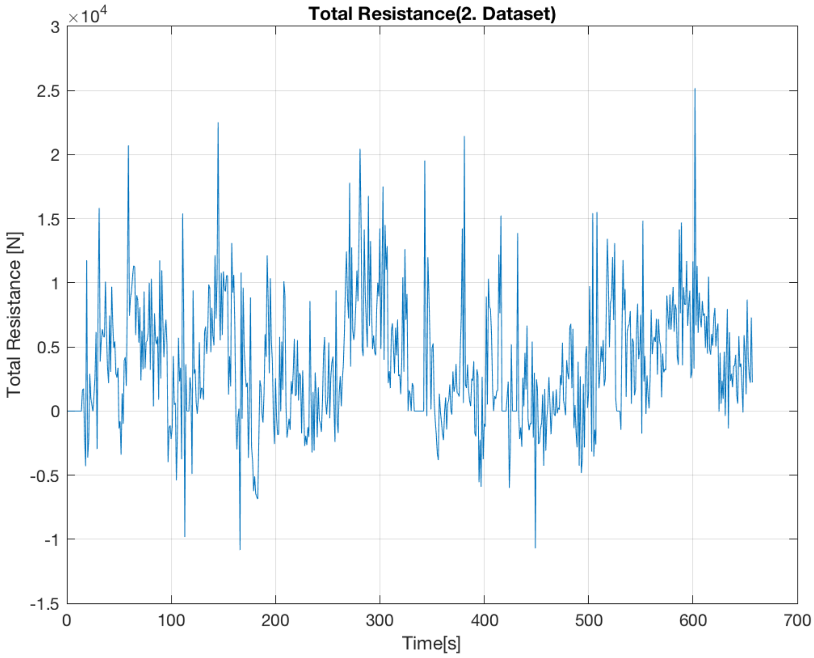

Figure D.10 : Total Resistance Map of 2.Measurement (1.(End point→ Start point))

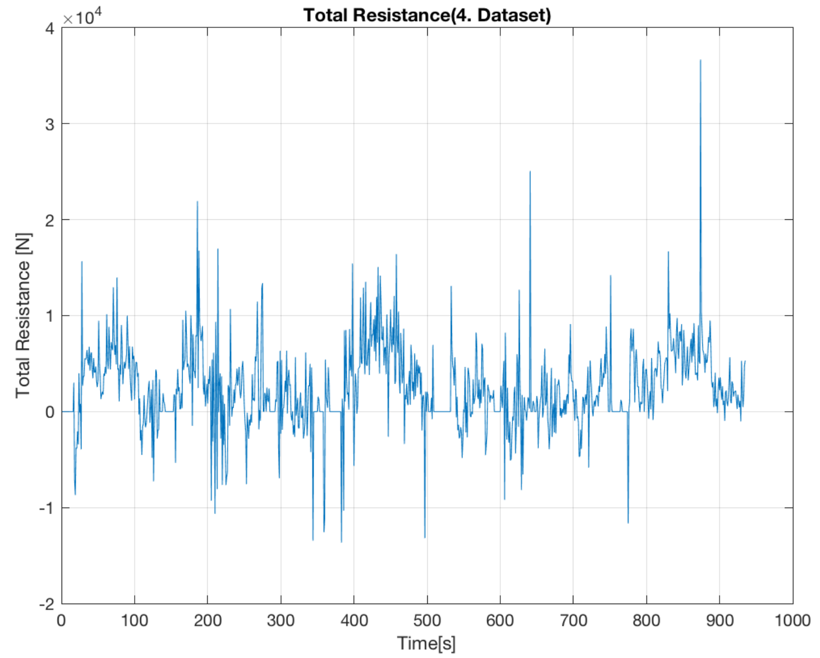

Figure D.11 : Total Resistance Map of 8.Measurement (4.(End point→ Start point))

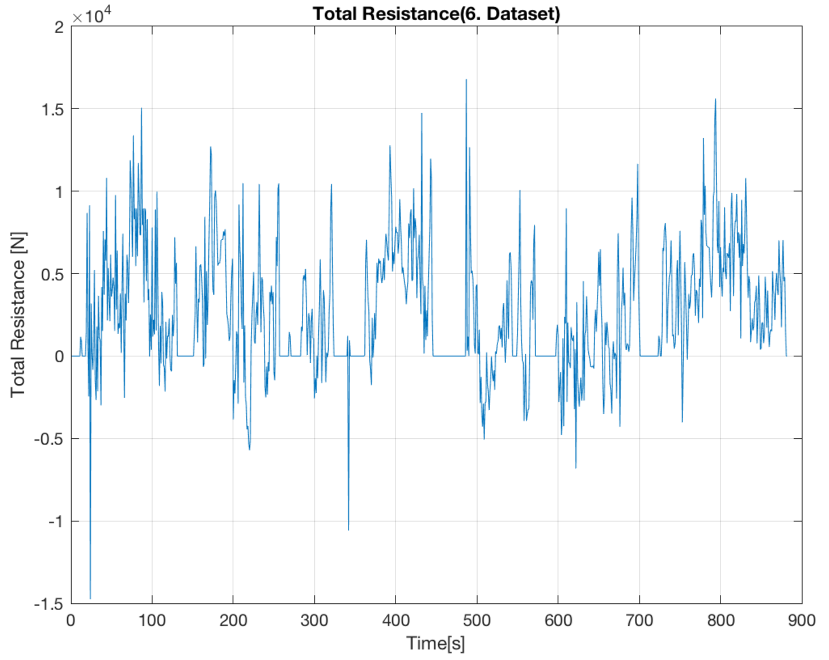

Figure D.12 : Total Resistance Map of 6.Measurement (3.(End point→ Start point))

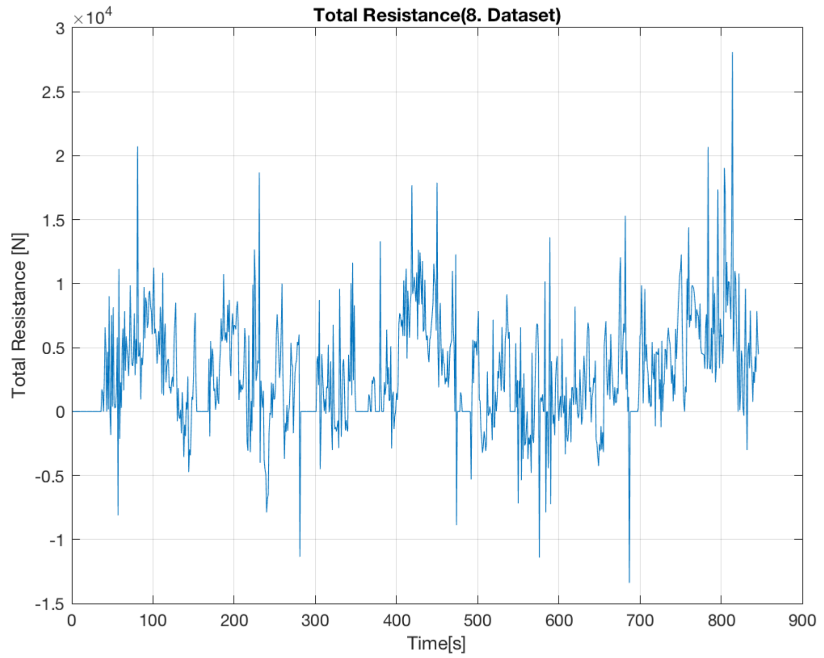

Figure D.13 : Total Resistance Map of 8.Measurement (4.(End point→ Start point))

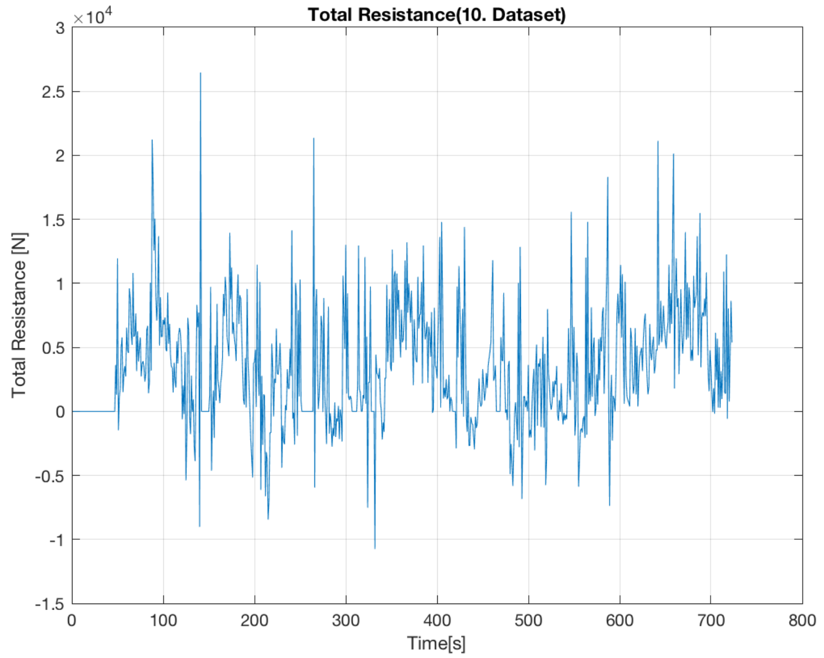

Figure D.14 : Total Resistance Map of 10.Measurement (5.(End point→ Start point))

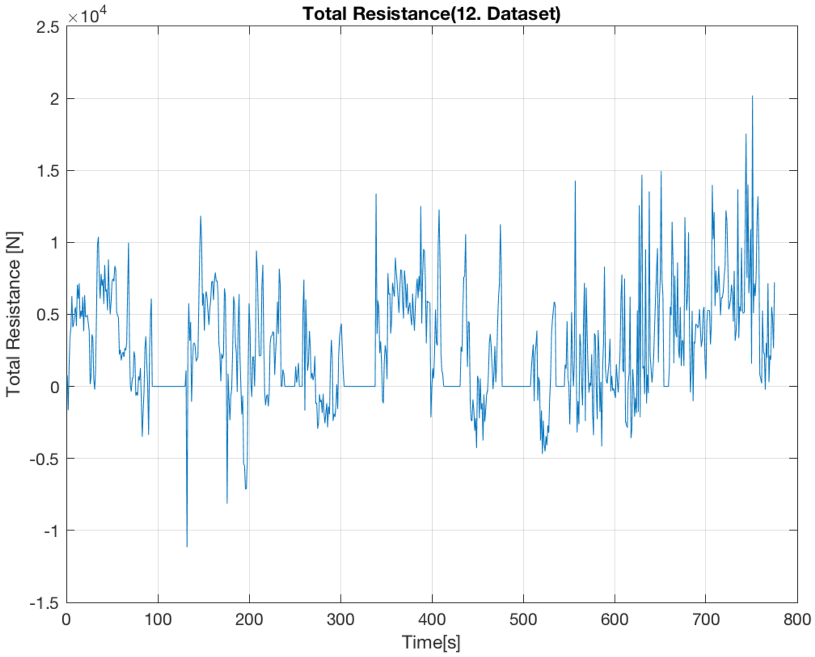

Figure D.15 : Total Resistance Map of 12.Measurement (6.(End point→ Start point))

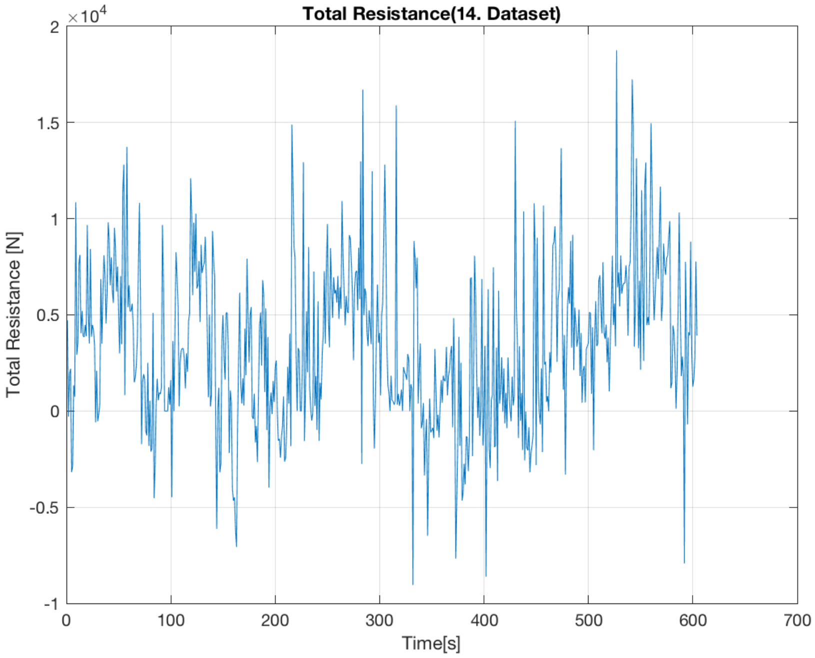

Figure D.16 : Total Resistance Map of 14.Measurement (7.(End point→ Start point))

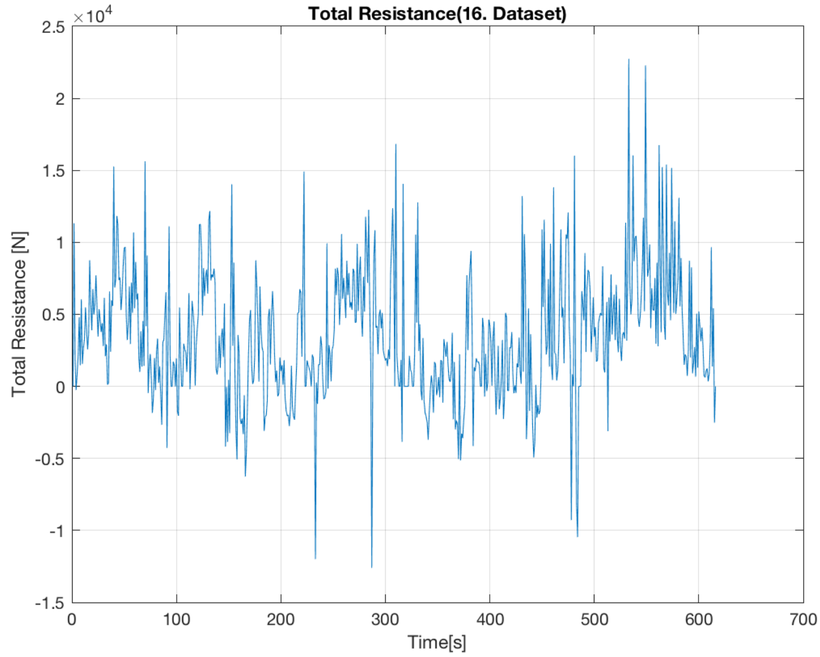

Figure D.17 : Total Resistance Map of 16.Measurement (8.(End point→ Start point))

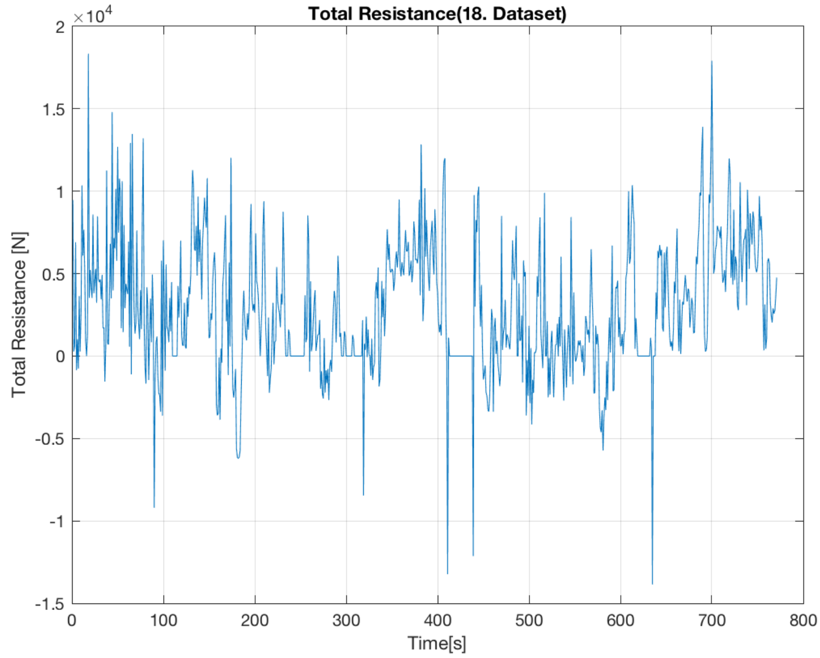

Figure D.18 : Total Resistance Map of 18.Measurement (9.(End point→ Start point))

APPENDIX E

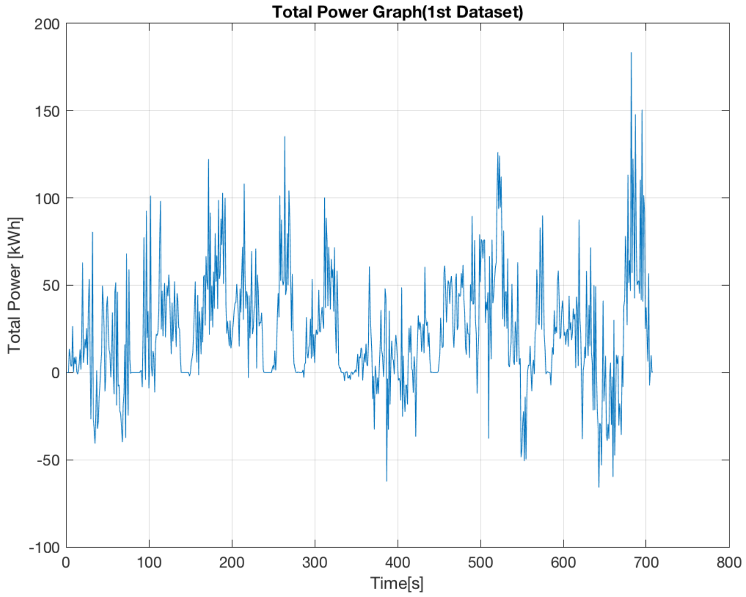

Figure E.1 : Total Power Map of 1.Measurement (1.(Start point → End point))

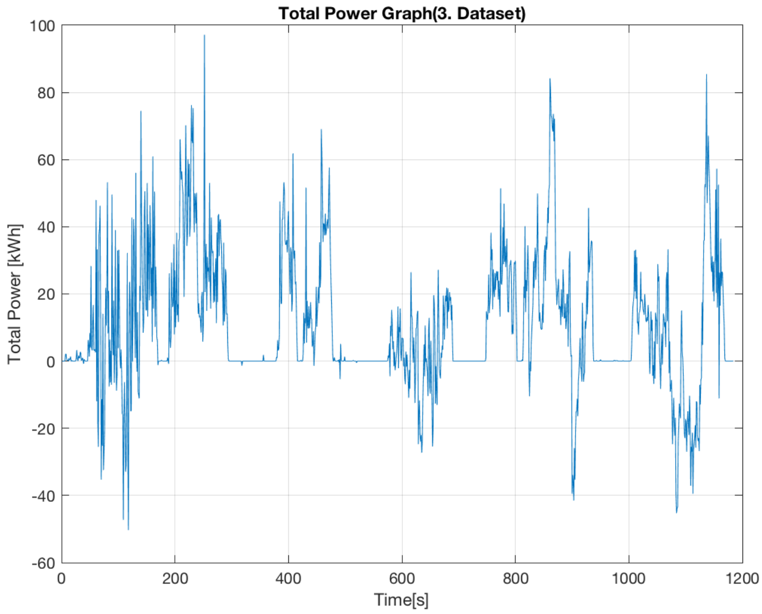

Figure E.2 : Total Power Map of 3.Measurement (2. (Start point → End point))

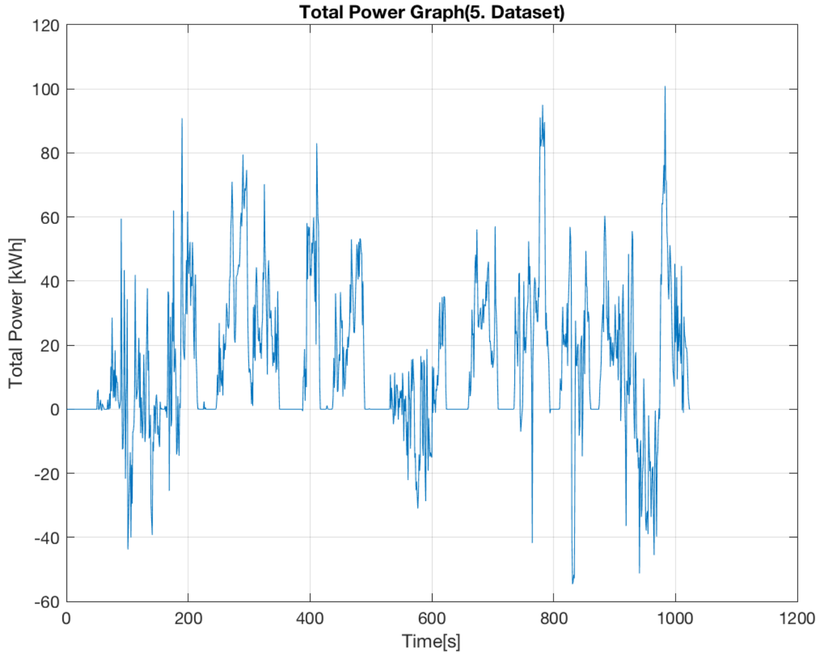

Figure E.3 : Total Power Map of 5.Measurement (3.(Start point → End point))

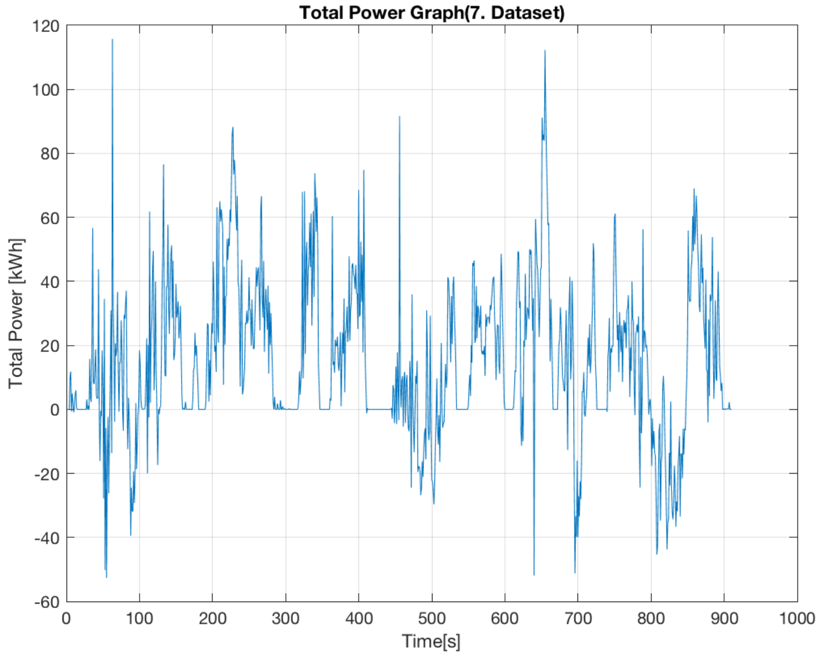

Figure E.4 : Total Power Map of 7.Measurement (4. (Start point → End point))

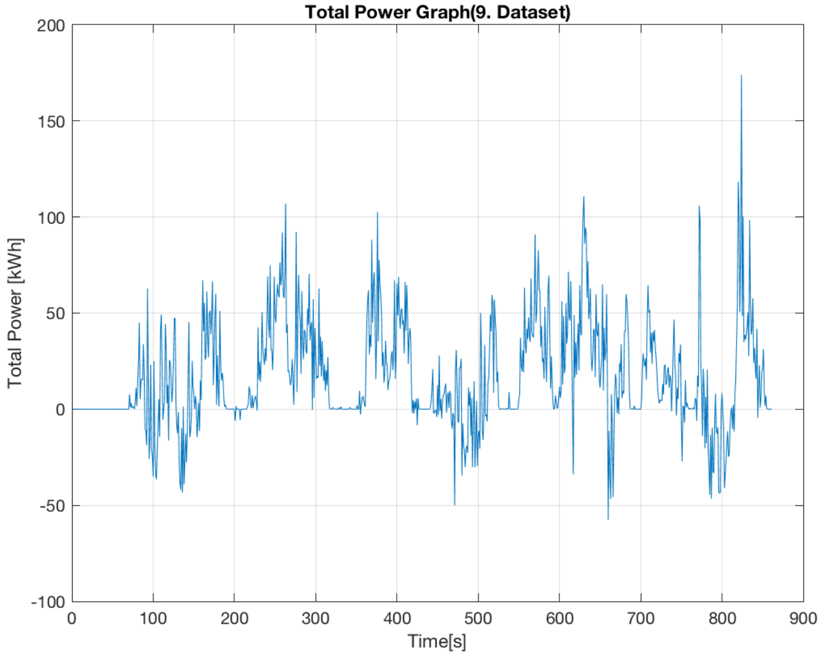

Figure E.5 : Total Power Map of 9.Measurement (5.(Start point → End point))

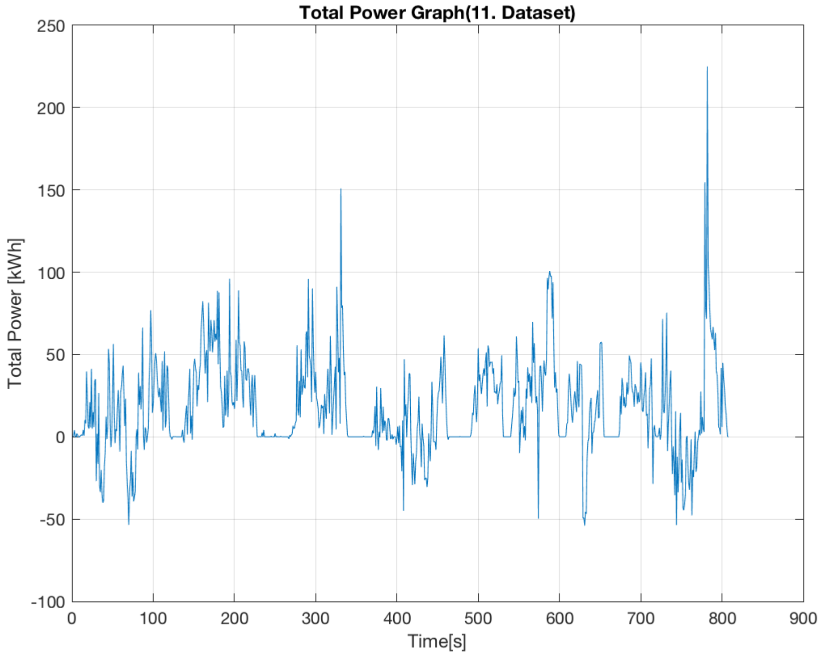

Figure E.6 : Total Power Map of 11.Measurement (6. (Start point → End point))

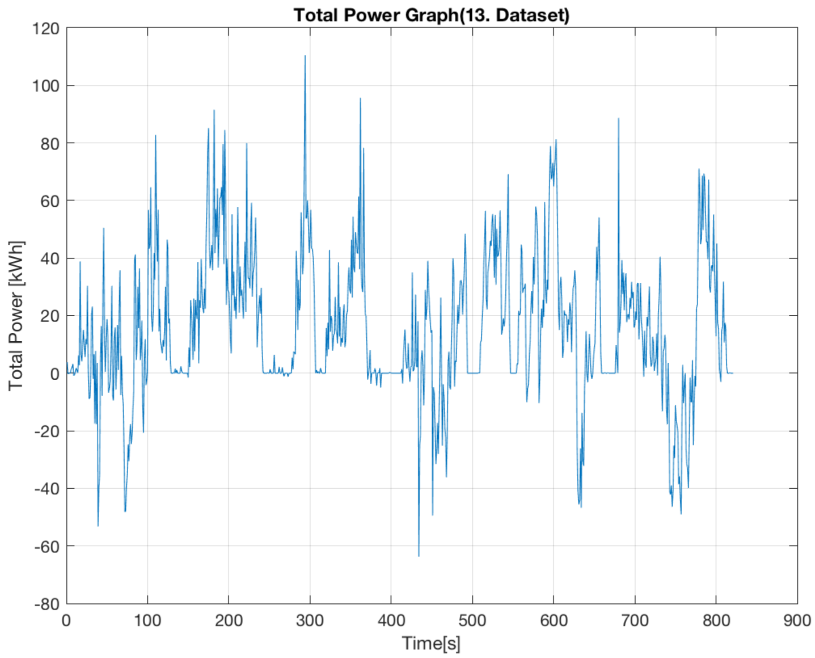

Figure E.7 : Total Power Map of 13.Measurement (7.(Start point → End point))

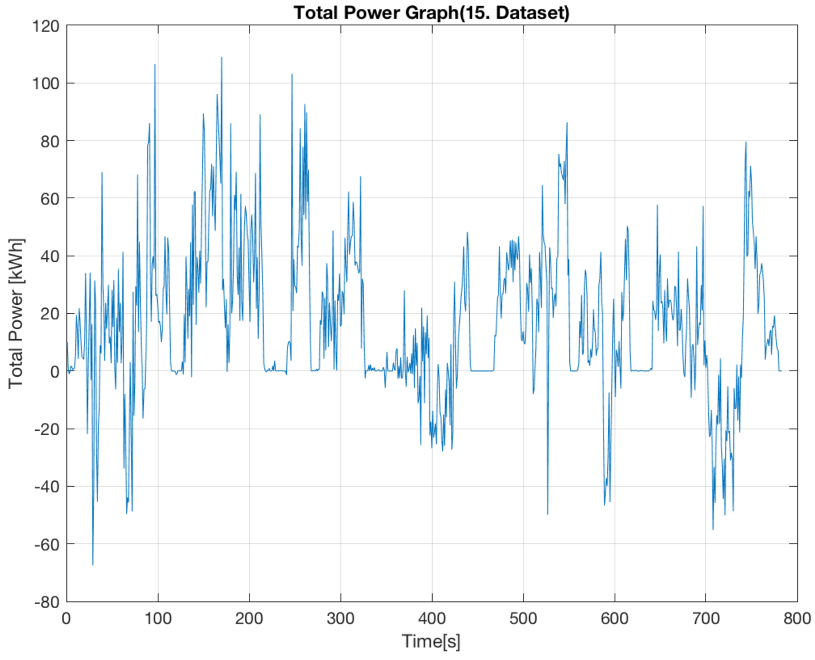

Figure E.8 : Total Power Map of 15.Measurement (8. (Start point → End point))

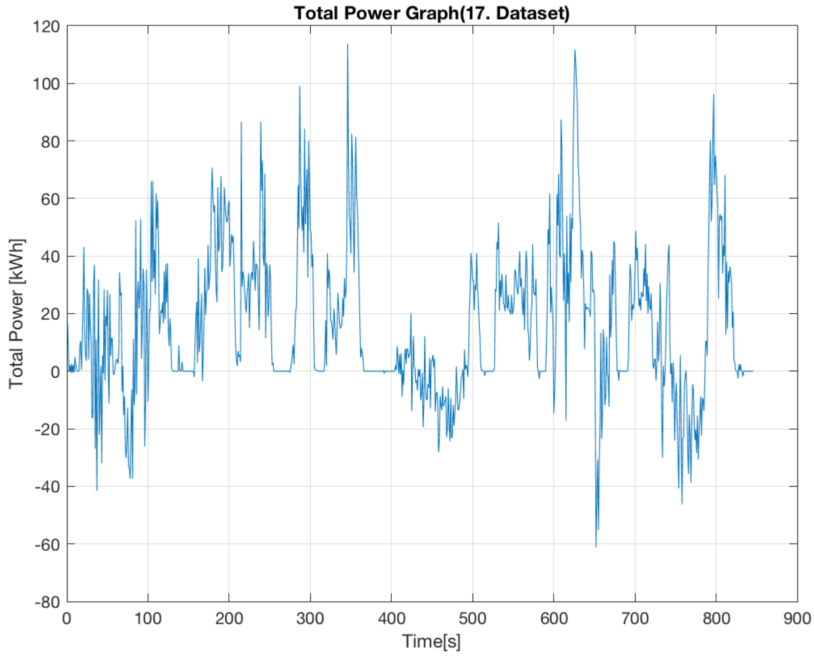

Figure E.9 : Total Power Map of 17.Measurement (9.(Start point → End point))

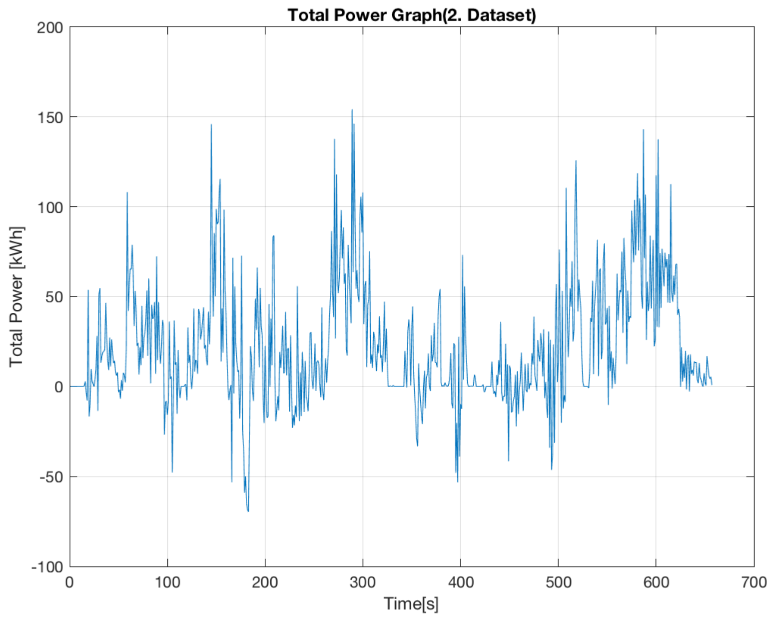

Figure E.10 : Total Power Map of 2.Measurement (1.(End point→ Start point))

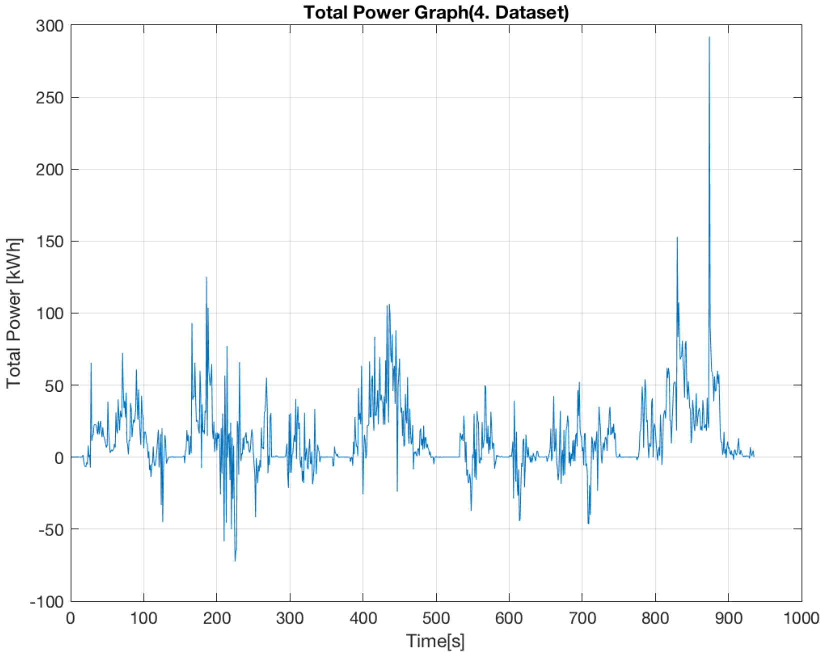

Figure E.11 : Total Power Map of 4.Measurement (2.(End point→ Start point))

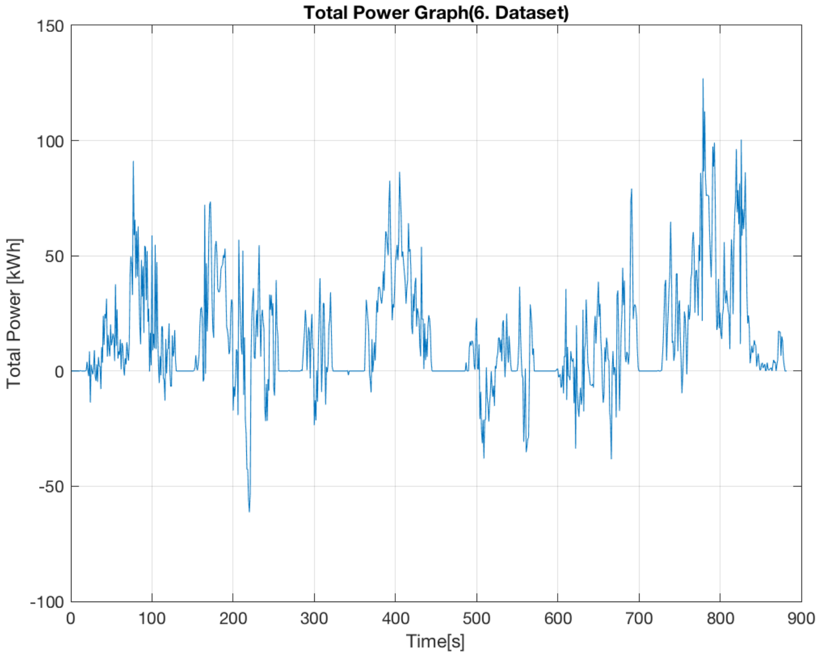

Figure E.12 : Total Power Map of 6.Measurement (3.(End point→ Start point))

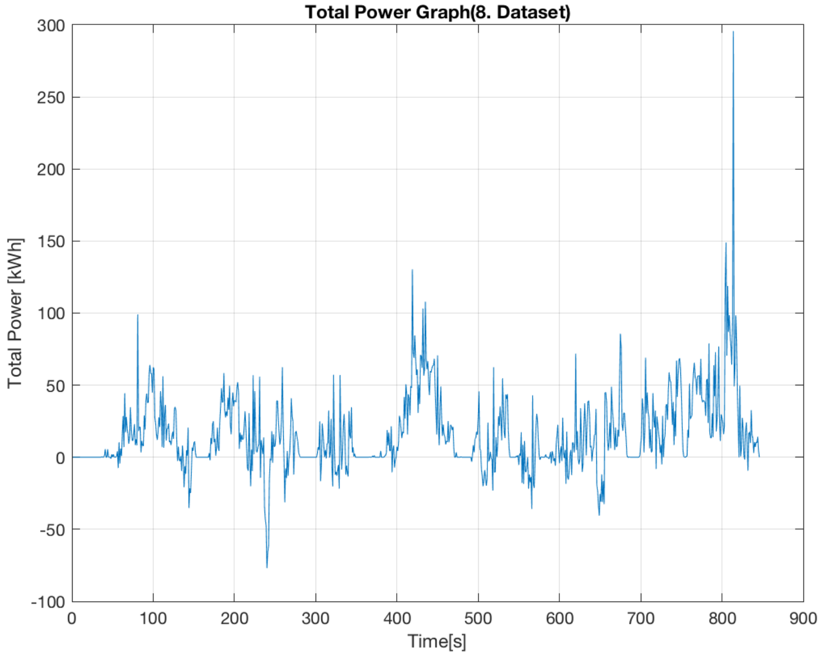

Figure E.13 : Total Power Map of 8.Measurement (4.(End point→ Start point))

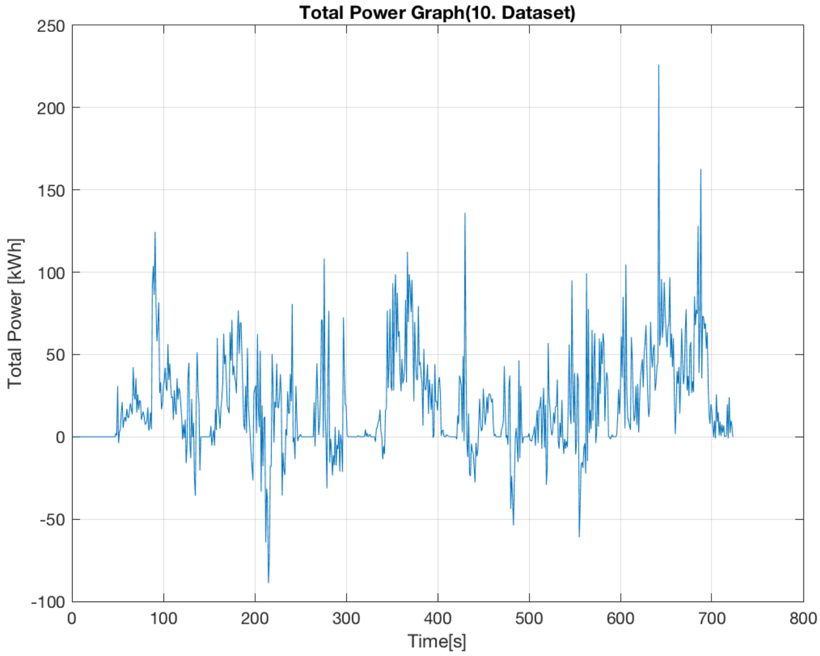

Figure E.14 : Total Power Map of 10.Measurement (5.(End point→ Start point))

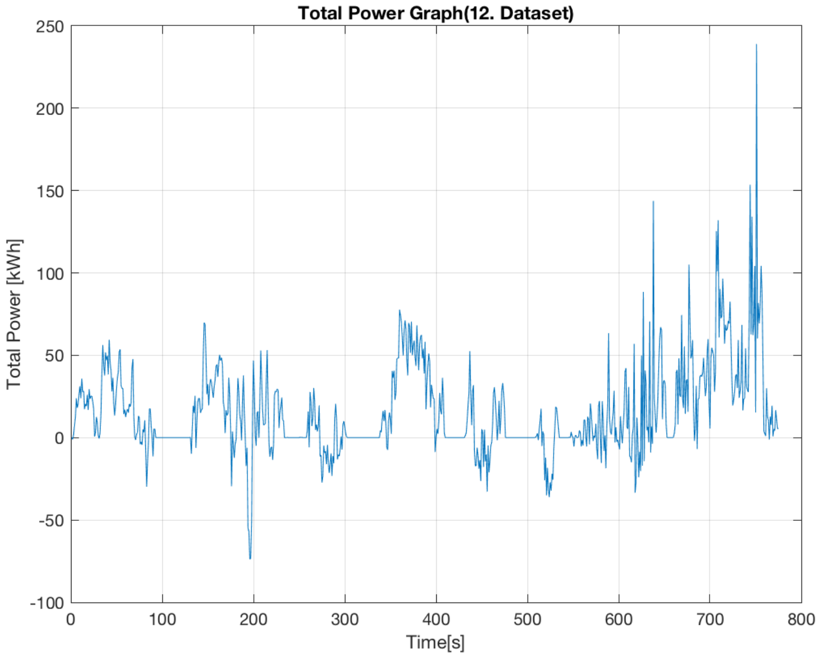

Figure E.15 : Total Power Map of 12.Measurement (6.(End point→ Start point))

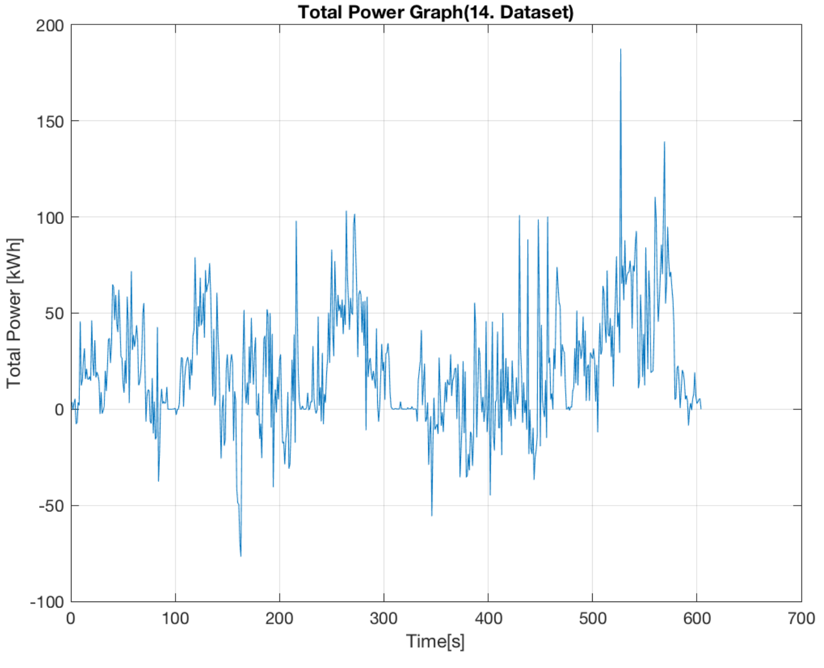

Figure E.16 : Total Power Map of 14.Measurement (7.(End point→ Start point))

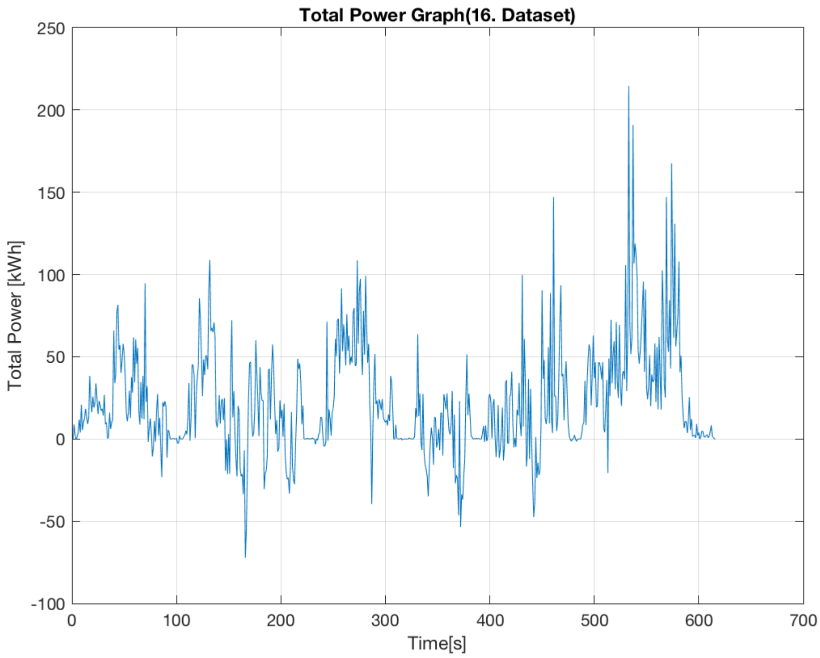

Figure E.17 : Total Power Map of 16.Measurement (8.(End point→ Start point))

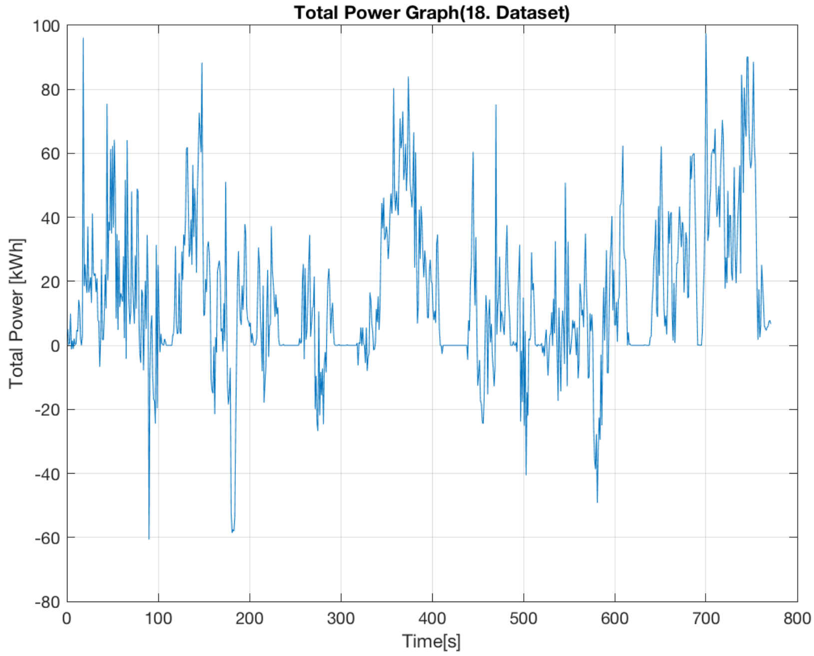

Figure E.18 : Total Power Map of 18.Measurement (9.(End point→ Start point))

APPENDIX F

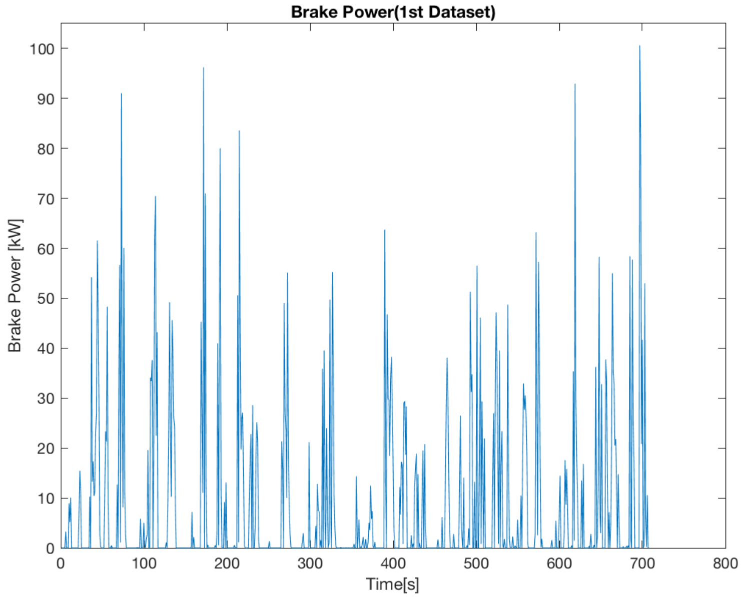

Figure F.1 : Brake Power Map of 1.Measurement (1.(Start point → End point))

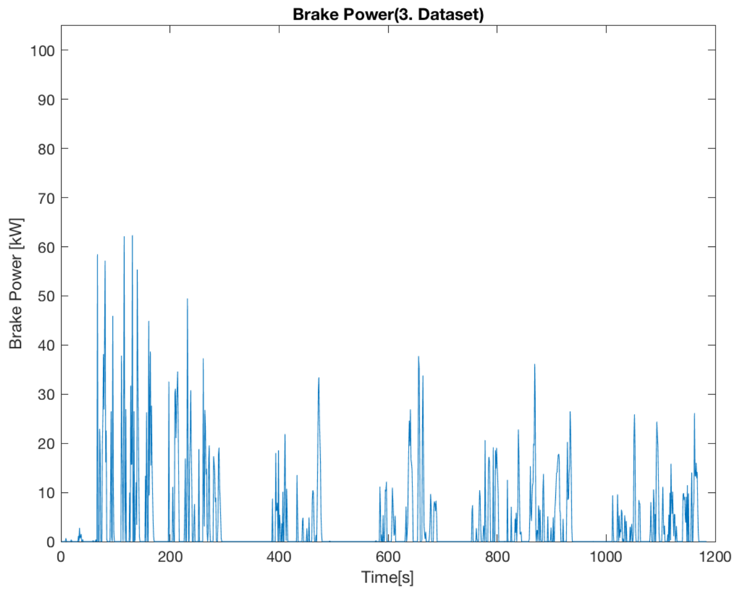

Figure F.2 : Brake Power Map of 3.Measurement (2. (Start point → End point))

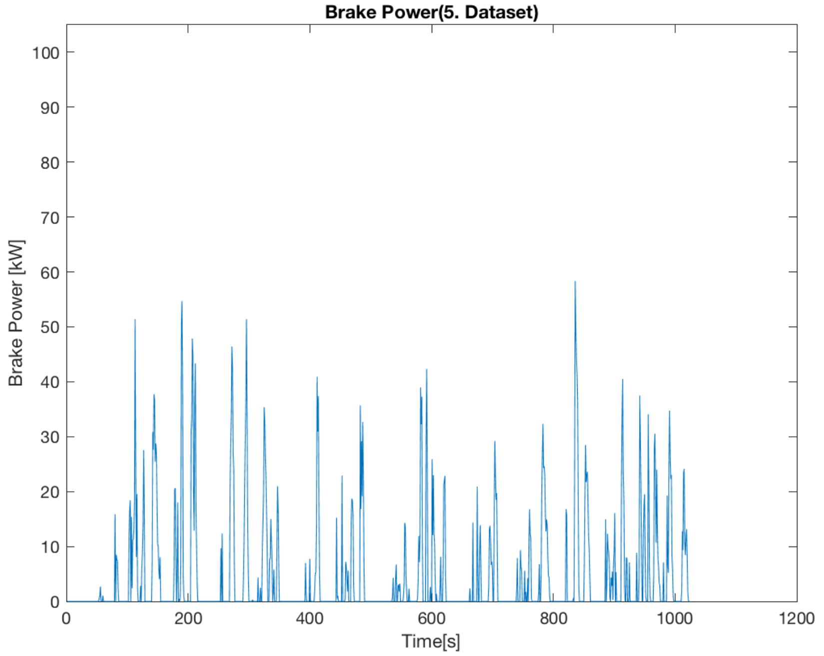

Figure F.3 : Brake Power Map of 5.Measurement (3.(Start point → End point))

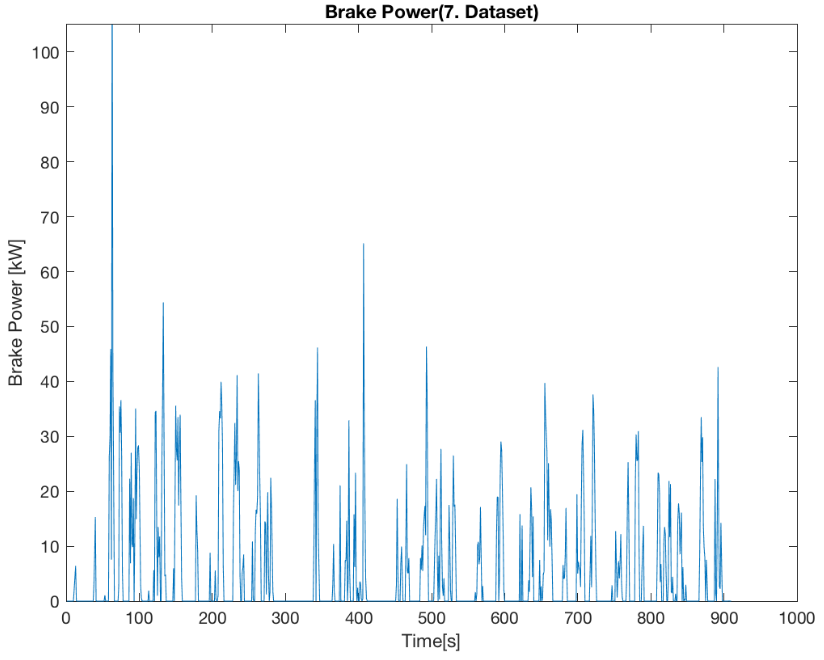

Figure F.4 : Brake Power Map of 7.Measurement (4. (Start point → End point))

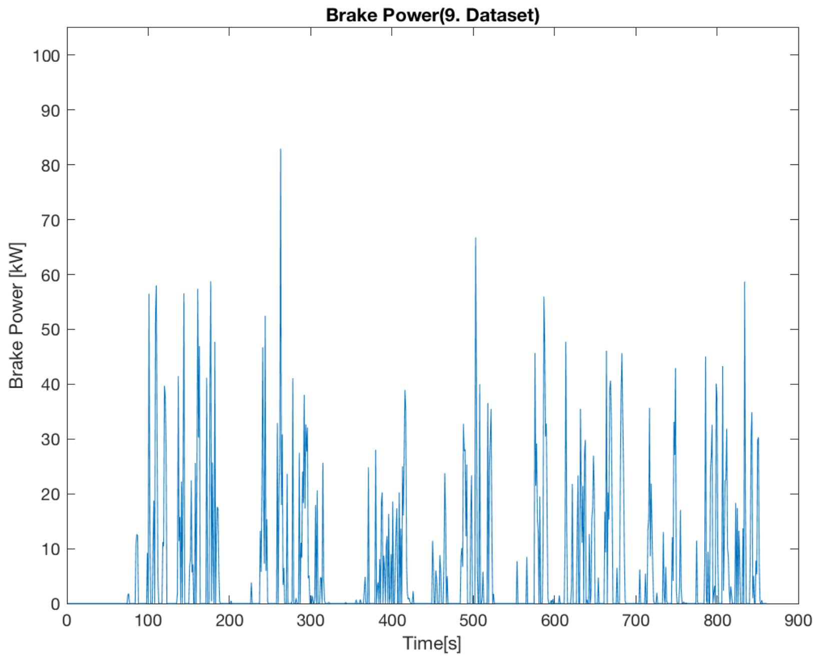

Figure F.5 : Brake Power Map of 9.Measurement (5.(Start point → End point))

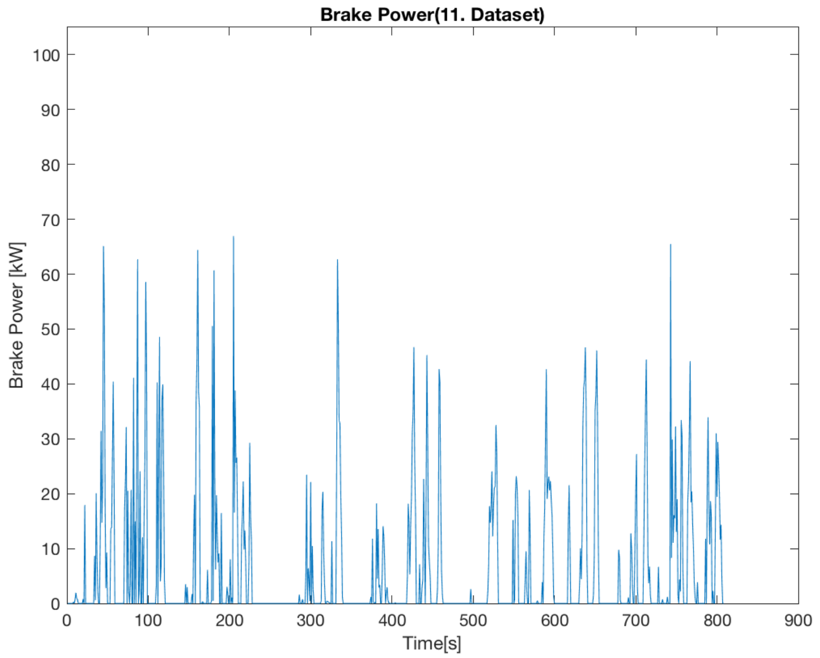

Figure F.6 : Brake Power Map of 11.Measurement (6. (Start point → End point))

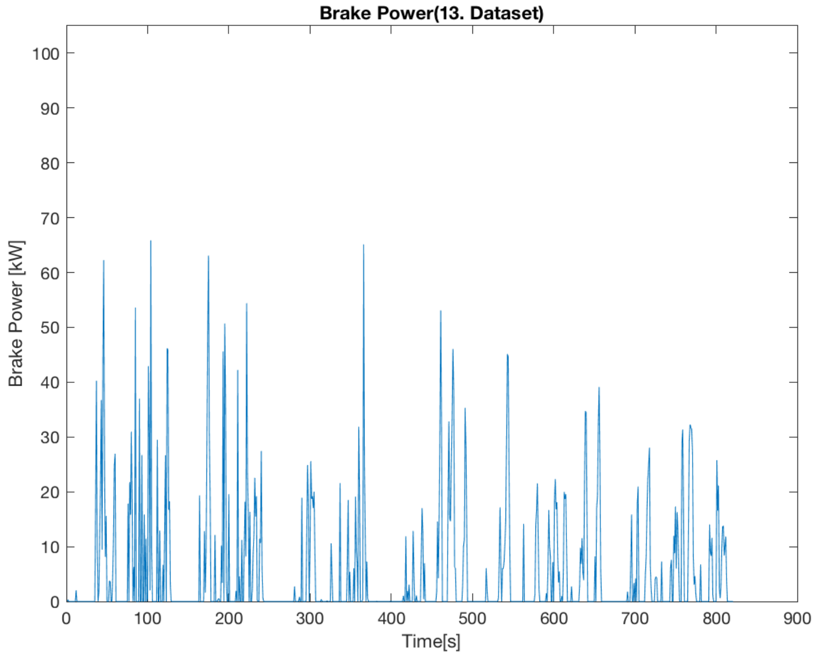

Figure F.7 : Brake Power Map of 13.Measurement (7.(Start point → End point))

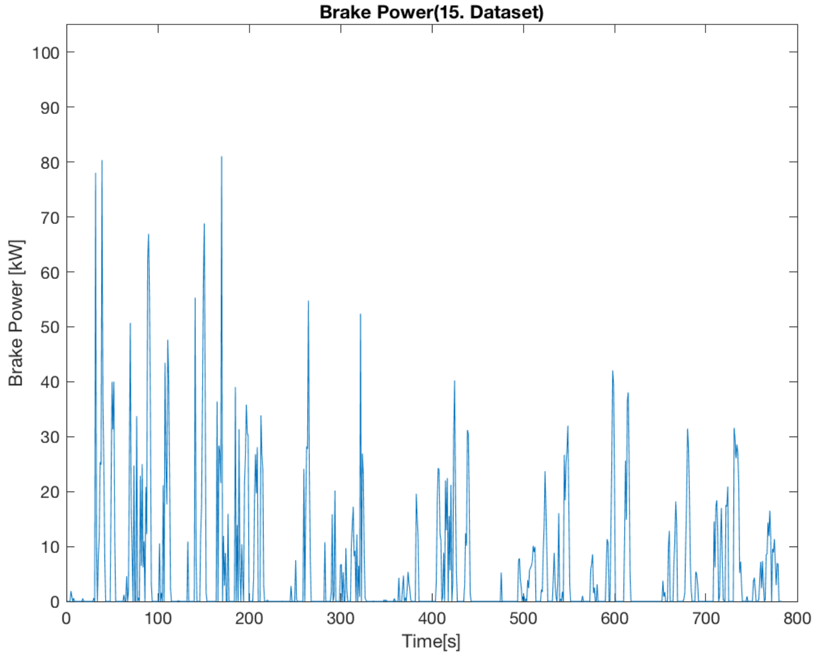

Figure F.8 : Brake Power Map of 15.Measurement (8. (Start point → End point))

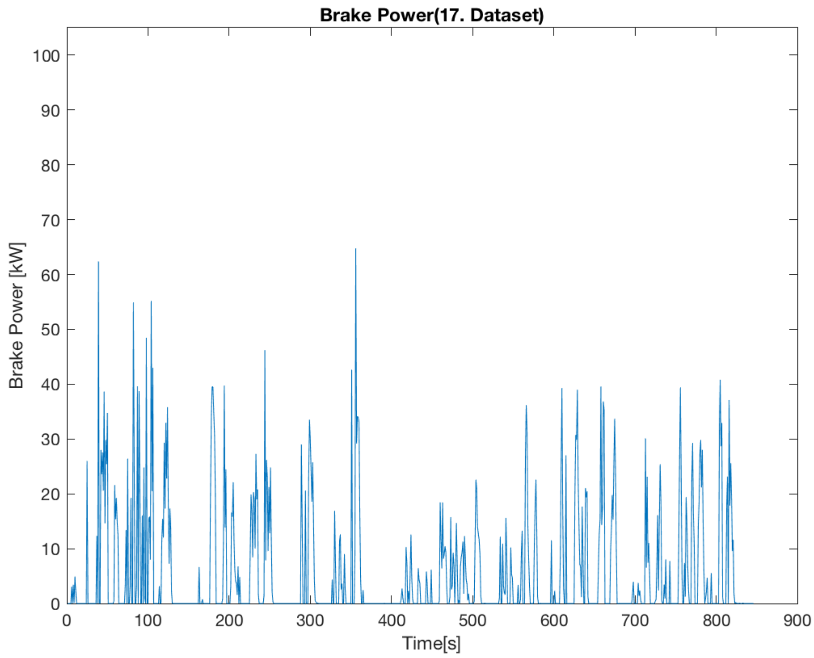

Figure F.9 : Brake Power Map of 17.Measurement (9.(Start point → End point))

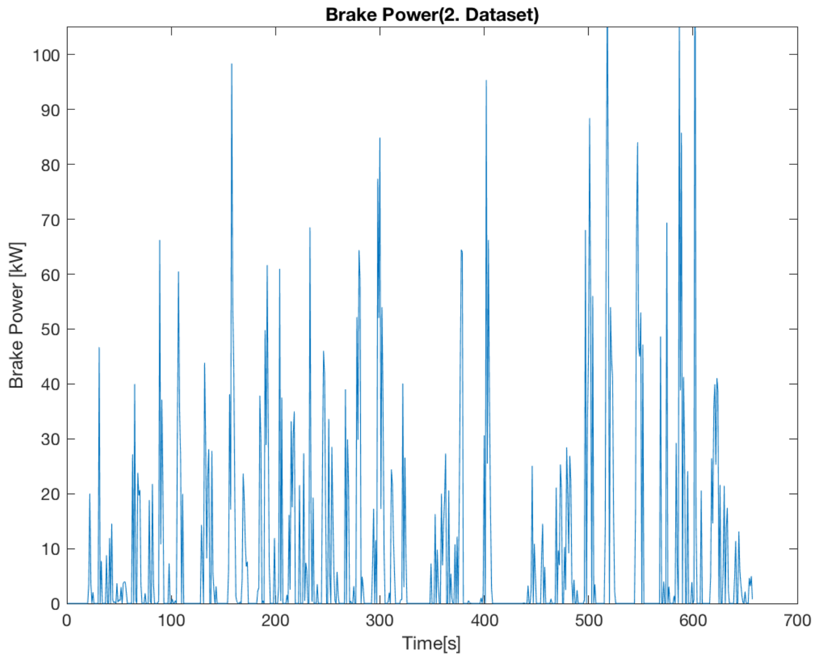

Figure F.10 : Brake Power Map of 2.Measurement (1.(End point→ Start point))

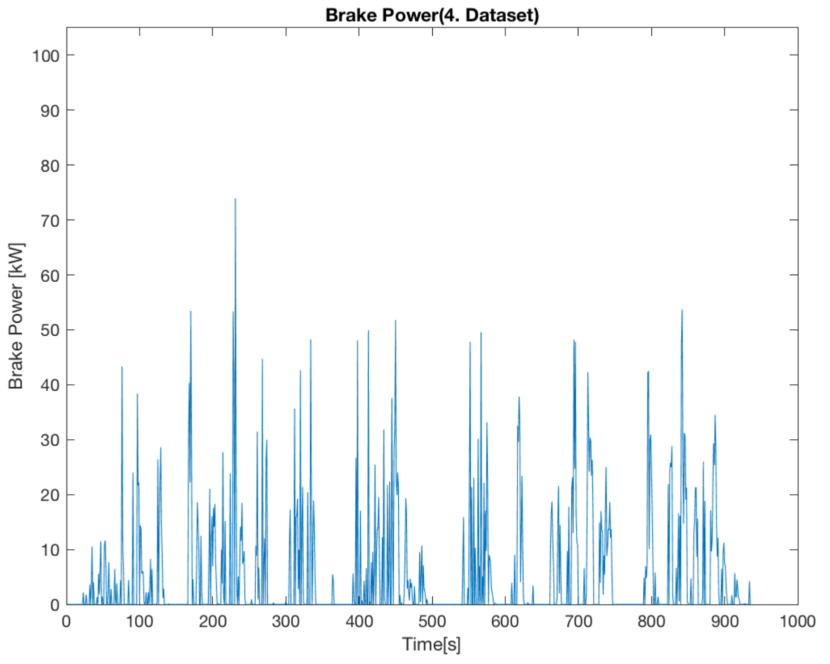

Figure F.11 : Brake Power Map of 4.Measurement (2.(End point→ Start point))

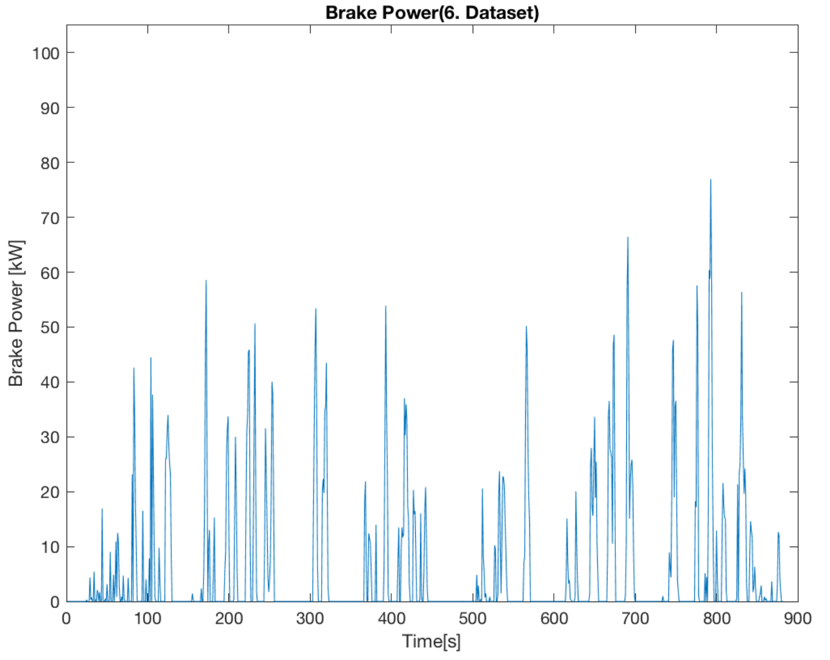

Figure F.12 : Brake Power Map of 6.Measurement (3.(End point→ Start point))

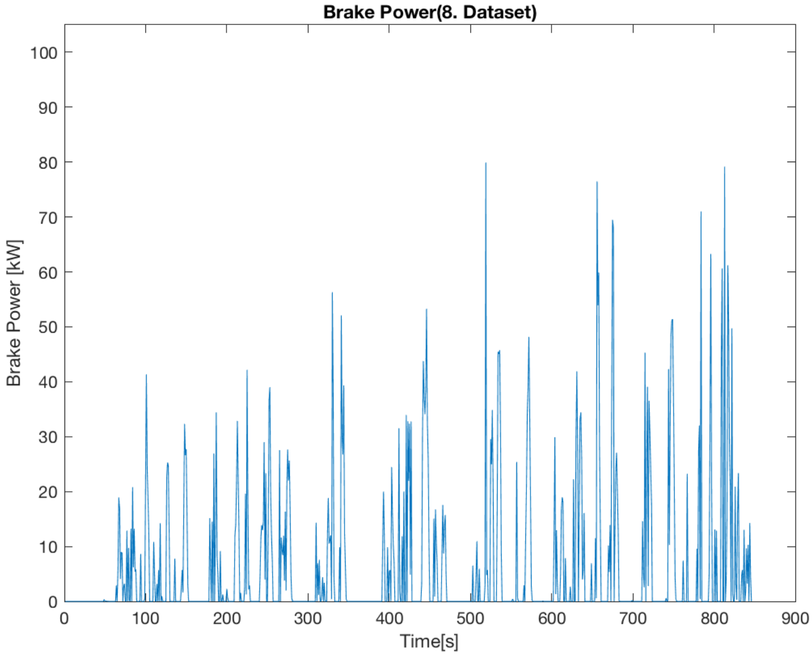

Figure F.13 : Brake Power Map of 8.Measurement (4.(End point→ Start point))

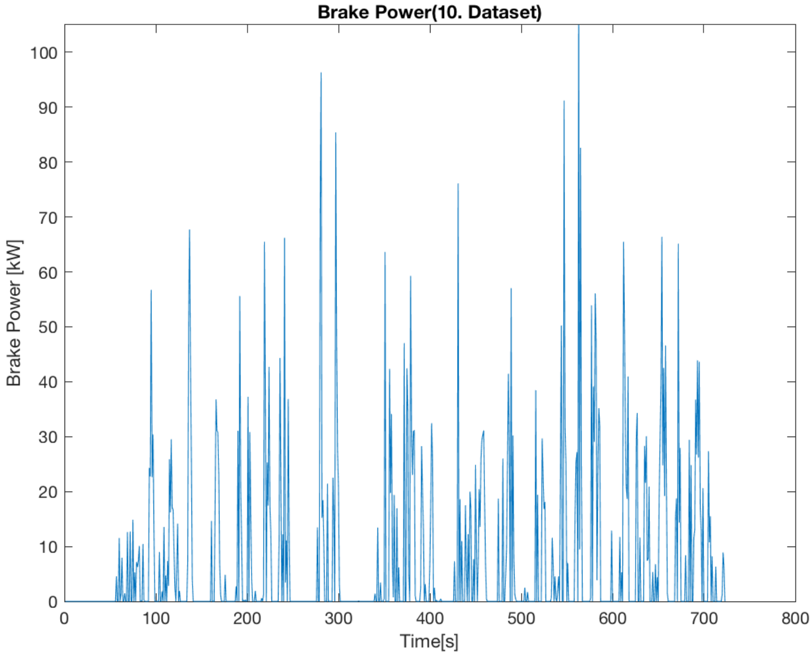

Figure F.14 : Brake Power Map of 10.Measurement (5.(End point→ Start point))

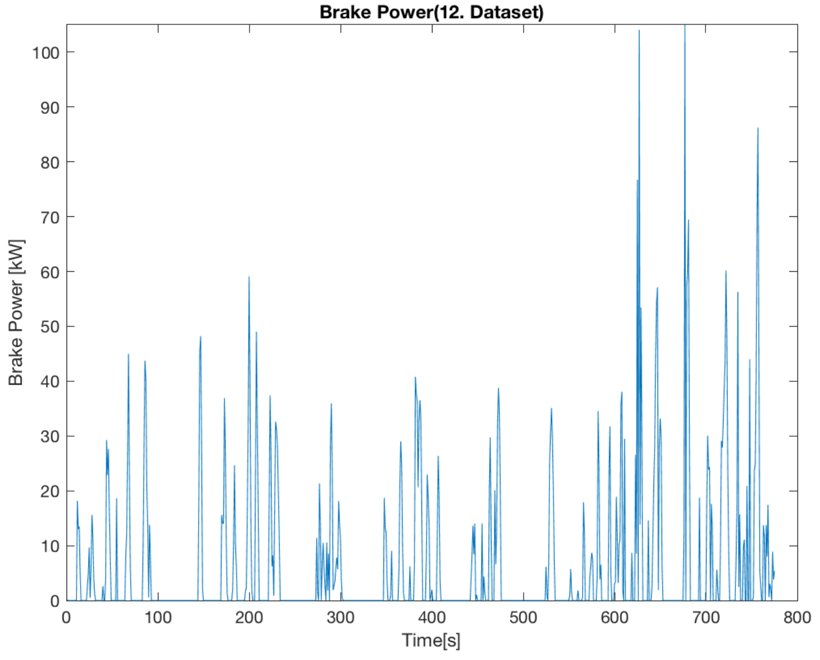

Figure F.15 : Brake Power Map of 12.Measurement (6.(End point→ Start point))

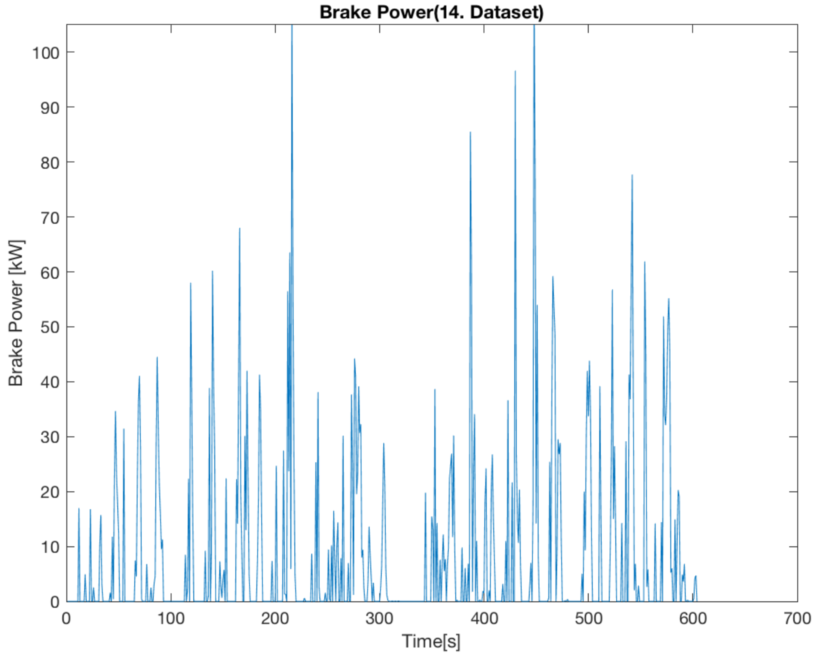

Figure F.16 : Brake Power Map of 14.Measurement (7.(End point→ Start point))

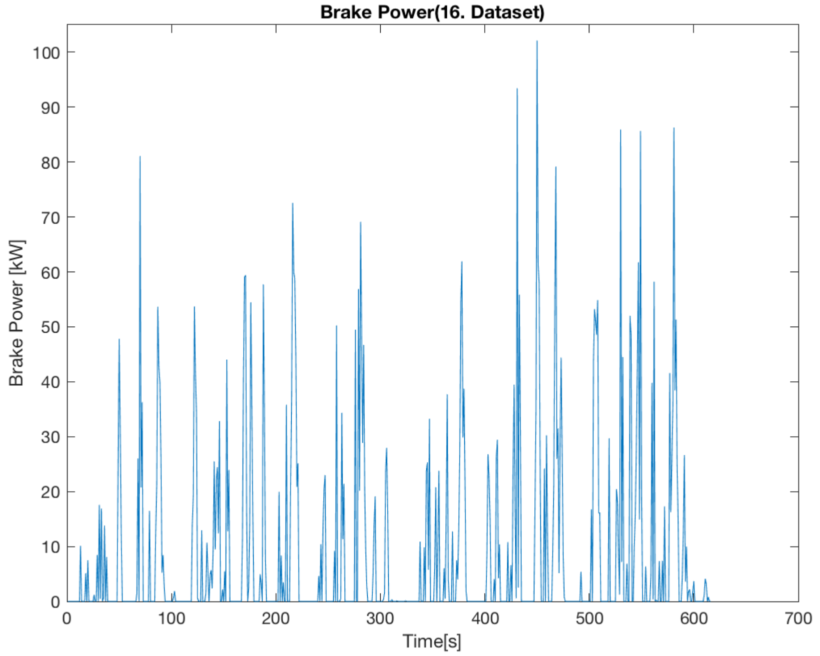

Figure F.17 : Brake Power Map of 16.Measurement (8.(End point→ Start point))

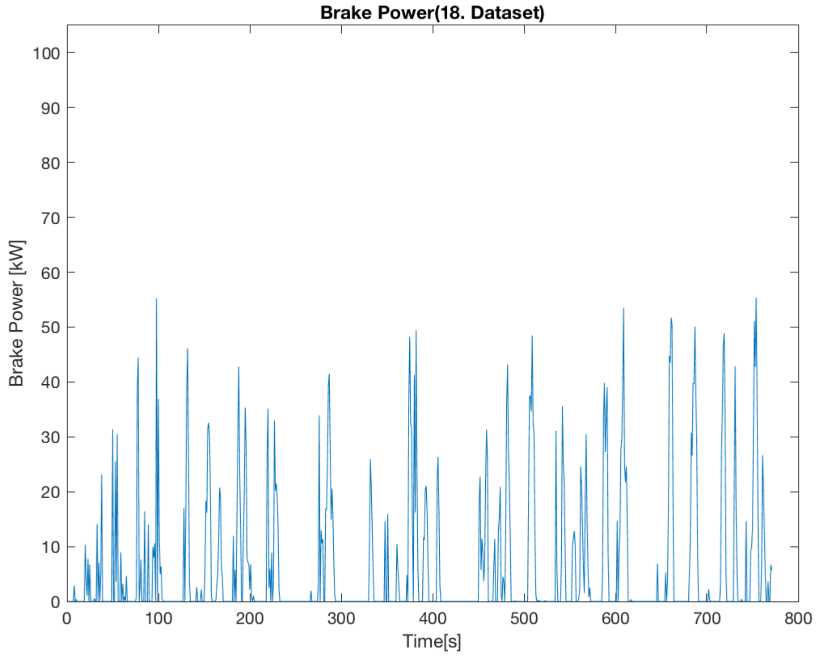

Figure F.18 : Brake Power Map of 18.Measurement (9.(End point→ Start point))

APPENDIX G

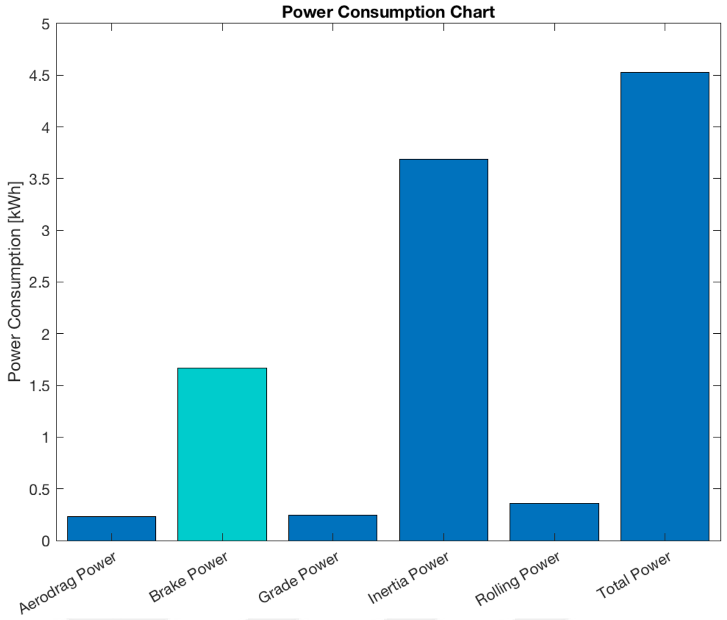

Figure G.1 : Power Consumption Chart of 1.Measurement (1.(Start point → End point))

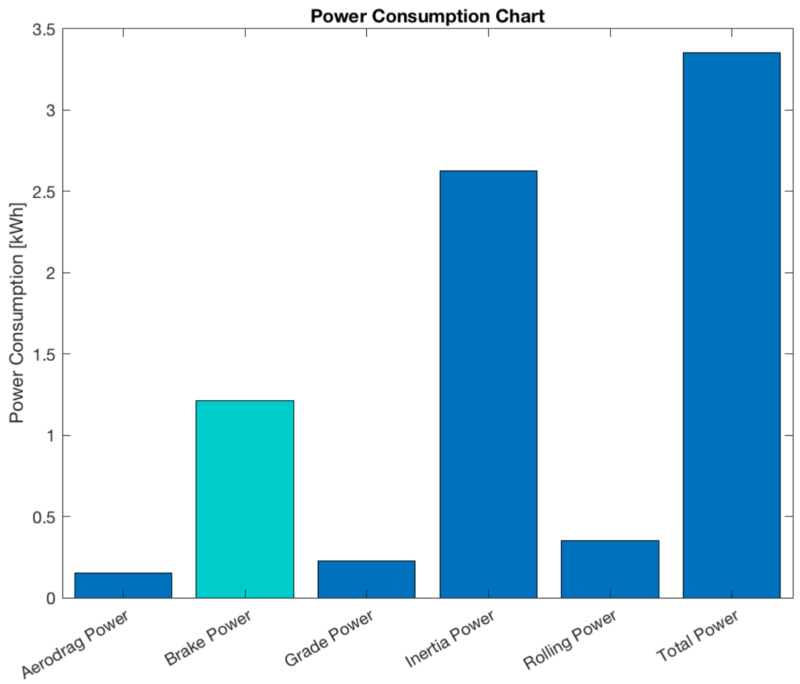

Figure G.2 : Power Consumption Chart of 3.Measurement (2. (Start point → End point))

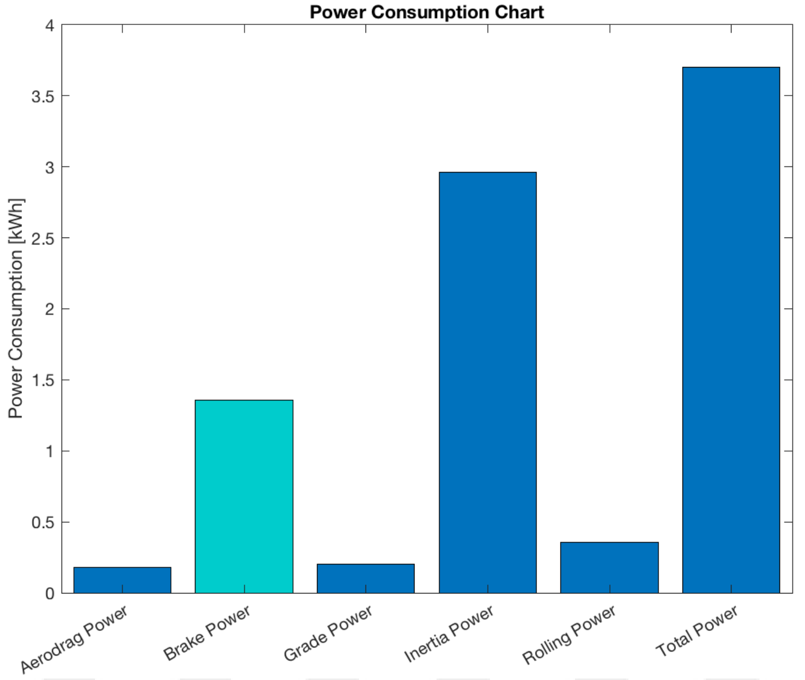

Figure G.3 : Power Consumption Chart of 5.Measurement (3.(Start point → End point))

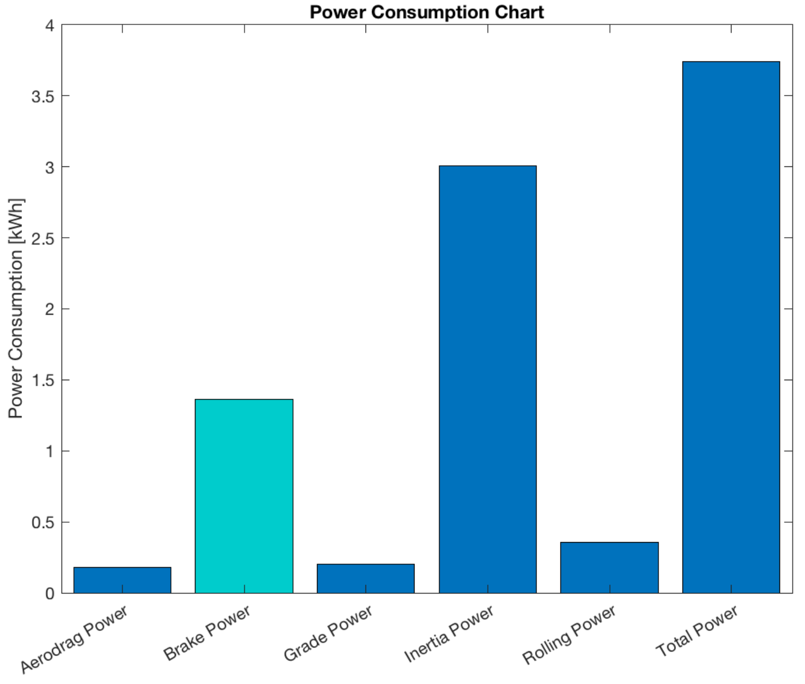

Figure G.4 : Power Consumption Chart of 7.Measurement (4. (Start point → End point))

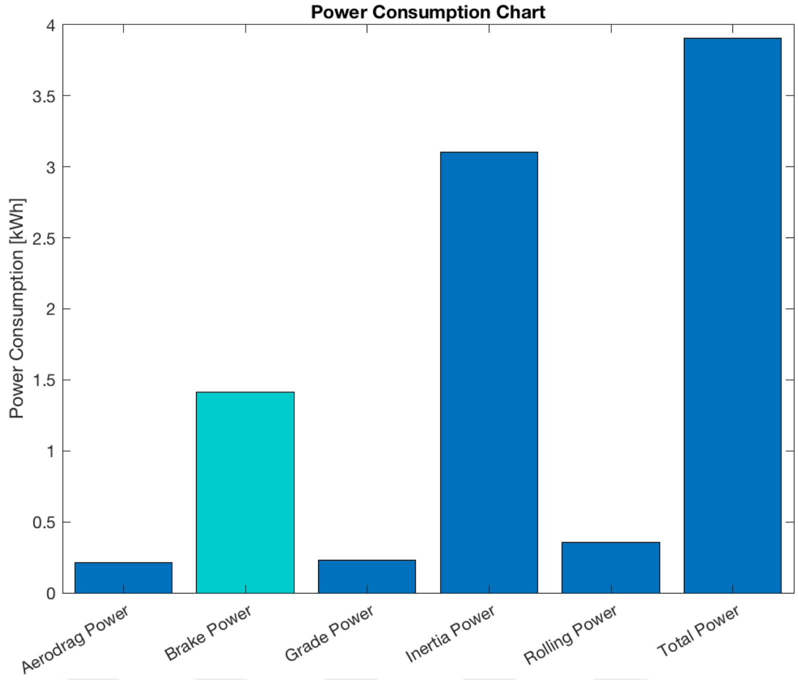

Figure G.5 : Power Consumption Chart of 9.Measurement (5.(Start point → End point))

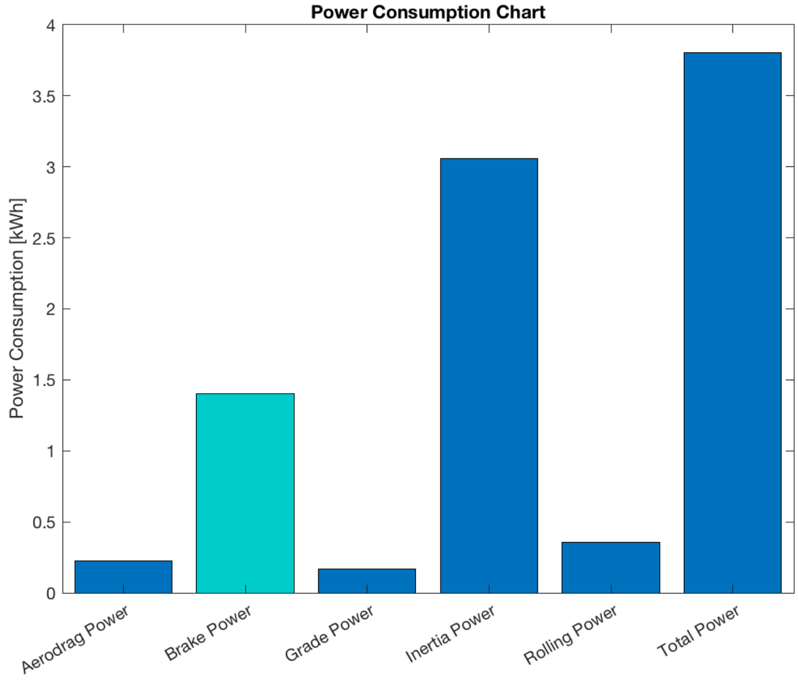

Figure G.6 : Power Consumption Chart of 11.Measurement (6. (Start point → End point))

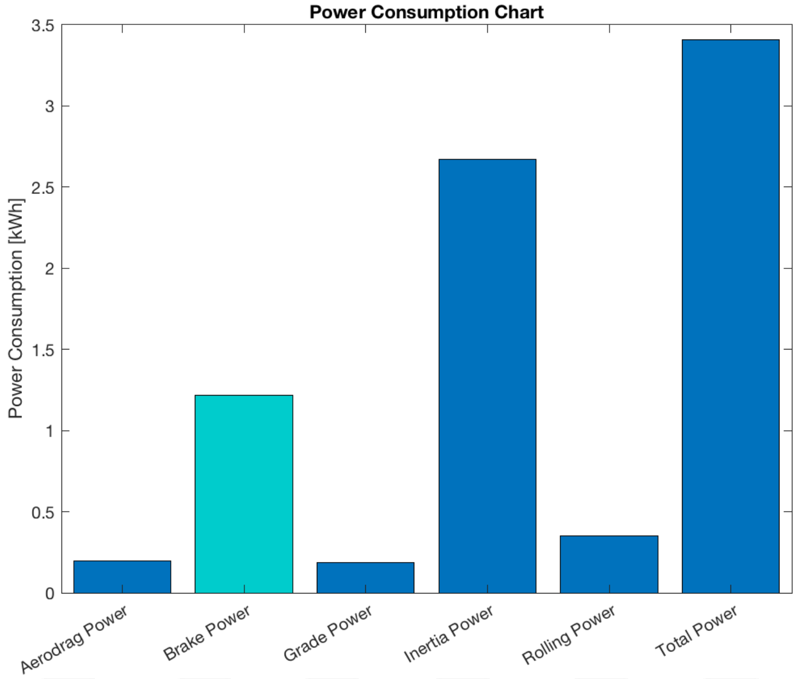

Figure G.7 : Power Consumption Chart of 13.Measurement (7.(Start point → End point))

Figure G.8 :

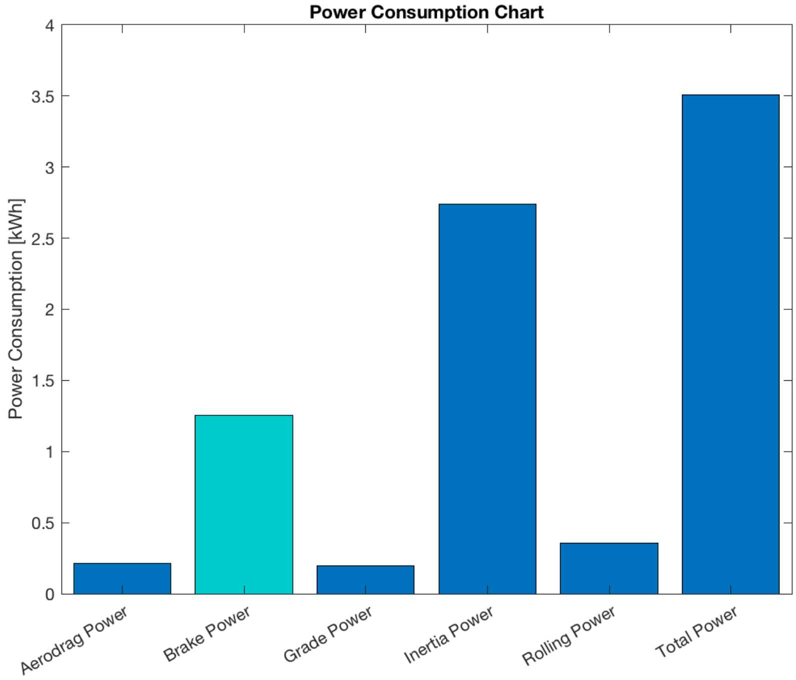

Figure G.9 : Power Consumption Chart of 17.Measurement (9.(Start point → End point))

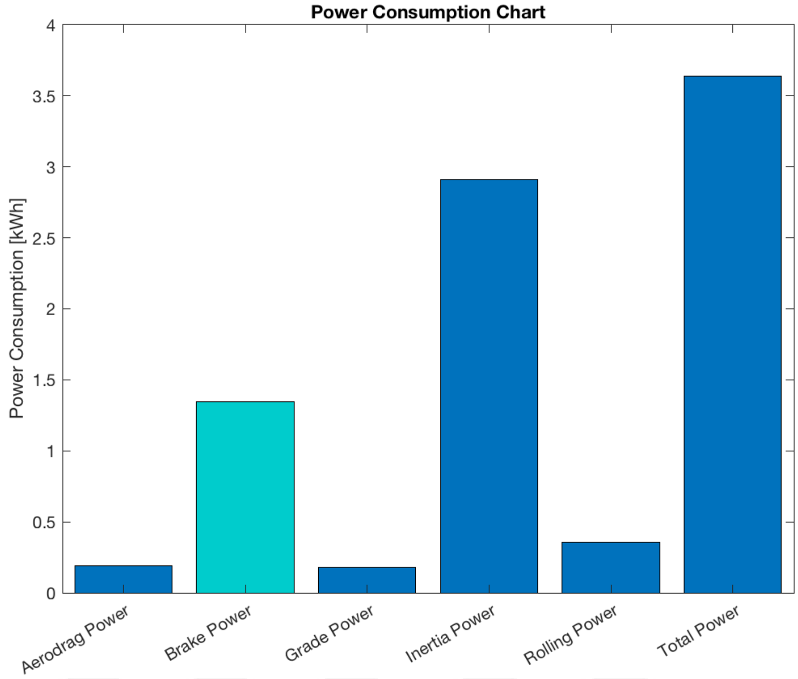

Figure G.10 : Power Consumption Chart of 2.Measurement (1.(End point→ Start point))

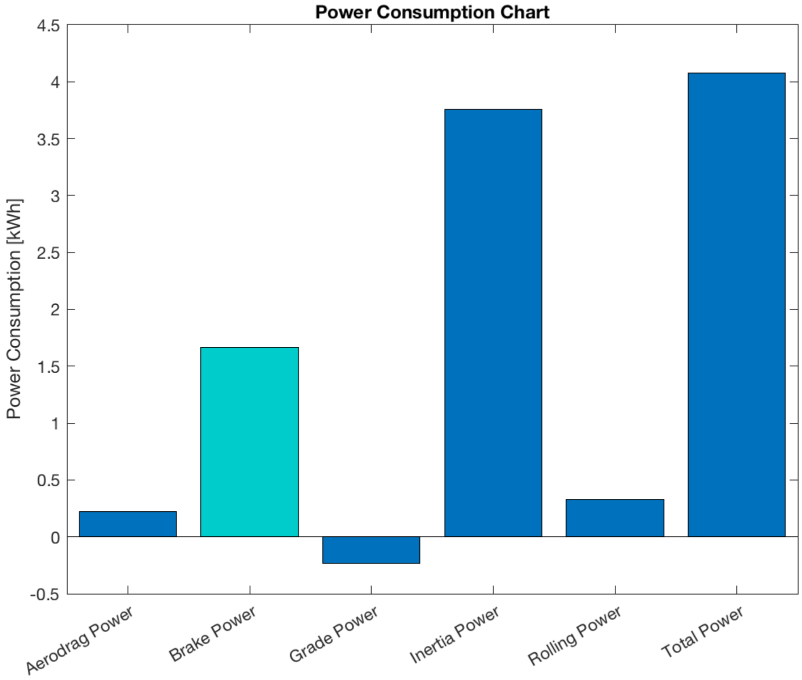

Figure G.11 : Power Consumption Chart of 4.Measurement (2.(End point→ Start point))

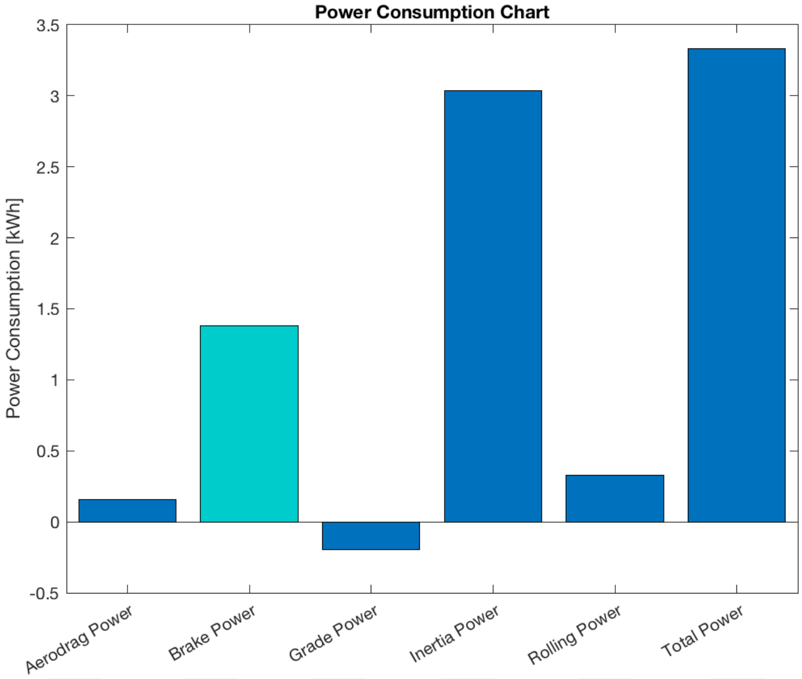

Figure G.12 : Power Consumption Chart of 6.Measurement (3.(End point→ Start point))

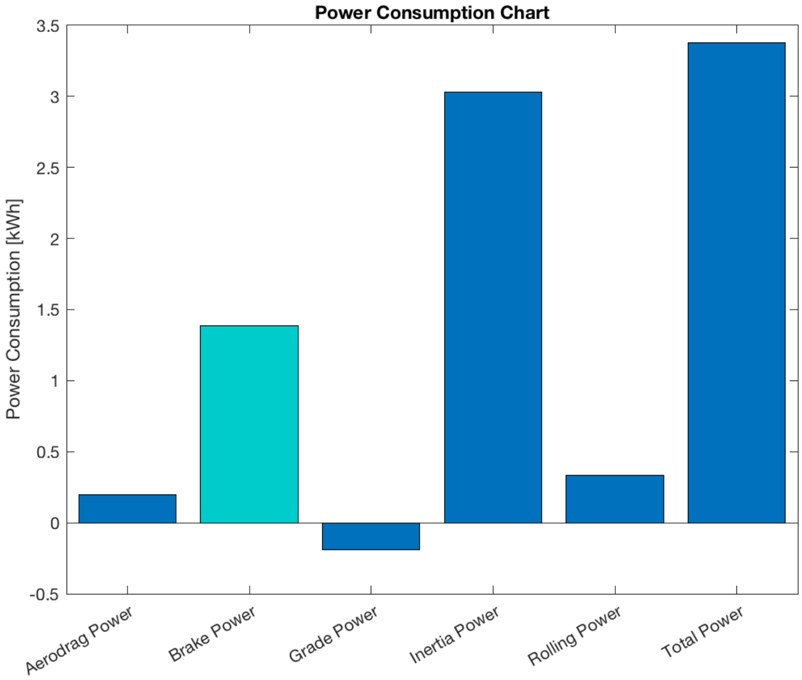

Figure G.13 : Power Consumption Chart of 8.Measurement (4.(End point→ Start point))

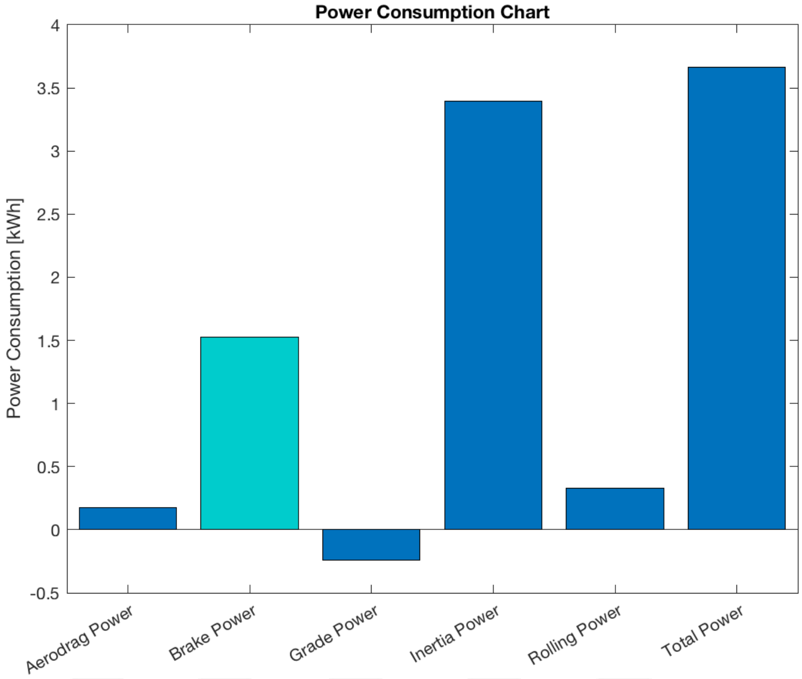

Figure G.14 : Power Consumption Chart of 10.Measurement (5.(End point→ Start point))

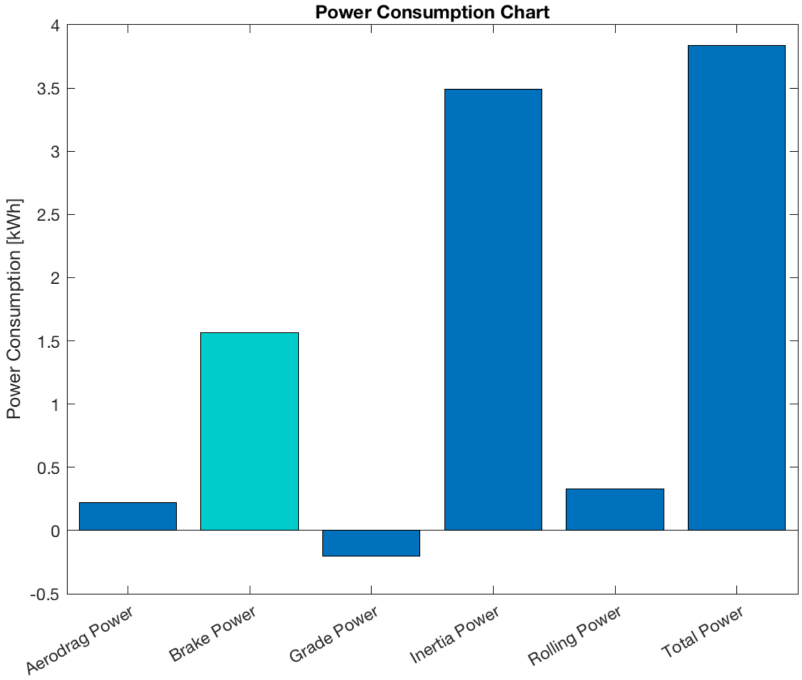

Figure G.15 : Power Consumption Chart of 12.Measurement (6.(End point→ Start point))

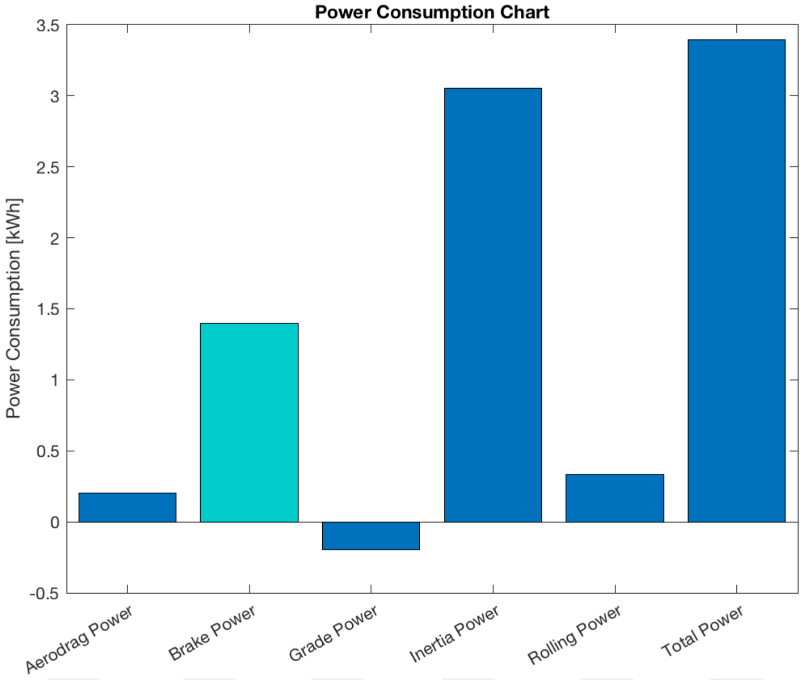

Figure G.16 : Power Consumption Chart of 14.Measurement (7.(End point→ Start point))

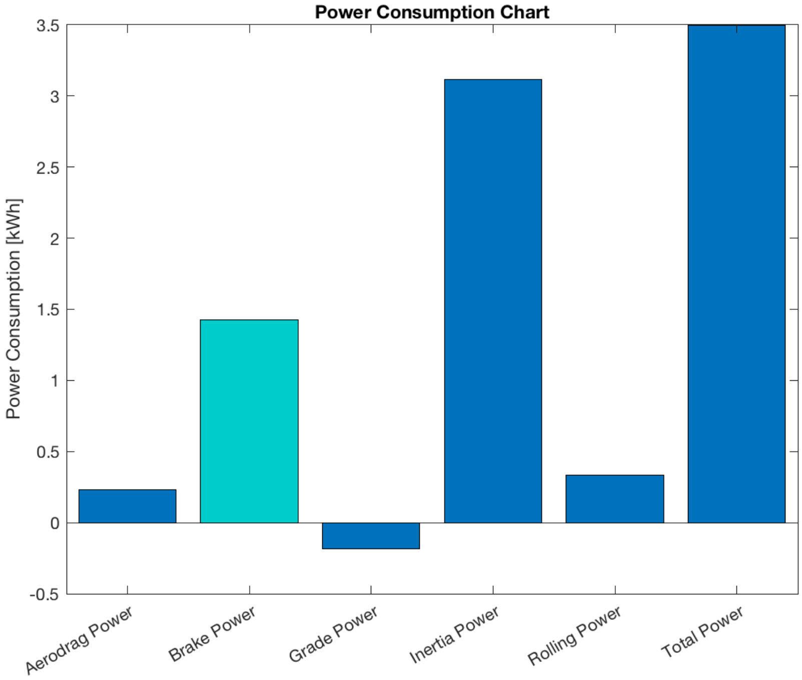

Figure G.17 : Power Consumption Chart of 16.Measurement (9.(End point→ Start point))

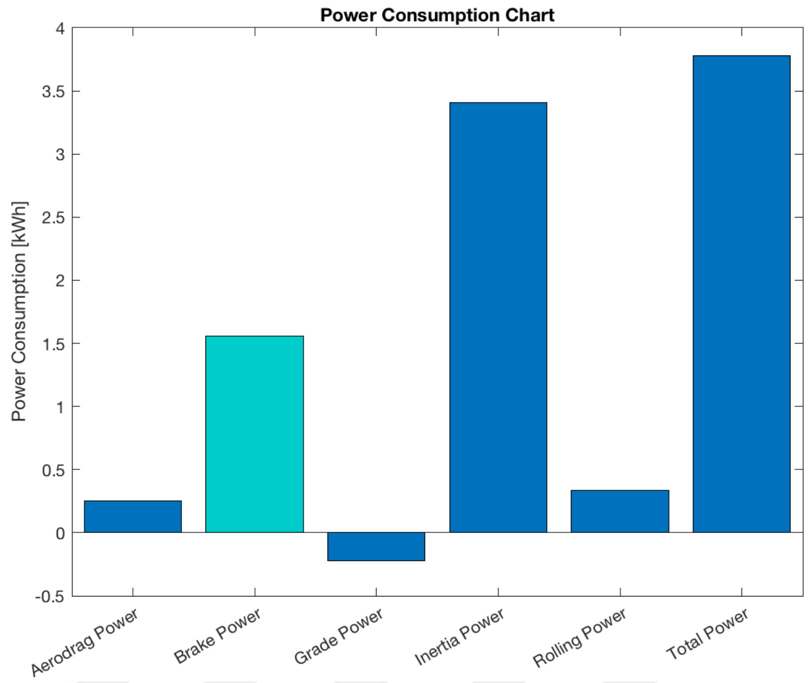

Figure G.18 : Power Consumption Chart of 18.Measurement (9.(End point→ Start point))

APPENDIX H

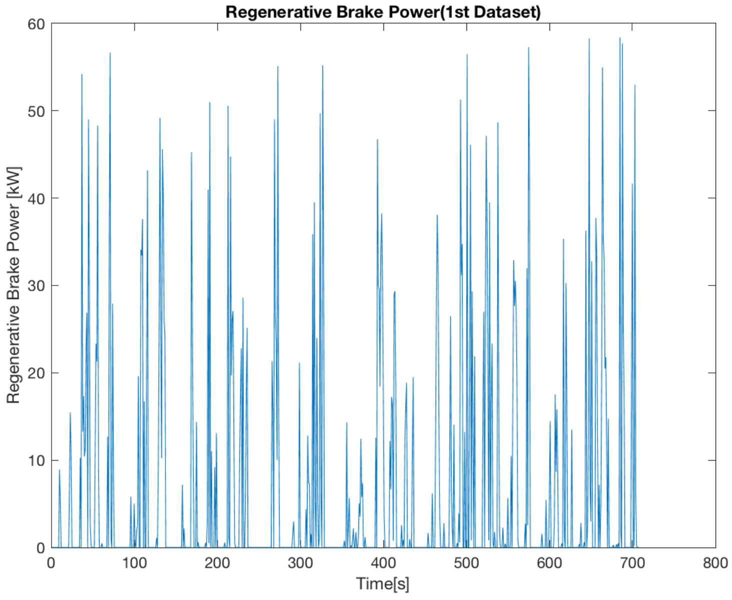

Figure H.1 : Regenerative Brake Power Map of 1.Measurement (1.(Start point → End point))

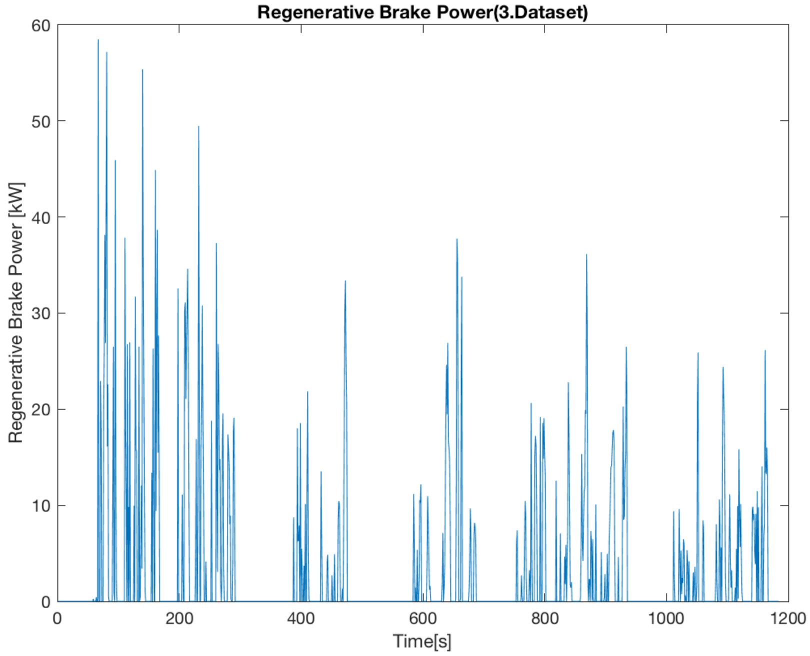

Figure H.2 : Regenerative Brake Power Map of 3.Measurement (2. (Start point → End point))

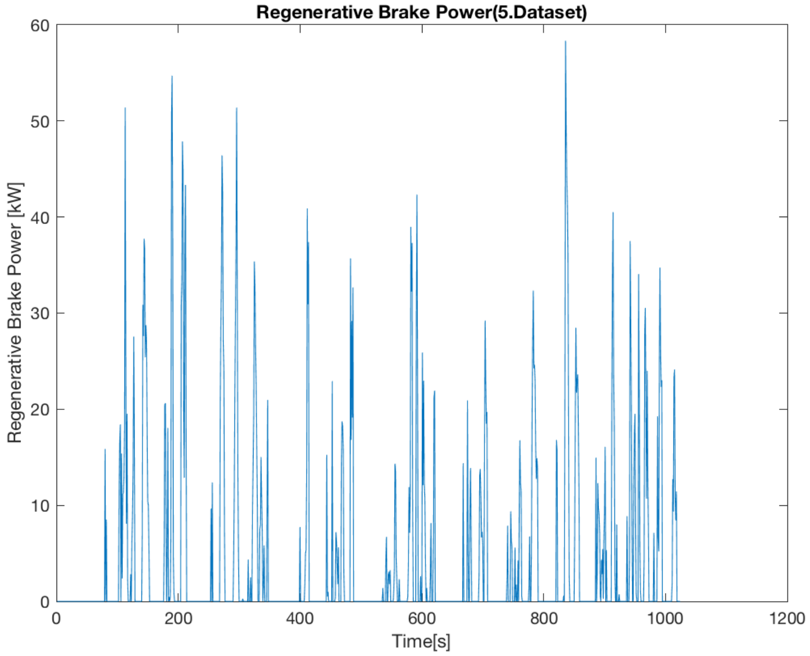

Figure H.3 : Regenerative Brake Power Map of 5.Measurement (3.(Start point → End point))

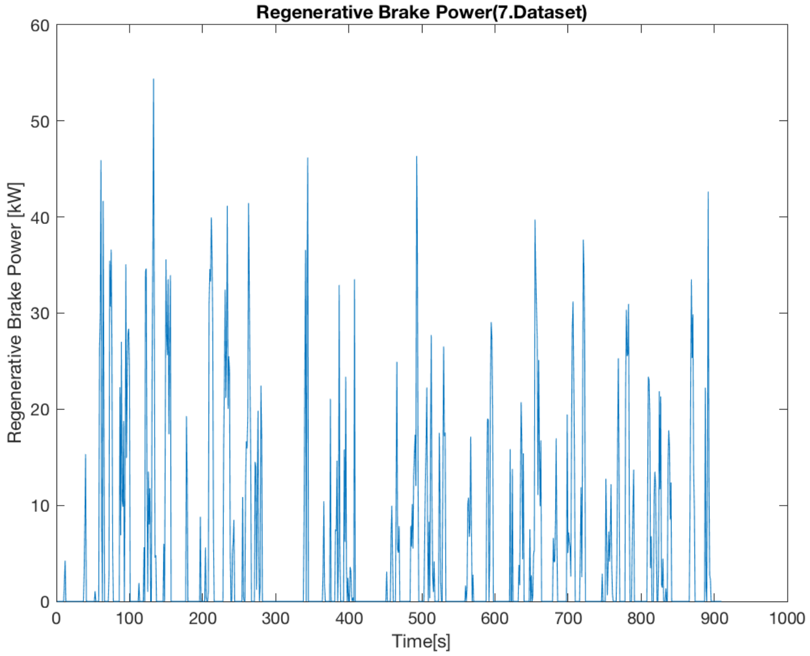

Figure H.4 : Regenerative Brake Power Map of 7.Measurement (4. (Start point → End point))

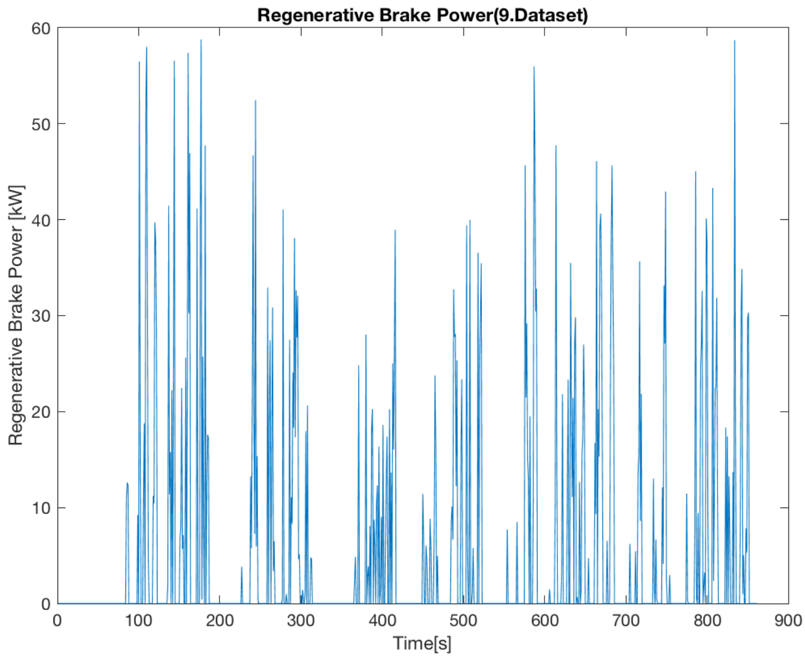

Figure H.5 : Regenerative Brake Power Map of 9.Measurement (5.(Start point → End point))

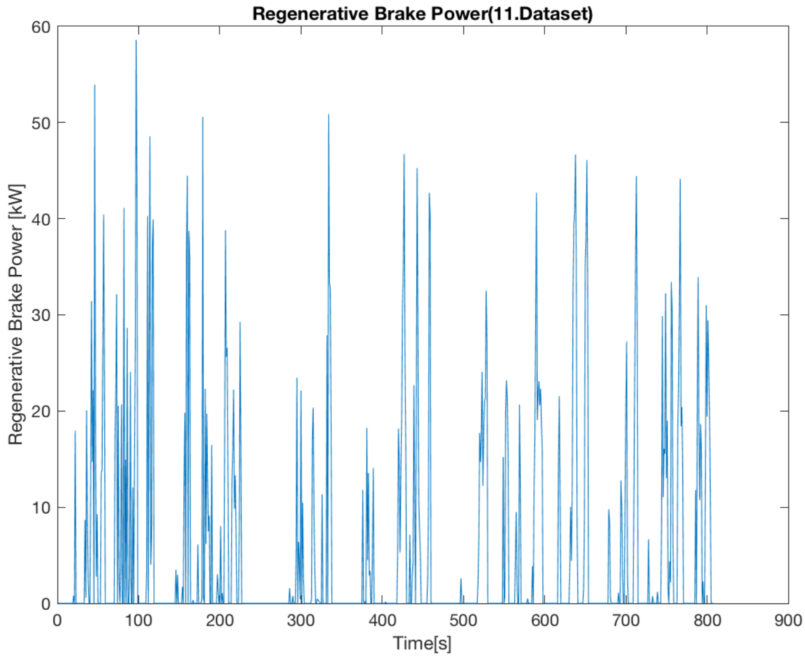

Figure H.6 : Regenerative Brake Power Map of 11.Measurement (6. (Start point → End point))

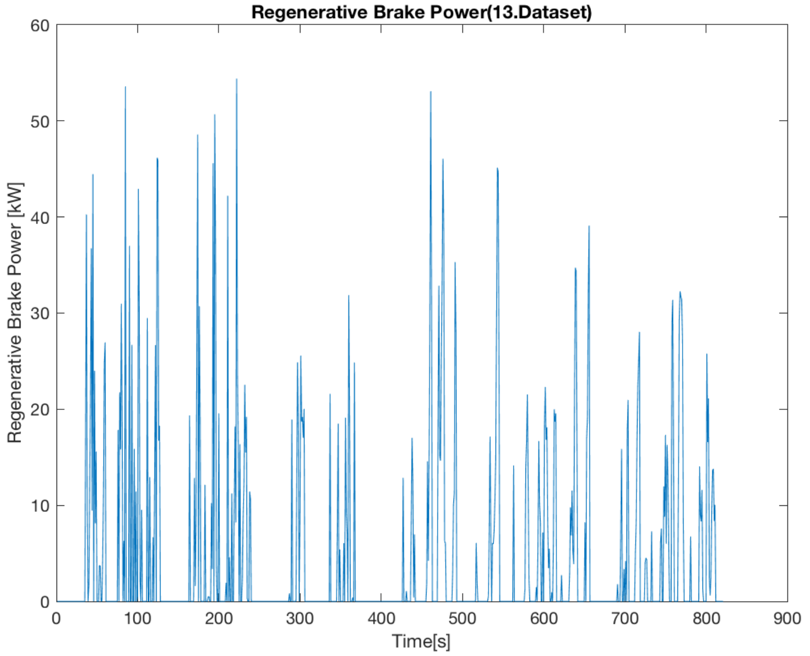

Figure H.7 : Regenerative Brake Power Map of 13.Measurement (7.(Start point → End point))

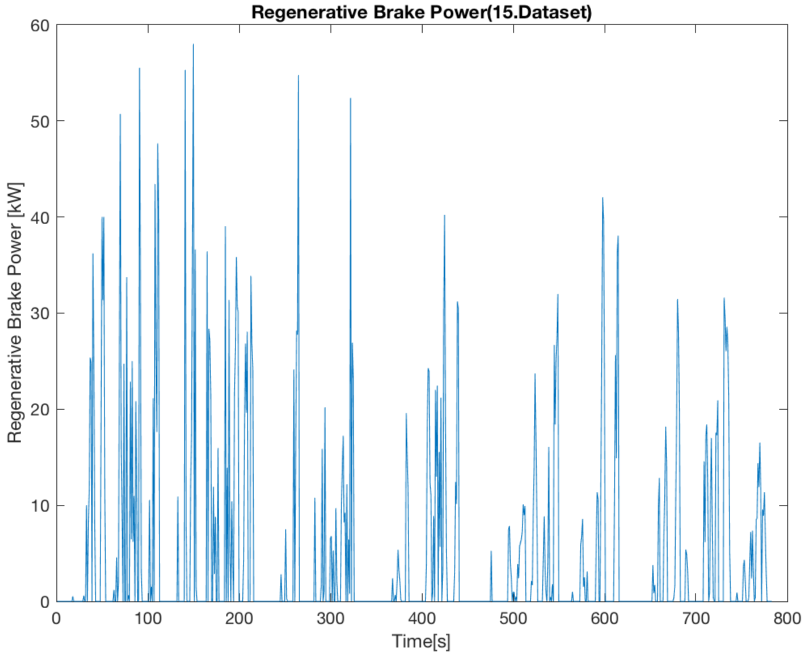

Figure H.8 : Regenerative Brake Power Map of 15.Measurement (8. (Start point → End point))

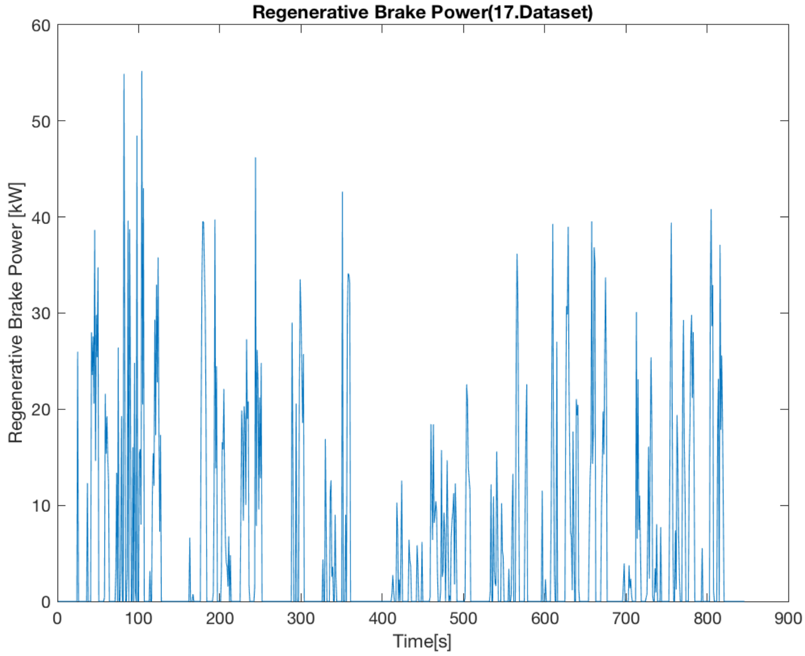

Figure H.9 : Regenerative Brake Power Map of 17.Measurement (9.(Start point → End point))

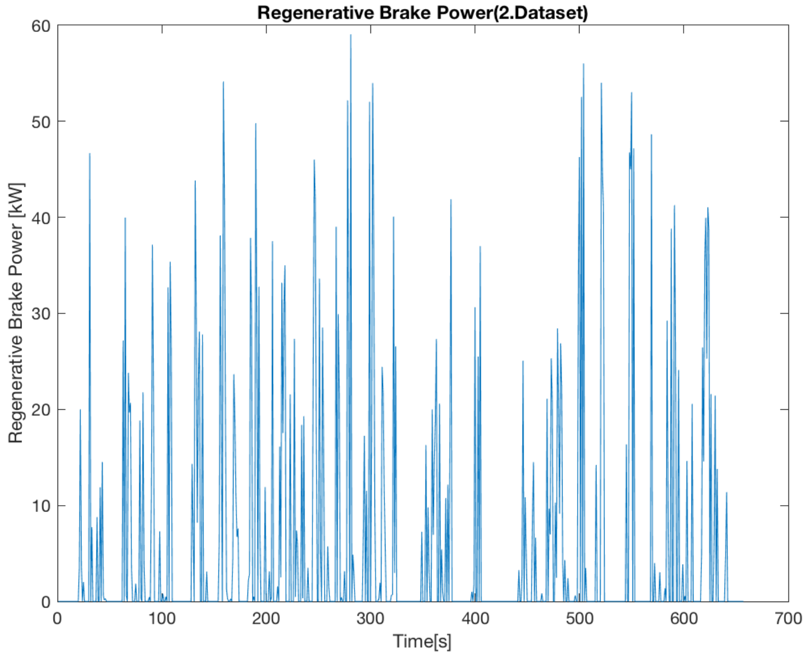

Figure H.10 : Regenerative Brake Power Map of 2.Measurement (1.(End point→ Start point))

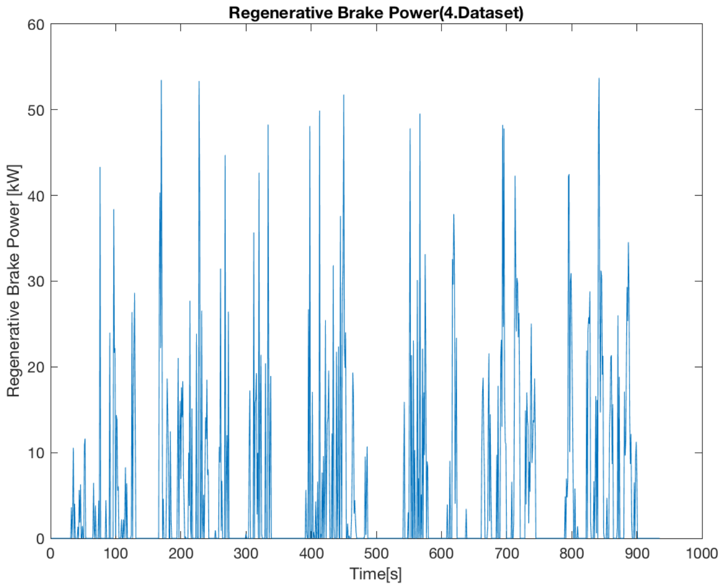

Figure H.11 : Regenerative Brake Power Map of 4.Measurement (2.(End point→ Start point))

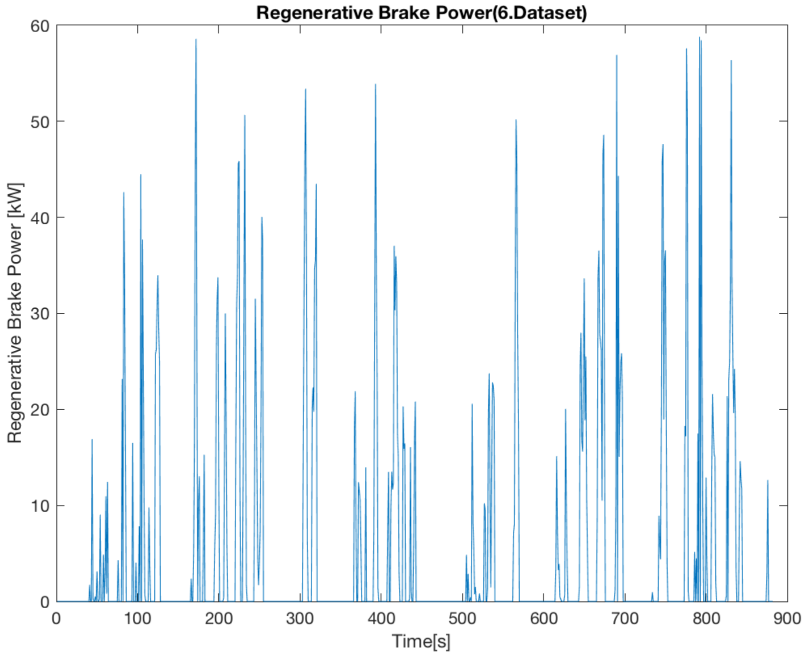

Figure H.12 : Regenerative Brake Power Map of 6.Measurement (3.(End point→ Start point))

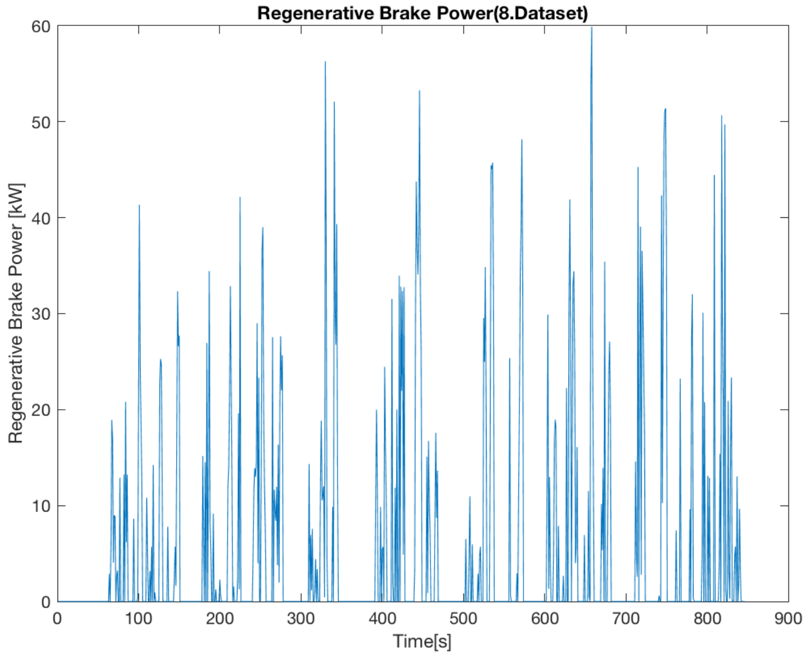

Figure H.13 : Regenerative Brake Power Map of 8.Measurement (4.(End point→ Start point))

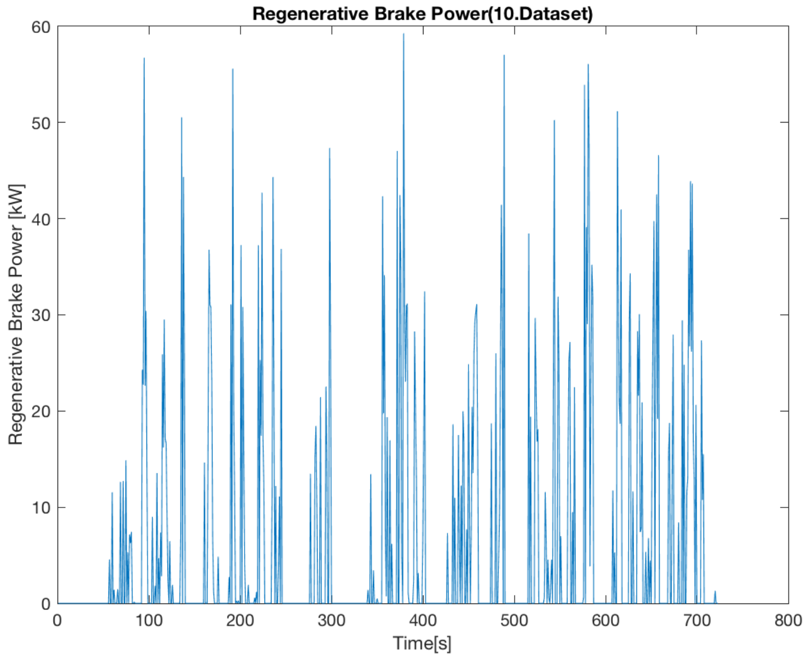

Figure H.14 : Regenerative Brake Power Map of 10.Measurement (5.(End point→ Start point))

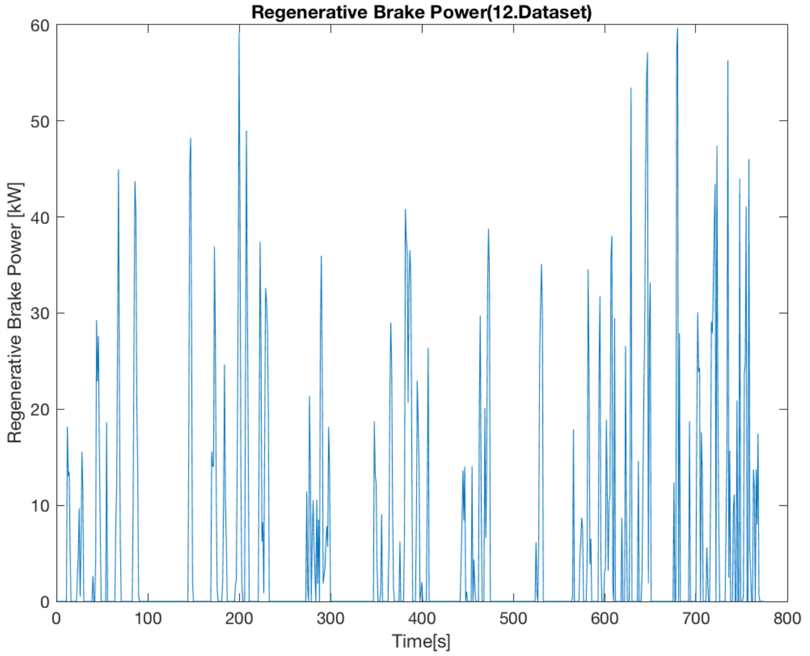

Figure H.15 : Regenerative Brake Power Map of 12.Measurement (6.(End point→ Start point))

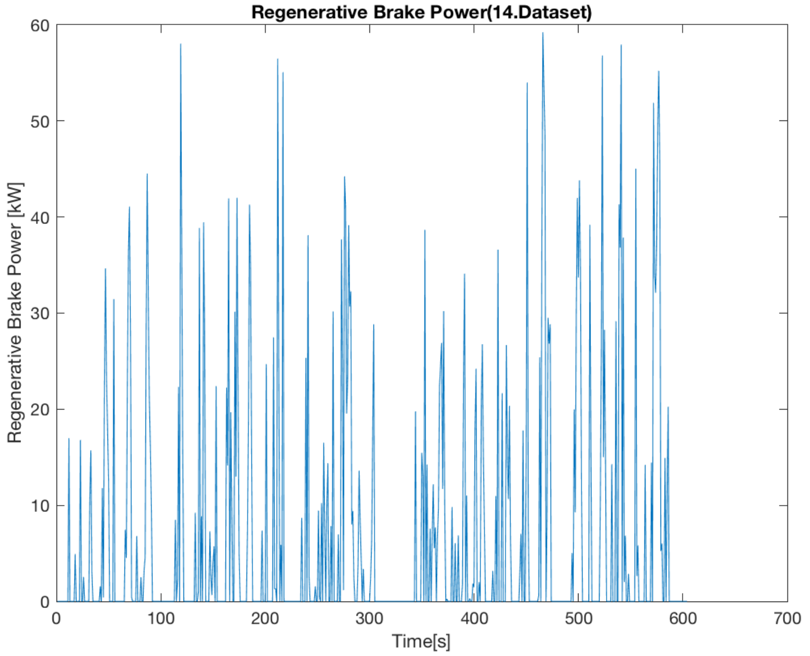

Figure H.16 : Regenerative Brake Power Map of 14.Measurement (7.(End point→ Start point))

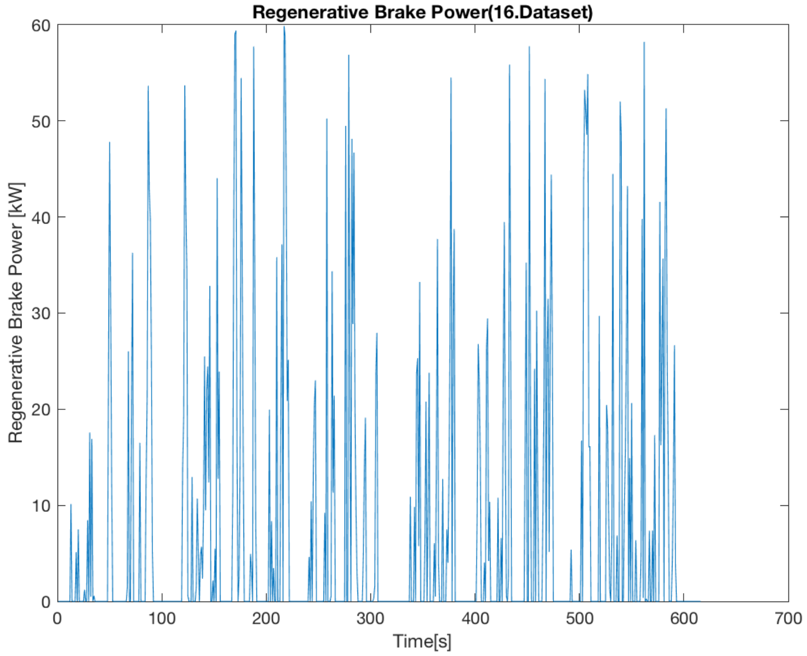

Figure H.17 : Regenerative Brake Power Map of 16.Measurement (8.(End point→ Start point))

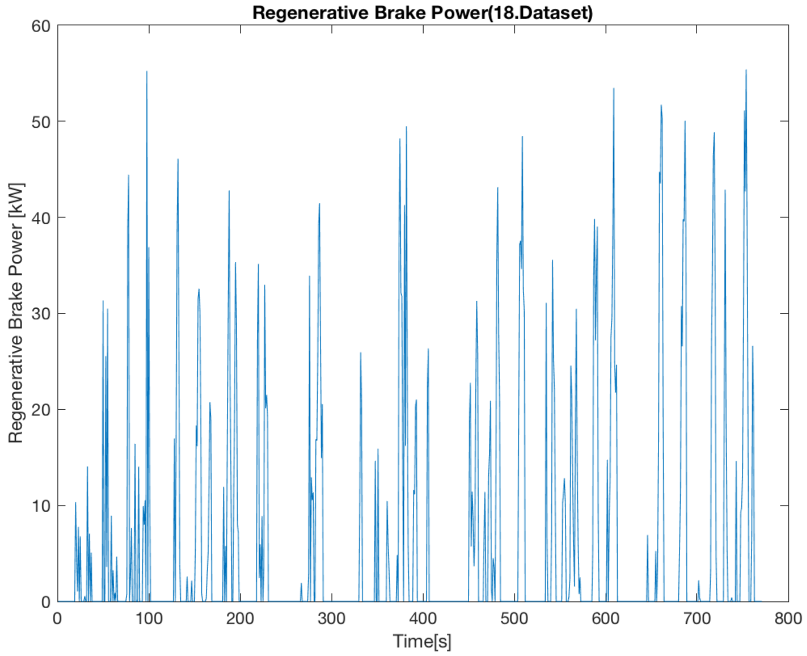

Figure H.18 : Regenerative Brake Power Map of 18.Measurement (9.(End point→ Start point))

CURRICULUM VITAE

Name Surname : Mehmet Ercan Tekin

Place and Date of Birth : Ankara, 21-04-1994

E-Mail : ercantekin94@gmail.com

EDUCATION :

- **B.Sc.** : 2016, Gazi University, Engineering Faculty, Mechanical Engineering

PROFESSIONAL EXPERIENCE AND REWARDS:

- Mechanical Design Engineer at Arçelik since September 2016